THE F_N METHOD IN KINETIC THEORY

by

Dimitris V. Valougeorgis

Dissertation submitted to the Faculty of the
Virginia Polytechnic Institute and State University
in partial fulfillment of the requirements for the degree of
DOCTOR OF PHILOSOPHY
in
Mechanical Engineering

APPROVED:

Dr. J.R. Thomas, Chairman

Dr. F.J. Pierce

Dr. E.W. Kohler

Dr. A. Moutsoglou

Dr. B. Vick

March, 1985
Blacksburg, Virginia

8/26/85 MCR

THE F_N METHOD IN KINETIC THEORY

by

Dimitris V. Valougeorgis

(ABSTRACT)

A complete formulation of the recently developed F_N method in kinetic theory is presented and the accuracy of this advanced semi-analytical-numerical technique is demonstrated by testing the method to several classical problems in rarefied gas dynamics.

The method is based on the existing analysis for the vector transport equation arising from the decomposition of the linearized BGK equation. Using full-range orthogonality, a system of singular integral equations for the distribution functions at the boundaries is established. The unknown distribution functions are then approximated by a finite expansion in terms of a set of basis functions and the coefficients of the expansion are found by requiring the set of the reduced algebraic equations to be satisfied at certain collocation points.

By studying the half-space heat transfer and weak evaporation problems and the problem of heat transfer between two parallel plates it is demonstrated that the F_N method is a viable solution technique yielding results of benchmark accuracy. Two different sets of basis functions are provided for half-space and finite media problems, respectively. In all cases, highly accurate numerical

results are computed and compared to existing exact solutions. The obtained numerical results help in judging the accuracy to expect of the method and indicate that the F_N method may be applied with confidence to problems for which, more exact methods of analysis do not appear possible.

Then, the cylindrical Poiseuille flow and thermal creep problems, which are not amenable to exact treatment, are solved. The F_N method is formulated and tested successfully for the first time in cylindrical geometry in kinetic theory. The complete solution of the two aforementioned problems is presented with the numerical results quoted as converged being of reference quality good for benchmark accuracy.

ACKNOWLEDGEMENTS

The author gratefully acknowledges the valuable guidance of Dr. James R. Thomas during the course of this research. Without his constant guidance, counseling and support this study would have been most difficult to complete.

The author would also like to express particular gratitude to Drs. F. J. Pierce, W. E. Kohler, A. Moutsoglou and B. Vick for many helpful suggestions and their consideration in serving on his committee. Professor C. E. Siewert of North Carolina State University also contributed valuable advice.

The financial support provided by the National Science Foundation is acknowledged with gratitude.

Special thanks go to the author's wife, , for her encouragement, support and typing the manuscript.

TABLE OF CONTENTS

LIST OF TABLES

LIST OF FIGURES

1. INTRODUCTION

The problem of the kinetic theory of gases is reduced to the mathematical problem of solving the Boltzmann transport equation, which is a nonlinear integro-differential equation for the distribution function $f(\bar{r},\bar{v},t)$. The single unknown f is a function of seven variables and already contains all the information about density, velocity, temperature, stresses, heat flux and flow rate.

The great complexity and the strong nonlinearity of the Boltzmann equation makes an analytical solution impossible and as a consequence it is necessary to resort to numerical techniques. However, the applied numerical analysis leads to the solution of a system of nonlinear partial differential equations, well known as the moment equations, which are in general harder to handle than even the Navier-Stokes equations.

One can simplify the calculations by utilizing the H-theorem that under an arbitrary initial condition any distribution $f(\bar{v},t)$ will be altered to approach the Maxwellian form as time goes to infinity, and thus replace the Boltzmann collision integral by a collision model. The most widely known collision model is usually called the Bhatnagar, Gross and Krook (BGK) model [1], although Welander [2] proposed it independently at about the same time. The nonlinearity of the proposed BGK model is much

worse than the nonlinearity of the true collision term but the main advantage is that for any given problem one can deduce integral equations for the macroscopic variables density, velocity and temperature. Another advantage of the BGK model is offered by its linearized form, which has a structure definitely simpler than the true linearized Boltzmann equation. It is to be remarked that the accuracy of kinetic models in nonlinear problems is less obvious than in the linearized ones and, provided linearization is permitted, then an exact analytical attack on the problem is possible.

The most elegant, concise and easy to handle method for providing these exact solutions is the normal-mode-expansion technique first developed by Case [3] in neutron transport theory and then applied to kinetic theory by Cercignani [4,5]. The effectiveness of the Case method in handling the typical problem of neutron transport is a result of its use of a complete set of elementary solutions. The general solution then follows as a superposition of these elementary solutions; by matching the boundary conditions, one is led to solving singular integral equations.

Case's method cannot be applied directly to the Boltzmann equation because of the strong nonlinear characteristics of the equation; neither can it be applied to the linearized equation because the linear collision operator has an infinite number of distinct eigenvalues. In

order to avoid this difficulty, and since the linearized BGK equation is identical to the linear Boltzmann equation for Maxwell molecules, Cercignani was able to split the linearized form of the BGK equation into five equations. This separation between the heat conduction effects and the viscosity effects is possible when there is a small departure from thermodynamic equilibrium and thus linearization is permitted. These five equations can be then treated by a procedure analogous to that of Case. The reader should refer to texts of Case and Zweifel [6] and Cercignani [4] for a complete exposition of the fundamentals.

Since its introduction the aforementioned work has been the focal point for many successful investigations and its importance for solving boundary value problems explains the enormous amount of literature.

The F_N method was first introduced by Siewert and Benoist [7] and Grandjean and Siewert [8] in the context of neutron transport theory. This method proved capable of utilizing aspects of the exact elementary solutions to establish an approximate solution that is particularly concise and accurate, minimizing computational time and effort. The method has been extensively developed in the field of neutron transport theory and radiative transfer.

It is the purpose of this work to demonstrate the general method of formulation of the F_N method in kinetic

theory. In addition, solutions of benchmark accuracy (correct to within +1, -1 in the last significant figure shown) to three kinetic theory problems are provided for judging the accuracy of the method. Finally, exact numerical results, not now available in the literature, which we believe to be of reference quality, are developed, for two more problems of rarefied gas dynamics.

In chapter 2, the literature review consists of two parts. First a survey of the literature on kinetic theory emphasizing the analytical techniques and solutions is given, followed by a comprehensive review on the recently introduced F_N method.

In the third chapter the general method of formulation of the F_N method is given. Singular integral equations for the distribution function at the boundaries are derived and solved by polynomial expansion and collocation. Once the boundary distributions are established, similar ideas can be used to find the desired distribution function at any location. With these quantities known, position-dependent macroscopic quantities like density, velocity and temperature and overall quantities like heat flux and flow rate follow immediately.

Chapter 4 is concerned with the demonstration of the method by solving two classical half-space problems: temperature jump and weak evaporation for the case of diffuse reflection only. In chapter 5 we turn to a problem

in a finite medium, that of heat transfer in a gas confined between parallel plates for arbitrary surface accommodation. Results for these problems computed to benchmark accuracy are reported.

Finally in chapter 6 the F_N method is used to develop a solution for the cylindrical Poiseuille flow and thermal creep problems based on the linearized BGK model written in cylindrical coordinates. The F_N method, extended for the first time to cylindrical geometry in kinetic theory, provides exact numerical results improving earlier results by Loyalka [37].

This work is ended in chapter 7, where the final conclusions are given and future applications of the F_N method in kinetic theory are suggested as a direct outgrowth of the present work.

2. REVIEW OF LITERATURE

As Boltzmann wrote more than a hundred years ago [9], in order to solve a boundary value problem in kinetic theory we need the Boltzmann equation and the boundary conditions. The boundary conditions are as important as the equation itself and were first investigated and presented by Maxwell [10], and for that reason they bear his name. The flow regime which is described by the Boltzmann equation is well known as the transition regime and is understood as covering the flows which cannot be predicted on the basis of either a continuum or a free molecule flow theory. Following the terminology introduced by H. Grad [11] flow regimes having the characteristics of the transition regime are transition layers such as the initial, boundary and shock layers.

The task of solving the Boltzmann equation assuming even the simplest boundary conditions, i.e., pure diffuse reflection on the wall, is a very complicated one. Attempts for overcoming these difficulties have been based on the BGK model and higher order models [1,2,12,13], and their applications are widely known [4,5]. These models are very helpful when they can be solved exactly or at least lead to closed form solutions; this is the case when linearization is permitted. It seems that the relation between the linearized BGK model and the linearized Boltzmann equation is much closer than the relation between the corresponding non-linear equations. Thus if one decides to resort to

heavy numerical computations, such as those involved in the moment and discrete ordinates methods, it seems advisable to use the full Boltzmann equation. We shall not review the fundamentals of these methods, which are appropriate for nonlinear problems and out of the scope of the present work. Kogan [14] and Bird [15] describe the fundamentals of these numerical techniques, which have continued to improve rapidly in recent years [16,17,18]. We only mention the fact that Monte Carlo simulation techniques seem especially suitable for computations of non-linear problems in which complicated scattering kernels describe gas surface interactions. Finally it has been found convenient to try direct numerical solutions, based on the discrete ordinate method, of the Boltzmann equation itself [5].

If we turn to analytic methods of solution, we have to face the unpleasant fact that the only available exact solutions are Maxwellians. This means that in order to make progress with analytical methods we must either make a qualitative study of the problem (existence, uniqueness, smoothness and asymptotic behavior of the solution) or to resort to perturbation methods based on the smallness of some parameter. The perturbation approach has been extensively used utilizing the Knudsen number and its inverse as perturbation parameters. The first instance of a perturbation expansion for solving the Boltzmann equation was due to Hilbert in 1912 [19,20]. The Hilbert expansion

fails to give uniformly valid solutions for specific initial and boundary value problems. Some of the troubles can be avoided, however, by not expanding the solutions, but the equations instead as was done by Chapman and Enskog [21] near the continuum regime and by Willis [21] near the free molecular regime. Expansions appropriate for the kinetic layer have been considered by Cercignani [23], Sone [24] and Darrozes [25] and more recently by Sone [26], Onishi [27,28] and Aoki [29]. As was pointed by H.Grad [30] the expansions in the Knudsen number or its inverse are singular and hence singular perturbation methods must be introduced in order to remove the singularities.

Let us consider now the first approach which has been successful in the case of the linearized Boltzmann equation. Systematic, accurate, and relatively simple methods of solution can be constructed for linearized transition flows. These methods are based on variational techniques and the method of elementary solutions.

The variational technique is based on the existence of a variational principle that is characteristic of the equation to be solved. The use of kinetic models in the form of integral equations leads to lengthy calculations even for very simple trial functions, but the results are very rewarding even if the guess is a poor one. The method has been developed and used extensively by Cercignani [5], and a number of heat transfer [31] and flow problems

[32,33,34,35] have been solved with great accuracy by using the BGK model. Loyalka [36,37] extended Cercignani's work by solving the thermal creep problem and providing more accurate results to the aforementioned problems. The same procedure can be applied to more complicated problems and models more general than the BGK [38,39,40,41]. The method appears to be more useful for evaluating integrated quantities when computation of the flow field is not required. Variational methods have been widely applied also to problems of neutron transport theory. There, of course the equation is linear and the method works quite well, although the choice of the trial functions is not a trivial one.

In 1960, Case [3] presented an elegant analytical technique providing rigorous solutions to the one-speed steady state neutron transport equation. The new approach was germinated when Van Kampen [42], studying stationary waves in plasmas, used an idea of Dirac [43] to propose solutions of a functional equation in the form of distributions or generalized functions. Case's method also utilized the classical theory of linear analysis by expressing the solution as a superposition of a set of normal modes and thus this method has come to be known as the normal-mode-expansion technique. The method is also known as the method of elementary solutions since the first step is to construct, using separation of variables, a

complete set of elementary solutions. Case's work was extended rapidly by other investigators to achieve rigorous analytical solutions to more complicated models in radiative transfer and neutron transport theory.

Cercignani [44] realized first that the method can be applied to other equations related to the neutron transport equation. Since the method cannot be applied directly to the Boltzmann equation or its linearized form he used the linearized BGK model to derive a complete set of elementary solutions. To achieve that he decomposed the linearized equation into a coupled pair of integro-differential equations and three uncoupled equations. Cercignani has solved the uncoupled equations, which are related to shear effects, by the normal mode expansion technique. He produced accurate results for the Kramers [45], the Couette flow [46] and the Poiseuille flow [47] problems in plane geometry, all of which are basic problems in the kinetic theory of gases. Ferziger [48], using methods developed for treating neutron transport problems in cylindrical geometry [49], obtained analytical expressions in the near-free-molecular and near-continuum regimes, and Loyalka [50] extended this work to the thermal transpiration problem in cylindrical geometry.

Kriese, et al. [51] employed the method of elementary solutions to solve the coupled integro-differential equations sufficient for determining temperature and density

effects. Kriese, et al. proved completeness and orthogonality of the singular eigenfunctions in the half and full range, and their work makes feasible highly accurate solutions involving heat transfer effects. It might also be mentioned that the fully-coupled kinetic equations have been approached via transform techniques of the Wiener-Hopf type by Pao [84]; however his results are not considered definitive for reasons given in [52].

Applying the half range analysis by Kriese, et al., Siewert and Thomas [52] solved with great precision a number of basic problems in kinetic theory. In particular they solved the temperature jump problem [53], the heat transfer problem between parallel plates [54,55], the weak and strong evaporation problem in a half space [56,57,58] and also the inverse temperature gradient problem in kinetic theory of evaporation [59], providing for the first time exact numerical results to five or six significant figures. Inspite of the work of Siewert and Thomas, who considered only temperature and density effects, in general the problem of determining the expansion coefficients is cast into solving a regular Fredholm equation of the second kind. Since the kernel of such Fredholm equations, although bounded, turns out to be quite complicated, detailed solutions that could be considered numerically exact, especially when we consider shear effects, have not been available. Loyalka [60] tried with success a further

exploration of the numerical aspects of the method of elementary solutions. However in our opinion the ultimate tool for the full exploitation of the method of elementary solutions,the most elegant of solutions, is provided by the recently introduced F_N method.

The F_N method introduced by Siewert, et al. [7,8] is an outgrowth of the C_N method. The C_N method of solving the transport equation has been developed at Saclay in France by Kavenoky and Benoist [61,62]. Its main advantage compared with the Carlson S_N method [63] and the collision probability method [64] is that the computing time is independent of the size of the medium considered. Similar with the C_N method the F_N method is based on a lemma proved by Placzek [65]. The Placzek lemma is used to establish a system of singular integral equations and constraints that is solved uniquely for a half-space or a finite medium to yield the exact exit distributions. These singular integral equations and constraints are also used to develop a new approximation, the F_N method, that turns out to yield surprisingly concise and accurate results. The method was used extensively by Siewert and his co-workers to solve both multi-region [66,67] and multigroup [68,69,70] problems in neutron transport theory, although the multigroup problems have been limited to down-scattering only. Very recently the method was used by Thomas and Siewert [71,72] for neutron transport calculations in cylindrical geometry to

clarify initial uncertainties about extension of the F_N method in cylindrical geometry. At the same time the method was applied for solving accurately problems in radiative transfer in plane and spherical geometry [73,74,75,76,77]. The complete solution for radiative transfer problems with reflecting boundaries and internal sources has been established [78] and also concise and accurate solutions have been developed [79] for computing the X and Y functions introduced by Chandrasekhar to solve the standard problem in radiative transfer. The only applications in kinetic theory have been to the problems of plane Poiseuille flow [80] and strong evaporation in a half space [81,82]. Of these only one [82] involved the fully coupled kinetic equations which arise from the linear BGK model equation for a gas with three degrees of freedom.

It is hoped that the present work establishes the formulation of the F_N method in kinetic theory and amplifies the horizons for future applications of the method to more complicated problems.

3. FORMULATION OF THE F_N METHOD IN KINETIC THEORY AND RAREFIED GAS DYNAMICS.

3.1 Introduction

The F_N method, as was mentioned earlier, has been introduced recently by Siewert, et al. [7,8] as a modified version of the C_N method which has been proved to be an accurate and economical method of solving problems in neutron transport theory. The F_N method yields more concise equations that can be solved numerically more efficiently and thus has been extensively used in the field of transport theory and radiative transfer. The method can be summarized in the following way. Using the tractable full-range orthogonality theorem developed by Kriese, et al. [51] a system of singular integral equations for the distribution functions at the boundaries is established. The exit distribution functions are eliminated using the boundary conditions and the appropriate constraints. The incoming distributions are then approximated by a finite expansion in terms of a set of basis functions, and the coefficients of the expansion are found by requiring the set of the reduced algebraic equations to be satisfied at certain collocation points. In a similar way, as discussed later in section 3.4, approximating the distribution functions at each x and utilizing the established distributions at the boundaries we

develop an x-dependent approximate solution. As a result, position-dependent quantities follow immediately. In this chapter we restrict our formulation to plane geometry only since demonstration of the F_N method in cylindrical geometry requires different analysis, although the basic characteristics remain the same. A detailed description of the F_N method of solving cylindrical geometry boundary value problems is given in chapter 6.

3.2 General Analysis of the Fully-Coupled Kinetic Equations

Splitting of the one-dimensional linearized BGK equation [4] results in a system of two coupled equations which describe heat transfer (temperature-density) effects, two uncoupled equations which describe shear effects and a fifth one which is easily solved. The coupled equations, written in vector form in terms of nondimensional variables, are [52]:

$$\mu \frac{\partial}{\partial x} \underset{\sim}{\psi}(x,\mu) + \underset{\sim}{\psi}(x,\mu) = \frac{1}{\sqrt{\pi}} \underset{\sim}{Q}(\mu) \int_{-\infty}^{\infty} \underset{\sim}{\tilde{Q}}(\mu') \underset{\sim}{\psi}(x,\mu') e^{-\mu'^2} d\mu', \qquad (3.1)$$

where

$$\underset{\sim}{Q}(\mu) = \begin{vmatrix} \sqrt{\frac{2}{3}} \left(\mu^2 - \frac{1}{2}\right) & 1 \\ \sqrt{\frac{2}{3}} & 0 \end{vmatrix}, \qquad (3.1a)$$

x is the distance from the origin measured in units of the

mean free path, μ the nondimensional velocity in the x-direction, and the components of

$$\underset{\sim}{\psi}(x,\mu) = \begin{vmatrix} \psi_1(x,\mu) \\ \psi_2(x,\mu) \end{vmatrix} \tag{3.1b}$$

are simply related to perturbations in the number density and temperature of the gas, respectively. A superscript tilde indicates the transpose operation.

The general solution of equation (3.1) is presented by Kriese, et al. [51] as:

$$\underset{\sim}{\psi}(x,\mu) = \sum_{\alpha=1}^{2} A_\alpha \, \underset{\sim}{\phi}_\alpha(\mu) + \sum_{\alpha=3}^{4} A_\alpha \, \underset{\sim}{\psi}_\alpha(x,\mu)$$

$$+ \sum_{\alpha=1}^{2} \int_{-\infty}^{\infty} A_\alpha(\eta) \, \underset{\sim}{\phi}_\alpha(\eta,\mu) \, e^{-\frac{x}{\eta}} \, d\eta \quad . \tag{3.2}$$

The elementary solutions consist of the four discrete eigenvectors

$$\underset{\sim}{\phi}_\alpha(\mu) = \underset{\sim}{Q}(\mu) \begin{vmatrix} \delta_{1\alpha} \\ \delta_{2\alpha} \end{vmatrix} , \quad \alpha = 1,2 \quad , \tag{3.3}$$

$$\underset{\sim}{\psi}_\alpha(x,\mu) = (\mu - x) \, \underset{\sim}{\phi}_{\alpha-2}(\mu) \quad , \quad \alpha = 3,4 \quad , \tag{3.4}$$

and the pair of degenerate continuum eigenvectors

$$\underset{\sim}{\phi}_1(\eta,\mu) = \begin{vmatrix} \frac{\eta}{\sqrt{\pi}}\left(\mu^2 - \frac{1}{2}\right) P\left(\frac{1}{\eta-\mu}\right) e^{-\eta^2} + \lambda_1(\eta) \, \delta(\eta-\mu) \\ \frac{\eta}{\sqrt{\pi}} P\left(\frac{1}{\eta-\mu}\right) e^{-\eta^2} + \left[\frac{1}{2} + \lambda_o(\eta)\right] \delta(\eta-\mu) \end{vmatrix} \tag{3.5}$$

and

$$\underset{\sim}{\phi}_2(\eta,\mu) = \begin{vmatrix} \frac{\eta}{\sqrt{\pi}} P\left(\frac{1}{\eta-\mu}\right) e^{-\eta^2} + \lambda_o(\eta)\ \delta(\eta-\mu) \\ \\ \frac{1}{2}\ \delta(\eta-\mu) \end{vmatrix} \quad , \tag{3.6}$$

where

$$\lambda_o(\eta) = 1 + \frac{\eta}{\sqrt{\pi}} P \int_{-\infty}^{\infty} e^{-\mu^2} \frac{d\mu}{\mu-\eta} \quad , \tag{3.7}$$

and

$$\lambda_1(\eta) = \frac{1}{2} + \left(\eta^2 - \frac{1}{2}\right) \lambda_o(\eta) \quad . \tag{3.8}$$

Having established the elementary solutions, the expansion coefficients A_α and $A_\alpha(\eta)$ are to be determined once the boundary conditions of a particular problem are specified.

Completeness and orthogonality theorems for the full range ($-\infty<\mu<\infty$) and the half range ($0<\mu<\infty$) are also presented by Kriese, et al. It is the full range results which are needed for the present work. In particular it is found that linear combinations of $\underset{\sim}{\phi}_\alpha(\mu)$, $\alpha=1,2$, $\underset{\sim}{\phi}_\alpha(\mu)=\underset{\sim}{\psi}_\alpha(0,\mu)$, $\alpha=3,4$ and $\underset{\sim}{\phi}_\alpha(\eta,\mu)$, $\alpha=1,2$ form a complete set of functions orthogonal on the full range. The orthonormal full range adjoint set can be written explicitly as [51]

$$\underset{\sim}{X}_1(\mu) = \frac{1}{5\sqrt{\pi}} \left[6\ \underset{\sim}{\phi}_3(\mu) - 2\sqrt{6}\ \underset{\sim}{\phi}_4(\mu)\right] \quad , \tag{3.9}$$

$$\underset{\sim}{X}_2(\mu) = \frac{1}{5\sqrt{\pi}} \left[-2\sqrt{6}\ \underset{\sim}{\phi}_3(\mu) + 14\ \underset{\sim}{\phi}_4(\mu)\right] \quad , \tag{3.10}$$

$$\underset{\sim}{X}_3(\mu) = \frac{1}{5\sqrt{\pi}} \left[6\ \underset{\sim}{\phi}_1(\mu) - 2\sqrt{6}\ \underset{\sim}{\phi}_2(\mu)\right] \quad , \tag{3.11}$$

$$\underset{\sim}{X}_4(\mu) = \frac{1}{5\sqrt{\pi}} \left[-2\sqrt{6}\ \underset{\sim}{\phi}_1(\mu) + 14\ \underset{\sim}{\phi}_2(\mu)\right] \quad , \tag{3.12}$$

$$\underset{\sim}{X}_1(\eta,\mu) = \frac{1}{N(\eta)} \left[N_{11}(\eta)\ \underset{\sim}{\phi}_2(\eta,\mu) - N_{12}(\eta)\ \underset{\sim}{\phi}_1(\eta,\mu)\right] \quad , \tag{3.13}$$

and

$$\underset{\sim}{X}_2(\eta,\mu) = \frac{1}{N(\eta)} \left[N_{11}(\eta)\ \phi_2(\eta,\mu) - N_{12}(\eta)\ \phi_1(\eta,\mu)\right] \quad , \tag{3.14}$$

where

$$N_{11}(\eta) = \left[\lambda_o(\eta) + \frac{1}{2}\right]^2 + \lambda_1^2(\eta) + \pi\eta^2 \left[\left[\left(\eta^2 - \frac{1}{2}\right)^2 + 1\right] e^{-2\eta^2}\right. \quad , \tag{3.15}$$

$$N_{12}(\eta) = \lambda_o(\eta)\cdot\lambda_1(\eta) + \frac{1}{2}\lambda_o(\eta) + \frac{1}{4} + \pi\eta^2\left(\eta^2 - \frac{1}{2}\right) e^{-2\eta^2} \tag{3.16}$$

$$N_{22}(\eta) = \lambda_o^2(\eta) + \frac{1}{4} + \pi\eta^2\ e^{-2\eta^2} \quad , \tag{3.17}$$

and

$$N(\eta) = \left[N_{11}(\eta)\ N_{22}(\eta) - N_{12}^2(\eta)\right] \eta e^{-2\eta^2} \quad . \tag{3.18}$$

The required orthogonality relations among the full-range basis and adjoint sets are [51]:

$$\int_{-\infty}^{\infty} \underset{\sim}{\tilde{X}}_\alpha(\mu)\ \underset{\sim}{\phi}_\beta(\mu)\ e^{-\mu^2}\ \mu d\mu = \delta_{\alpha,\beta} \quad , \quad \alpha,\beta = 1,2,3,4 \quad , \tag{3.19}$$

$$\int_{-\infty}^{\infty} \tilde{\underset{\sim}{X}}_{\alpha}(\mu)\, \underset{\sim}{\phi}_{\beta}(\eta,\mu)\, e^{-\mu^2}\, \mu d\mu = 0 \quad , \quad \alpha = 1,2,3,4,\ \beta = 1,2 \quad , \qquad (3.20)$$

$$\int_{-\infty}^{\infty} \tilde{\underset{\sim}{X}}_{\alpha}(\eta',\mu)\, \underset{\sim}{\phi}_{\beta}(\eta,\mu)\, e^{-\mu^2}\, \mu d\mu = \delta(\eta-\eta')\, \delta_{\alpha,\beta} \quad , \quad \alpha,\beta = 1,2 \quad , \qquad (3.21)$$

$$\int_{-\infty}^{\infty} \tilde{\underset{\sim}{X}}_{\alpha}(\eta',\mu)\, \underset{\sim}{\phi}_{\beta}(\mu)\, e^{-\mu^2}\, \mu d\mu = 0 \quad , \quad \alpha = 1,2,\ \beta = 1,2,3,4 \quad . \qquad (3.22)$$

We note that exact analysis based on the method of elementary solutions, utilizing the half range orthogonality theorem, has been developed in order to solve the fully-coupled kinetic equations. In principle these equations could be solved numerically to yield the desired solution. In the present work we rely on the full-range orthogonality to develop an approximate solution. It is this reliance on the full-range orthogonality alone which makes the F_N method promising for application to many difficult boundary value problems.

3.3 The F_N Method for Half Space and Finite Media Applications

Using the full range orthogonality relations (3.19-3.22) and the general solution given by (3.2) all the expansion coefficients may be expressed immediately in terms of inner products:

$$A_\alpha = \int_{-\infty}^{\infty} \tilde{\underset{\sim}{X}}_\alpha(\mu)\ \underset{\sim}{\psi}(0,\mu)\ \mu e^{-\mu^2}\ d\mu \quad , \qquad \alpha = 1,2,3,4 \quad , \tag{3.23}$$

$$A_\alpha(\eta) = \int_{-\infty}^{\infty} \tilde{\underset{\sim}{X}}_\alpha(\eta,\mu)\ \underset{\sim}{\psi}(0,\mu)\ \mu e^{-\mu^2}\ d\mu \quad , \qquad \alpha = 1,2 \quad , \tag{3.24}$$

and

$$A_\alpha(-\eta) = \int_{-\infty}^{\infty} \tilde{\underset{\sim}{X}}\ (-\eta,\mu)\ \underset{\sim}{\psi}(0,\mu)\ \mu e^{-\mu^2}\ d\mu \quad , \qquad \alpha = 1,2 \quad , \tag{3.25}$$

where

$$\underset{\sim}{\psi}(0,\mu) = \sum_{\alpha=1}^{4} A_\alpha\ \underset{\sim}{\phi}_\alpha(\mu) + \sum_{\alpha=1}^{2} \int_{-\infty}^{\infty} A_\alpha(\eta)\ \underset{\sim}{\phi}_\alpha(\eta,\mu)\ d\eta \quad . \tag{3.26}$$

A similar set of expressions can be established at any physical boundary where the behavior of the gas is described by a rarefied Knudsen layer. At $x=\delta$ we obtain:

$$A_\alpha - \delta\ A_{\alpha+2} = \int_{-\infty}^{\infty} \tilde{\underset{\sim}{X}}_\alpha(\mu)\ \underset{\sim}{\psi}(\delta,\mu)\ \mu e^{-\mu^2}\ d\mu \quad , \qquad \alpha = 1,2 \quad , \tag{3.27}$$

$$A_\alpha = \int_{-\infty}^{\infty} \tilde{\underset{\sim}{X}}_\alpha(\mu)\ \underset{\sim}{\psi}(\delta,\mu)\ \mu e^{-\mu^2}\ d\mu \quad , \qquad \alpha = 3,4 \quad , \tag{3.28}$$

$$A_\alpha(\eta) = e^{\frac{\delta}{\eta}} \int_{-\infty}^{\infty} \tilde{\underset{\sim}{X}}_\alpha(\eta,\mu)\ \underset{\sim}{\psi}(\delta,\mu)\ \mu e^{-\mu^2}\ d\mu \quad , \qquad \alpha = 1,2 \quad , \tag{3.29}$$

and

$$A_\alpha(-\eta) = e^{-\frac{\delta}{\eta}} \int_{-\infty}^{\infty} \tilde{\underset{\sim}{X}}_\alpha(-\eta,\mu)\ \underset{\sim}{\psi}(\delta,\mu)\ \mu e^{-\mu^2}\ d\mu \quad , \qquad \alpha = 1,2 \quad , \tag{3.30}$$

where

$$\underset{\sim}{\psi}(\delta,\mu) = \sum_{\alpha=1}^{2} A_\alpha \, \underset{\sim}{\phi}_\alpha(\mu) + \sum_{\alpha=3}^{4} (\mu-\delta) \, \underset{\sim}{\phi}_{\alpha-2} \, A_\alpha$$

$$+ \sum_{\alpha=1}^{2} \int_{-\infty}^{\infty} A_\alpha(\eta) \, \underset{\sim}{\phi}_\alpha(\eta,\mu) \, e^{-\frac{\delta}{\eta}} \, d\eta \quad , \tag{3.31}$$

represents the general solution at the second boundary.

Having established the above formulation we note that the number of derived expressions for A_α $\alpha=1,2,3,4$, $A_\alpha(\eta)$ and $A_\alpha(-\eta)$, $\alpha=1,2$, is in general twice the number of the expansion coefficients to be determined. In particular for the finite media applications the presence of a second Knudsen layer yields a second set of equations (3.27-3.30) similar to (3.23-3.25), while for the semi-infinite medium problems half of the expansion coefficients are easily defined to satisfy the equilibrium conditions at infinity. This basic characteristic allows elimination of the expansion coefficients by simple algebraic operations. The resulting expressions clearly represent a system of singular integral equations; after applying the boundary conditions they can be regularized to give a system of Fredholm equations for the unknown distribution. However, rather than purse the exact analysis developed by Kriese, et al., we wish to invoke the F_N approximation.

The F_N approximation consists of a finite expansion in basis functions while the unknown coefficients of the expansion are found by solving the derived system of

algebraic equations. The type of the basis functions differs for each particular problem and depends on the geometry and the physics of the problem. It is important that the behavior of the basis functions describe as closely as possible the approximated distribution function. A closed form expression for the unknown distribution is sometimes essential in order to choose the correct set of basis functions. It turns out that half-space problems require an approximate solution in the form $1/(\nu_\alpha+\mu)$ while for finite geometries the simpler basis functions μ^α are adequate. Minor modifications of the proposed basis functions may be appropriate for each particular problem in order to have a valid solution through the range of Knudsen number. The number of the required F_N approximations should match the number of physical boundaries of the problem. Generally speaking, half space problems require one approximation while slab problems require two F_N approximations.

Substitution of the F_N approximation and evaluation of the singular integral equations at certain collocation points results in a set of linear algebraic equations which can be solved straightforwardly using standard techniques. Of course, the manner in which these points are chosen can affect the accuracy of the method. Some preliminary work shows that the best values of the collocation points are usually the zeros of the Hermite or Chebyshev polynomials.

It is evident that with increasing the order of the approximation, convergence of the solution is essential and the only justification of the correctness and accuracy of the results. Estimation of the coefficients of the expansion leads to evaluation of overall quantities like flow rate and heat flux or slip conditions on the wall in terms of surface quantities only.

3.4 Position-Dependent Approximate Solution

Once the F_N expansion coefficients are computed, the expansion coefficients A_α $\alpha=1,2,3,4$, $A_\alpha(\eta)$ and $A_\alpha(-\eta)$ are available from the aforementioned full range orthogonality expressions. This leads immediately, through (3.2),

$$N(x) = C_1 \left| \begin{matrix} 1 \\ 0 \end{matrix} \right|^T \int_{-\infty}^{\infty} \underset{\sim}{\psi}(x,\mu)\, e^{-\mu^2}\, d\mu \quad , \tag{3.32}$$

and

$$T(x) = C_2 \int_{-\infty}^{\infty} \left| \begin{matrix} \mu^2 - \frac{1}{2} \\ 1 \end{matrix} \right|^T \underset{\sim}{\psi}(x,\mu)\, e^{-\mu^2}\, d\mu \quad , \tag{3.33}$$

where C_1, C_2 are constants depending on each particular problem, to expressions for the density and temperature.

However a different approach can be used to give the profiles directly as well as the reduced molecular distribution function. The equations (3.27-3.30) are a

special case of the more general singular integral equations

$$A_\alpha - x\, A_{\alpha+2} = \int_{-\infty}^{\infty} \tilde{\underset{\sim}{X}}_\alpha(\mu)\, \underset{\sim}{\psi}(x,\mu)\, \mu e^{-\mu^2}\, d\mu \quad , \quad \alpha = 1,2 \quad , \tag{3.34}$$

$$A_\alpha = \int_{-\infty}^{\infty} \tilde{\underset{\sim}{X}}_\alpha(\mu)\, \underset{\sim}{\psi}(x,\mu)\, \mu e^{-\mu^2}\, d\mu \quad , \quad \alpha = 3,4 \quad , \tag{3.35}$$

$$A_\alpha(\eta) = e^{\frac{x}{\eta}} \int_{-\infty}^{\infty} \tilde{\underset{\sim}{X}}_\alpha(\eta,\mu)\, \underset{\sim}{\psi}(x,\mu)\, \mu e^{-\mu^2}\, d\mu \quad , \quad \alpha = 1,2 \quad , \tag{3.36}$$

and

$$A_\alpha(-\eta) = e^{-\frac{x}{\eta}} \int_{-\infty}^{\infty} \tilde{\underset{\sim}{X}}_\alpha(-\eta,\mu)\, \underset{\sim}{\psi}(x,\mu)\, \mu e^{-\mu^2}\, d\mu \quad , \quad \alpha = 1,2 \quad . \tag{3.37}$$

Eliminating the expansion coefficients between (3.23-3.25) and((3.34-3.37) by simple algebraic operations, and having established the distributions at the boundaries, the unknown distribution functions at each x are approximated in a similar manner used in introducing the F_N approximation at the boundaries. We then evaluate the integral equations at the same collocation points and solve the system of linear algebraic equations for any selected value of $x>0$ to establish the coefficients of the expansion which, in correlation with the basis functions, represent directly the approximated distribution function at each x. This approach allows us to calculate directly the reduced distribution function and as a result the temperature and

density profiles follow immediately, through (3.32) and (3.33) in addition to any desired quantity of the problem.

4. EVAPORATION AND HEAT TRANSFER INTO A HALF SPACE

4.1 Introduction

The problem of weak evaporation of a pure substance from an interface and the problem of heat conduction in a gas adjacent to a solid wall are studied on the basis of the linearized BGK equation and purely diffuse reflection at the surface. We consider the linearized problems [82,83,84,85,56,57] for which mathematical theory exists and the solutions are uniquely determined. Pao [82,83] formulated the two problems into the same pair of Wiener-Hopf equations and reported exact values for the microscopic temperature and density jumps. Thomas and Siewert [56] solved these two problems by the method of elementary solutions to establish the complete temperature and density profiles, correcting the earlier results of Pao [83].

Here we wish to solve the two half space problems using the F_N method in order to check and demonstrate the efficiency of this method for providing solutions of benchmark accuracy to kinetic theory problems. Siewert and Thomas [58] have also tried to approach the strong evaporation problem, which is basically a non-linear problem [87,88,89,90,91], through linear analysis simply by linearizing the distribution function about a downstream

Maxwellian distribution. During the course of this work the F_N method [81,58] had been used successfully to reproduce the exact results obtained by the method of elementary solutions.

For the evaporation problem we consider a gas evaporating at the plane x=0 into a vacuum which occupies the region x>0. We assume that the liquid-vapor interface in maintained at x=0 and the condensed phase in the space x<0 is kept at a constant temperature. The vapor occupies the half space x>0 and as a result of the evaporation process there is a flow of mass and energy in the x-direction in the vapor. Following the formulation by Thomas [52] the state of the gas is described by the linearized BGK model,

$$c_x \frac{\partial}{\partial x} f(x,\underset{\sim}{c}) + f(x,\underset{\sim}{c}) = \frac{1}{\pi^{3/2}} [N(x) + (c^2 - \frac{3}{2}) T(x) + 2 c_x V(x)] \quad , \qquad (4.1)$$

where the perturbed density N(x), temperature T(x), and mass flow rate V(x) are given by

$$N(x) = \int_{-\infty}^{\infty} f(x,\underset{\sim}{c})\, e^{-c^2}\, d^3c \quad , \qquad (4.2a)$$

$$T(x) = \frac{2}{3} \int_{-\infty}^{\infty} f(x,\underset{\sim}{c})\, (c^2 - \frac{3}{2})\, e^{-c^2}\, d^3c \quad , \qquad (4.2b)$$

and

$$V(x) = \int_{-\infty}^{\infty} f(x,\underset{\sim}{c})\, c_x\, e^{-c^2}\, d^3c \quad . \tag{4.2c}$$

Here f(x,c) is the perturbation of the particle distribution function in terms of which the boundary condition at x=0 becomes

$$f(0,\underset{\sim}{c}) = 0 \quad , \quad \text{for } c_x > 0 \tag{4.3a}$$

since we assume no specular reflection, and the physical constraints at infinity can be written as

$$\lim_{x\to\infty} \frac{d}{dx} N(x) = \lim_{x\to\infty} \frac{d}{dx} T(x) = 0 \quad . \tag{4.3b}$$

By integrating (4.1) with the weight factor $\exp(-c^2)$, we have the result that V(x) is a constant, say V. If now we introduce a new function h(x,c) as

$$h(x,\underset{\sim}{c}) = f(x,\underset{\sim}{c}) - \frac{2}{\pi^{3/2}} V \tag{4.4}$$

equation (4.1) may be written as

$$c_x \frac{\partial}{\partial x} h(x,\underset{\sim}{c}) + h(x,\underset{\sim}{c}) = \frac{1}{\pi^{3/2}} [N(x) + (c^2 - \tfrac{3}{2})\, T(x)] \quad . \tag{4.5}$$

Since we are concerned here only with density and temperature effects we choose to decompose equation (4.5) in the manner suggested by Cercignani [44] to obtain

$$\mu \frac{\partial}{\partial x} \underset{\sim}{\psi}(x,\mu) + \underset{\sim}{\psi}(x,\mu) = \frac{1}{\sqrt{\pi}} \underset{\sim}{Q}(\mu) \int_{-\infty}^{\infty} \tilde{\underset{\sim}{Q}}(\mu) \underset{\sim}{\psi}(x,\mu') e^{-\mu'^2} d\mu \quad , \tag{4.6}$$

where $\underset{\sim}{Q}(\mu)$ is defined by equation (3.1a) and the density and temperature profiles follow from the two-vector $\underset{\sim}{\psi}(x,\mu)$ by

$$N(x) = \sqrt{\pi} \begin{vmatrix} 1 \\ 0 \end{vmatrix}^T \int_{-\infty}^{\infty} \underset{\sim}{\psi}(x,\mu) e^{-\mu^2} d\mu \quad , \tag{4.7}$$

and

$$T(x) = \frac{2}{3} \sqrt{\pi} \int_{-\infty}^{\infty} \begin{vmatrix} \mu^2 - \frac{1}{2} \\ 1 \end{vmatrix} \underset{\sim}{\psi}(x,\mu) e^{-\mu^2} d\mu \quad . \tag{4.8}$$

After the splitting of equation (4.5) the boundary conditions at x=0 and infinity become

$$\underset{\sim}{\psi}(0,\mu) = - \frac{2V}{\pi} \mu \begin{vmatrix} 1 \\ 0 \end{vmatrix} \quad , \tag{4.9a}$$

$$\lim_{x\to\infty} \frac{d}{dx} \begin{vmatrix} 1 \\ 0 \end{vmatrix}^T \int_{-\infty}^{\infty} \underset{\sim}{\psi}(x,\mu) e^{-\mu^2} d\mu = 0 \quad , \tag{4.9b}$$

and

$$\lim_{x\to\infty} \int_{-\infty}^{\infty} \begin{vmatrix} \mu^2 - \frac{1}{2} \\ 1 \end{vmatrix}^T \underset{\sim}{\psi}(x,\mu) e^{-\mu^2} d\mu = 0 \quad . \tag{4.9c}$$

Next we consider the heat conduction problem for which a gas in the half-space x>0 is in contact with a solid wall

of a different temperature at x=0. There is an energy flow in the x-direction in the form of heat conduction while there can be no mass flow in the gas since no evaporation or condensation takes place, and thus V=0. For the heat transfer problem we seek a solution of the same integro-differential equation as (4.5) with the same boundary solution at x=0 as (4.3a). For the boundary condition at infinity we impose that

$$\lim_{x\to\infty} \frac{d}{dx} T(x) = - \lim_{x\to\infty} \frac{d}{dx} N(x) = 1 \quad . \tag{4.10}$$

Following the same procedure as for the evaporation problem by splitting equation (4.5) according to Cercignani [44], we seek a solution of equation (4.6) which satisfies the boundary conditions

$$\underset{\sim}{\psi}(0,\mu) = 0 \quad , \tag{4.11a}$$

$$\lim_{x\to\infty} \frac{d}{dx} \sqrt{\pi} \begin{vmatrix} 1 \\ 0 \end{vmatrix}^T \int_{-\infty}^{\infty} \underset{\sim}{\psi}(x,\mu)\, e^{-\mu^2}\, d\mu = -1 \quad , \tag{4.11b}$$

and

$$\lim_{x\to\infty} \frac{d}{dx} \frac{2}{3} \sqrt{\pi} \int_{-\infty}^{\infty} \begin{vmatrix} \mu^2 - \frac{1}{2} \\ 1 \end{vmatrix}^T \underset{\sim}{\psi}(x,\mu)\, e^{-\mu^2}\, d\mu = 1 \quad . \tag{4.11c}$$

After deriving the elementary solutions $\underset{\sim}{\phi}_{\alpha}(\mu)$, $\underset{\sim}{\psi}_{\alpha}(x,\mu)$, and $\underset{\sim}{\phi}_{\alpha}(\eta,\mu)$ which are given explicitly in section 3.2, Kriese,

et al. [51] have given the general solution of equation (4.6) in the form

$$\underset{\sim}{\psi}(x,\mu) = \sum_{\alpha=1}^{2} A_\alpha \phi_\alpha(\mu) + \sum_{\alpha=3}^{4} A_\alpha \psi_\alpha(x,\mu) + \sum_{\alpha=1}^{2} \int_{-\infty}^{\infty} A_\alpha(\eta) \phi_\alpha(\eta,\mu) e^{-\frac{x}{\eta}} d\eta \quad , \tag{4.12}$$

where the A_α and $A_\alpha(\eta)$ are arbitrary coefficients to be determined by the boundary conditions.

Clearly once $\underset{\sim}{\psi}(x,\mu)$ is established for each particular problem the density and temperature jumps (microscopic and macroscopic) follow immediately from the definitions [83]

$$\begin{aligned} &\lim_{x\to\infty} N(x) = -2V c_1 \quad , \quad \lim_{x\to\infty} T(x) = -2V d_1 \quad , \\ &N(0) = -2V \gamma_1 \quad , \quad T(0) = -2V \delta_1 \end{aligned} \tag{4.13}$$

for the evaporation problem, and

$$\begin{aligned} &\lim_{x\to\infty} [N(x) + x] = -c_2 \quad , \quad \lim_{x\to\infty} [T(x) - x] = d_2 \quad , \\ &N(0) = -\gamma_2 \quad , \quad T(0) = \delta_2 \end{aligned} \tag{4.14}$$

for the heat transfer problem.

4.2 Basic Analysis of the Evaporation Problem

Equations (4.9) and (4.12) with V given constitute the mathematical formulation of the linearized evaporation

problem. It can easily be determined that $\underset{\sim}{\psi}(x,\mu)$ will satisfy the conditions (4.9b) and (4.9c) if we take $A_3=A_4=0$, and $A_\alpha(\eta)=0$, $\eta<0$, $\alpha=1,2$. Evaluating the resulting solution at x=0 we have

$$\underset{\sim}{\psi}(0,\mu) = \sum_{\alpha=1}^{2} A_\alpha \underset{\sim}{\phi}_\alpha(\mu) + \sum_{\alpha=1}^{2} \int_0^\infty A_\alpha(\eta)\, \underset{\sim}{\phi}_\alpha(\eta,\mu)\, d\eta \quad , \quad \mu > 0 \tag{4.15}$$

and

$$\underset{\sim}{\psi}(0,-\mu) = \sum_{\alpha=1}^{2} A_\alpha \underset{\sim}{\phi}_\alpha(-\mu) + \sum_{\alpha=1}^{2} \int_0^\infty A_\alpha(\eta)\, \underset{\sim}{\phi}_\alpha(\eta,-\mu)\, d\eta \quad , \quad \mu > 0 \, . \tag{4.16}$$

Using the full range orthogonality relations of Kriese, Chang and Siewert [51], we obtain the singular equations

$$\int_{-\infty}^{\infty} \underset{\sim}{\tilde{X}}_b(\mu)\, \underset{\sim}{\psi}(0,\mu)\, \mu e^{-\mu^2}\, d\mu = 0 \quad , \quad b = 3,4 \quad , \tag{4.17}$$

$$\int_{-\infty}^{\infty} \underset{\sim}{\tilde{X}}_b(-\eta,\mu)\, \underset{\sim}{\psi}(0,\mu)\, \mu e^{-\mu^2}\, d\mu = 0 \quad , \quad b = 1,2 \quad , \tag{4.18}$$

$$\int_{-\infty}^{\infty} \underset{\sim}{\tilde{X}}_b(\mu)\, \psi(0,\mu)\, \mu e^{-\mu^2}\, d\mu = A_b \quad , \quad b = 1,2 \quad , \tag{4.19}$$

and

$$\int_{-\infty}^{\infty} \underset{\sim}{\tilde{X}}_b(\eta,\mu)\, \psi(0,\mu)\, \mu e^{-\mu^2}\, d\mu = A_b(\eta) \quad , \quad b = 1,2 \quad , \tag{4.20}$$

where the eigenvectors $\underset{\sim}{X}_b(\mu)$ and $\underset{\sim}{X}_b(\eta,\mu)$ are given explicitly in section 3.2. Entering equations (3.3), (3.5), and (3.6) into equation (4.16), as is discussed in section

9.1 of the appendices, we approximate the distribution function approaching the interface as

$$\underset{\sim}{\psi}(0,-\mu) = \underset{\sim}{Q}(\mu) \left\{ \begin{bmatrix} A_1 \\ A_2 \end{bmatrix} + \frac{1}{\sqrt{\pi}} \sum_{\alpha=1}^{\infty} \begin{bmatrix} \sqrt{\frac{3}{2}}\, A_1(\eta_\alpha) \\ A_2(\eta_\alpha) \end{bmatrix} \frac{\eta_\alpha}{\eta_\alpha+\mu} e^{-\eta_\alpha^2} \right\} ,$$

$$\mu > 0 \quad . \tag{4.21}$$

Since $\underset{\sim}{\psi}(0,\mu)$ is known for $\mu>0$ from the boundary condition (4.9a) we attempt, on the basis of the derived expression (4.21), an approximation

$$\underset{\sim}{\psi}(0,-\mu) = \underset{\sim}{Q}(\mu) \left[\underset{\sim}{C}_o + \sum_{\alpha=1}^{N} \frac{\underset{\sim}{C}_\alpha}{\nu_\alpha+\mu} \right] , \quad \mu > 0 \quad , \tag{4.22}$$

where $\underset{\sim}{Q}(\mu)$ is the same polynomial matrix used in equation (4.6), $\underset{\sim}{C}_\alpha$ are 2-vectors to be determined, the ν_α, $0<\nu_\alpha<\infty$ are chosen to be the positive zeros of the Hermite polynomial of degree 2N, and $1/(\nu_\alpha+\mu)$ are the basis functions. It is seen that an approximation of order N involves N+1 unknown vectors $\underset{\sim}{C}_\alpha$, or a total of 2N+2 unknowns. Substitution of the boundary condition (4.9a) and the approximation (4.22) into equations (4.17) and (4.18) yields the equations

$$\int_0^\infty \underset{\sim}{\tilde{X}}_b(-\mu)\, \underset{\sim}{Q}(\mu) \left[\underset{\sim}{C}_o + \sum_{\alpha=1}^{N} \frac{\underset{\sim}{C}_\alpha}{\nu_\alpha+\mu} \right] \mu e^{-\mu^2}\, d\mu$$

$$= -\frac{2V}{\pi} \int_0^\infty \underset{\sim}{\tilde{X}}_b(-\eta,\mu)\, \mu^2\, e^{-\mu^2}\, d\mu \Bigg|_0^1 , \quad b = 3,4 \quad , \tag{4.23}$$

and

$$\int_{-\infty}^{\infty} \tilde{\underset{\sim}{X}}_b(-\eta,-\mu)\ \underset{\sim}{Q}(\mu) \left[\underset{\sim}{C}_o + \sum_{\alpha=1}^{N} \frac{\underset{\sim}{C}_\alpha}{\nu_\alpha+\mu}\right] \mu e^{-\mu^2}\, d\mu$$

$$= -\frac{2V}{\pi} \int_0^{\infty} \tilde{\underset{\sim}{X}}_b(-\eta,\mu)\ \mu^2 e^{-\mu^2}\, d\mu \left|\begin{matrix} 1 \\ 0 \end{matrix}\right| , \quad b = 1,2 \quad . \tag{4.24}$$

Most of the integrals which involve the discrete eigenvectors $\underset{\sim}{X}_b(\mu)$ can be evaluated analytically in terms of identities of the gamma functions. The resulting set of equations can be written as

$$\left|\begin{matrix} \frac{7}{2\sqrt{\pi}} \\ -\sqrt{\frac{3}{2\pi}} \end{matrix}\right|^T \underset{\sim}{C}_o + \sum_{\alpha=1}^{N} \tilde{\underset{\sim}{P}}_3(\nu_\alpha)\ \underset{\sim}{C}_\alpha = 0 \quad , \tag{4.25}$$

$$\left|\begin{matrix} -\sqrt{\frac{3}{2\pi}} \\ \frac{6}{\sqrt{\pi}} \end{matrix}\right|^T \underset{\sim}{C}_o + \sum_{\alpha=1}^{N} \tilde{\underset{\sim}{P}}_4(\nu_\alpha)\ \underset{\sim}{C}_\alpha = -\frac{5V}{\pi} \quad , \tag{4.26}$$

$$\tilde{\underset{\sim}{R}}_b(\eta)\ \underset{\sim}{C}_o + \sum_{\alpha=1}^{N} \tilde{\underset{\sim}{R}}_b(\eta,\nu_\alpha)\ \underset{\sim}{C}_\alpha = -\frac{2V}{\pi}\, \tilde{\underset{\sim}{S}}_b(\eta) \left|\begin{matrix} 1 \\ 0 \end{matrix}\right| , \quad b = 1,2 \quad , \tag{4.27}$$

where

$$\tilde{\underset{\sim}{P}}_b(\nu_\alpha) = \int_0^{\infty} \tilde{\underset{\sim}{X}}_b(-\mu)\ \underset{\sim}{Q}(\mu)\ \mu e^{-\mu^2} \frac{d\mu}{\nu_\alpha+\mu} \quad , \quad b = 3,4 \quad , \tag{4.28}$$

$$\tilde{\underset{\sim}{R}}_b(\eta) = \int_0^{\infty} \tilde{\underset{\sim}{X}}_b(-\eta,-\mu)\ \underset{\sim}{Q}(\mu)\ \mu e^{-\mu^2}\, d\mu \quad , \quad b = 1,2 \quad , \tag{4.29}$$

$$\tilde{\underset{\sim}{R}}_b(\eta,\nu_\alpha) = \int_0^\infty \tilde{\underset{\sim}{X}}_b(-\eta,-\mu)\ \underset{\sim}{Q}(\mu)\cdot e^{-\mu^2}\ \frac{d\mu}{\nu_\alpha+\mu} \quad , \quad b = 1,2 \quad , \tag{4.30}$$

and

$$\tilde{\underset{\sim}{S}}_b(\eta) = \int_0^\infty \tilde{\underset{\sim}{X}}_b(-\eta,\mu)\ \mu^2 e^{-\mu^2}\ d\mu \quad , \quad b = 1,2 \quad . \tag{4.31}$$

The integrals in equation (4.28-4.31) can all be reduced, (see section 9.2), to combinations of the basic integral

$$I(\xi) = \int_0^\infty \frac{e^{-\mu^2}}{\mu+\xi}\ d\xi \quad ,$$

which we evaluate numerically using Gaussian quadrature. If we now evaluate equations (4.27) at N selected values of $\eta=\eta_j$, $j=1,2,\ldots N$, along with equations (4.25) and (4.26) then clearly we arrive at a system of 2N+2 linear algebraic equations for the 2N+2 unknowns $\{C_{1\alpha}\}$ and $\{C_{2\alpha}\}$ where $C_{1\alpha}$ and $C_{2\alpha}$ denote the elements of $\underset{\sim}{C}_\alpha$. This system can be solved straightforwardly using standard methods. Once these coefficients are computed the perturbed distribution function $\underset{\sim}{\psi}(0,\mu)$ for $-\infty<\mu<\infty$ can be established easily and the microscopic density and temperature jumps follow immediately from equations (4.7) and (4.8). For a complete solution of the problem the required expansion coefficients A_α and $A_\alpha(\eta)$, $\alpha=1,2$ used in equation (4.12) are available from the aforementioned full range orthogonality. If we substitute the boundary condition for $\mu>0$ and the F_N

approximation for $\mu<0$ in equations (4.19) and (4.20) we obtain

$$A_b = -\frac{2V}{\pi}\int_0^\infty \tilde{\underset{\sim}{X}}_b(\mu)\,\mu^2\,e^{-\mu^2}\,d\mu \,\Big|\begin{matrix}1\\0\end{matrix}\Big| - \int_0^\infty \tilde{\underset{\sim}{X}}_b(-\mu)\,\underset{\sim}{Q}(\mu)\left[\underset{\sim}{C}_o + \sum_{\alpha=1}^{N}\frac{\underset{\sim}{C}_\alpha}{\nu_\alpha+\mu}\right]\mu e^{-\mu^2}\,d\mu \quad , \quad b = 1,2 \quad , \tag{4.32}$$

and

$$A_b(\eta) = -\frac{2V}{\pi}\int_0^\infty \tilde{\underset{\sim}{X}}_b(\eta,\mu)\,\mu^2 e^{-\mu^2}\,d\mu \,\Big|\begin{matrix}1\\0\end{matrix}\Big| - \int_0^\infty \tilde{\underset{\sim}{X}}_b(\eta,-\mu)\,\underset{\sim}{Q}(\mu)\left[\underset{\sim}{C}_o + \sum_{\alpha=1}^{N}\frac{\underset{\sim}{C}_\alpha}{\nu_\alpha+\mu}\right]\mu e^{-\mu^2}\,d\mu \quad , \quad b = 1,2\,. \tag{4.33}$$

Since the F_N expansion coefficients are known, numerical computation of the integrals in equations (4.32) and (4.33) yields A_b and $A_b(\eta)$, b=1,2. Substituting equation (4.15) in equations (4.7) and (4.8) we find the following expressions for the density and temperature perturbations:

$$N(x) = \pi A_2 + \sqrt{\pi}\int_0^\infty A_2(\eta)\,e^{-\eta^2 - \frac{x}{\eta}}\,d\eta \tag{4.34}$$

$$T(x) = \pi\sqrt{\frac{2}{3}}\,A_1 + \sqrt{\pi}\int_0^\infty A_1(\eta)\,e^{-\eta^2 - \frac{x}{\eta}}\,d\eta \tag{4.35}$$

which lead immediately to values of the density and temperature profiles.

4.3 Basic Analysis of the Heat Transfer Problem

We define the heat transfer problem as the problem consisting of equations (4.11) and (4.12). In order to satisfy the boundary conditions (4.11b) and (4.11c) we must take

$$A_3 = -\sqrt{\frac{3}{2}}\,\pi^{-1} \quad , \quad A_4 = \pi^{-1}$$

and $A_\alpha(\eta)=0$, $\eta<0$, $\alpha=1,2$. Evaluating the resulting solution at $x=0$ we have

$$\underset{\sim}{\psi}(0,\mu) = \sum_{\alpha=1}^{2} A_\alpha \underset{\sim}{\phi}_\alpha(\mu) - \frac{1}{\pi}\sqrt{\frac{2}{3}}\,\mu\,\underset{\sim}{\phi}_1(\mu) + \frac{1}{\pi}\,\mu\,\underset{\sim}{\phi}_2(\mu)$$

$$+ \sum_{\alpha=1}^{2} \int_0^\infty A_\alpha(\eta)\,\underset{\sim}{\phi}_\alpha(\eta,\mu)\,d\eta \qquad (4.36)$$

and

$$\psi(0,-\mu) = \sum_{\alpha=1}^{2} A_\alpha \underset{\sim}{\phi}_\alpha(-\mu) + \frac{1}{\pi}\sqrt{\frac{2}{3}}\,\mu\,\underset{\sim}{\phi}_1(-\mu) - \frac{1}{\pi}\,\mu\,\underset{\sim}{\phi}_2(-\mu)$$

$$+ \sum_{\alpha=1}^{2} \int_0^\infty A_\alpha(\eta)\,\underset{\sim}{\phi}_\alpha(\eta,-\mu)\,d\eta \quad . \qquad (4.37)$$

For this case, full-range orthogonality applied to the general solution (4.36) yields the singular integral equations

$$\int_{-\infty}^{\infty} \underset{\sim}{\tilde{X}}_b(\mu)\,\underset{\sim}{\psi}(0,\mu)\,\mu e^{-\mu^2}\,d\mu = A_b \quad , \quad b = 3,4 \quad , \qquad (4.38)$$

$$\int_{-\infty}^{\infty} \tilde{\underset{\sim}{X}}_b(-\eta,\mu)\ \underset{\sim}{\psi}(0,\mu)\ \mu e^{-\mu^2}\ d\mu = 0 \quad , \quad b = 1,2 \quad , \tag{4.39}$$

$$\int_{-\infty}^{\infty} \tilde{\underset{\sim}{X}}_b(\mu)\ \underset{\sim}{\psi}(0,\mu)\ \mu e^{-\mu^2}\ d\mu = A_b \quad , \quad b = 1,2 \quad , \tag{4.40}$$

and

$$\int_{-\infty}^{\infty} \tilde{\underset{\sim}{X}}_b(\eta,\mu)\ \underset{\sim}{\psi}(0,\mu)\ \mu e^{-\mu^2}\ d\mu = A_b(\eta) \quad , \quad b = 1,2 \quad . \tag{4.41}$$

After we substitute the expressions for the discrete and continuum eigenvectors in equation (4.37), as is shown in section 9.1 of the appendices, the distribution function approaching the boundary can be written as

$$\underset{\sim}{\psi}(0,-\mu) = Q(\mu) \left\{ \begin{vmatrix} A_1 \\ A_2 \end{vmatrix} - \frac{\mu}{\pi} \begin{vmatrix} -\sqrt{\frac{3}{2}} \\ 1 \end{vmatrix} + \frac{1}{\sqrt{\pi}} \sum_{\alpha=1}^{\infty} \begin{vmatrix} \sqrt{\frac{3}{2}}\, A_1(\eta_\alpha) \\ A_2(\eta_\alpha) \end{vmatrix} \frac{\eta_\alpha}{\eta_\alpha+\mu} e^{-\eta_\alpha^2} \right\} . \tag{4.42}$$

Trying to describe as closely as possible the expression (4.42) we attempt an approximation in the form

$$\underset{\sim}{\psi}(0,-\mu) = \underset{\sim}{Q}(\mu) \left[\underset{\sim}{C}_o - \frac{\mu}{\pi} \begin{vmatrix} -\sqrt{\frac{3}{2}} \\ 1 \end{vmatrix} + \sum_{\alpha=1}^{N} \frac{\underset{\sim}{C}_\alpha}{\nu_\alpha+\mu} \right] . \tag{4.43}$$

Inserting this approximation and the boundary condition (4.11) into equations (4.38) and (4.39) we find the equations

$$\int_0^\infty \tilde{\underset{\sim}{X}}_b(-\mu)\ \underset{\sim}{Q}(\mu)\left[\underset{\sim}{C}_o + \sum_{\alpha=1}^{N} \frac{\underset{\sim}{C}_\alpha}{\nu_\alpha+\mu}\right]\mu e^{-\mu^2}\, d\mu$$

$$= -A_b + \int_0^\infty \tilde{\underset{\sim}{X}}_b(-\mu)\ \underset{\sim}{Q}(\mu)\ \frac{\mu}{\pi}\begin{vmatrix} -\sqrt{\frac{3}{2}} \\ 1 \end{vmatrix} \mu e^{-\mu^2}\, d\mu \quad , \quad b = 3,4 \quad , \tag{4.44}$$

and

$$\int_0^\infty \tilde{\underset{\sim}{X}}_b(-\eta,-\mu)\ \underset{\sim}{Q}(\mu)\left[\underset{\sim}{C}_o + \sum_{\alpha=1}^{N} \frac{\underset{\sim}{C}_\alpha}{\nu_\alpha+\mu}\right]\mu e^{-\mu^2}\, d\mu$$

$$= \int_0^\infty \tilde{\underset{\sim}{X}}_b(-\eta,-\mu)\ \underset{\sim}{Q}(\mu)\ \frac{\mu}{\pi}\begin{vmatrix} -\sqrt{\frac{3}{2}} \\ 1 \end{vmatrix} \mu e^{-\mu^2}\, d\mu \quad , \quad b = 1,2 \quad . \tag{4.45}$$

After we evaluate analytically some of the integrals which include the discrete eigenvectors using identities of the gamma function [105] we obtain

$$\begin{vmatrix} \frac{7}{2\sqrt{\pi}} \\ -\sqrt{\frac{3}{2\pi}} \end{vmatrix}^T \underset{\sim}{C}_o + \sum_{\alpha=1}^{N} \tilde{\underset{\sim}{P}}_3(\nu_\alpha)\ \underset{\sim}{C}_\alpha = \frac{5}{2\pi}\sqrt{\frac{3}{2}} \quad , \tag{4.46}$$

$$\begin{vmatrix} -\sqrt{\frac{3}{2\pi}} \\ \frac{6}{\sqrt{\pi}} \end{vmatrix}^T \underset{\sim}{C}_o + \sum_{\alpha=1}^{N} P_4(\nu_\alpha)\ \underset{\sim}{C}_\alpha = -\frac{5}{2\pi} \quad , \tag{4.47}$$

and

$$\tilde{\underset{\sim}{R}}(\eta)\ \underset{\sim}{C}_o + \sum_{\alpha=1}^{N} \tilde{\underset{\sim}{R}}_b(\eta,\nu_\alpha)\ \underset{\sim}{C}_\alpha = \frac{1}{\pi}\,\tilde{\underset{\sim}{T}}_b(\eta) \begin{vmatrix} -\sqrt{\frac{3}{2}} \\ 1 \end{vmatrix}, \quad b = 1,2 \ . \tag{4.48}$$

Here $\tilde{\underset{\sim}{P}}_b(\nu_\alpha)$, $\tilde{\underset{\sim}{R}}_b(\eta)$, and $\tilde{\underset{\sim}{R}}_b(\eta,\nu_\alpha)$ represent the same integrals as for the evaporation problem and

$$\tilde{\underset{\sim}{T}}_b(\eta) = \int_0^\infty \tilde{\underset{\sim}{X}}_b(-\eta,-\mu)\ \underset{\sim}{Q}(\mu)\ \mu^2 e^{-\mu^2}\, d\mu \quad , \quad b = 3,4 \ . \tag{4.49}$$

The procedure is exactly the same as for the evaporation problem and thus for the sake of space we give no more details. The expansion coefficients A_α and $A_\alpha(\eta)$, $\alpha=1,2$ used in equation (4.12) can be reduced by substituting the approximation (4.43) and the boundary condition (4.11a) into equations (4.40) and (4.41). The resulting expressions can be written as

$$A_b = -\int_0^\infty \tilde{\underset{\sim}{X}}_b(-\mu)\ \underset{\sim}{Q}(\mu) \left[\underset{\sim}{C}_o - \frac{\mu}{\pi} \begin{vmatrix} -\sqrt{\frac{3}{2}} \\ 1 \end{vmatrix} + \sum_{\alpha=1}^{N} \frac{\underset{\sim}{C}_\alpha}{\nu_\alpha+\mu} \right] \mu e^{-\mu^2}\, d\mu \ ,$$

$$b = 1,2 \quad , \tag{4.50}$$

and

$$A_b(\eta) = -\int_0^\infty \tilde{\underset{\sim}{X}}_b(\eta,-\mu)\ \underset{\sim}{Q}(\mu) \left[\underset{\sim}{C}_o - \frac{\mu}{\pi} \begin{vmatrix} -\sqrt{\frac{3}{2}} \\ 1 \end{vmatrix} + \sum_{\alpha=1}^{N} \frac{\underset{\sim}{C}_\alpha}{\nu_\alpha+\mu} \right] \mu e^{-\mu^2}\, d\mu \ ,$$

$$b = 1,2 \tag{4.51}$$

while the density and temperature profiles follow

immediately in a similar way from

$$N(x) = \pi A_2 - x + \sqrt{\pi} \int_0^\infty A_2(\eta)\, e^{-\eta^2 - \frac{x}{\eta}}\, d\eta \quad , \tag{4.52}$$

and

$$T(x) = \pi \sqrt{\frac{2}{3}} A_1 + x + \sqrt{\pi} \int_0^\infty A_1(\eta)\, e^{-\eta^2 - \frac{x}{\eta}}\, d\eta \quad , \tag{4.53}$$

along with equations (4.50) and (4.51).

4.4 Numerical Results

To establish the constants $\{C_{1\alpha}\}$ and $\{C_{2\alpha}\}$ of the F_N approximation we first must define a strategy for selecting the collocation points η. Then we must compute accurately the known matrix elements and inhomogeneous terms in the two systems of linear algebraic equations (4.46-4.48) for the evaporation problem and (4.25-4.27) for the heat transfer problem. We find that choosing the η_j, $j=1,2,\ldots,N$ to be the positive zeros of the Hermite polynomial of degree 2N, we maximize computational efficiency. The computation of the elements of the known matrix and the right-hand-side vector is based upon a useful Gaussian formula [92]

$$\int f(x)\, dx = \sum_{i=0}^{\eta} w_i\, f(x_i)$$

where x_i are the roots of the Hermite polynomial of degree 2n+1 and w_i the corresponding weight factors. The above

expression is based upon the orthogonality property of the Hermite polynomials. The system of linear algebraic equations is solved in two different ways, first by standard techniques using Gaussian elimination with equilibration and partial pivoting, and secondly by an algorithm based on the singular value decomposition (SVD) [93,94], which is a reliable technique to determine the "numerical" rank of a real matrix. It turns out that the second technique leads to more accurate results especially when high order approximations are required. In particular, solutions with the singular value decomposition method leads in general to results accurate to one more significant figure than the results obtained using the conventional Gaussian elimination. The SVD method is based on the statement that for any real n by p matrix A, there is an n by n orthogonal matrix U and a p by p orthogonal matrix V such that U^TAV assumes one of the two following forms:

$$1.\quad U^T A V = \begin{vmatrix} \Sigma \\ 0 \end{vmatrix} \qquad \text{if } n \geq P$$

$$2.\quad U^T A V = [\Sigma \quad 0] \qquad \text{if } n \leq P$$

Here $\Sigma = \text{diag}\,(\sigma_1, \sigma_2, \ldots, \sigma_m)$, where $m = \min(n,p)$, and

$$\sigma_1 \geq \sigma_2 \geq \cdots \geq \sigma_m \geq 0$$

This decomposition is called the singular value

decomposition of A and can be used to solve a linear system of equations. For example the linear system

$$Ax = b$$

can be solved by applying the above technique since it is equivalent to the system

$$(U^T AV)(V^{-1}x) = (U^T b)$$

which can be reduced to

$$x = V\Sigma^{-1} U^T b$$

All the computations were performed in double-precision arithmetic on an IBM 370/4341 machine.

In Tables 4.1 and 4.3 we show the rate of convergence of the F_N method for the two problems under investigation, as the order of the approximation is increased. The computed results are the various slip coefficients as defined by equations (4.13) and (4.14) with V=0.5. It is evident that convergence is faster for quantities evaluated at $x \to \infty$ (c_1, d_1, c_2, d_2) than for quantities evaluated at x=0 $(\gamma_1, \delta_1, \gamma_2, \delta_2)$. This is expected since in the limit of large x the integral terms disappear in equations (4.34,4.35) and (4.52,4.53). We note that in general only a fourth order approximation is enough and consequently minimum computational effort and time is required to achieve accuracy up to four significant figures while 6-figure accuracy is achieved for $20<N<28$.

Converged numerical results for the temperature and

density profiles for the evaporation problem and the heat transfer problem are presented respectively in Tables 4.2 and 4.3 as computed from equations (4.34,4.35) and (4.52,4.53); for the evaporation problem we have normalized the temperature and density profiles by taking V=0.5. Our results are in excellent agreement with the exact results of Thomas [52]. The 6-figure accuracy is achieved with a relatively low-order approximation (20<N<28).

Finally figures 4.1 through 4.4 give the density and temperature profiles with respect to distance x from the interface, and also some information about the physics of the evaporation and heat transfer problems as they are described by the mathematical modeling. Near the interface the behavior of the gas for both problems is described by a rarefied Knudsen layer a few mean free paths thick in which the collisional effects are only of secondary importance. Here and at the interface the temperature and density undergo important changes, similar to those known as temperature and density jumps. Finally, the kinetic theory solutions recover the features of the continuum regime as x becomes large.

Table 4.1 Convergence of the slip coefficients for the half-space evaporation problem

N	TEMPERATURE		DENSITY	
	$x=0, \delta_1$	$x\to\infty, d_1$	$x=0, \gamma_1$	$x\to\infty, c_1$
4	0.204798	0.223374	0.661082	0.842620
6	0.204800	0.223379	0.661090	0.842628
8	0.204797	0.223378	0.661109	0.842633
10	0.204795	0.223377	0.661116	0.842637
12	0.204794	0.223377	0.661118	0.842638
14	0.204793	0.223376	0.661120	0.842640
16	0.204792	0.223376	0.661122	0.842641
18	0.204791	0.223376	0.661124	0.842642
20	0.204791	0.223376	0.661125	0.842642
22	0.204791	0.223375	0.661125	0.842642
24	0.204791	0.223376	0.661126	0.842642
26	0.204791	0.223375	0.661126	0.842643
28	0.204790	0.223375	0.661127	0.842643
30	0.204790	0.223375	0.661128	0.842644
Converged Results	0.204790	0.223375	0.661128	0.842644
Exact [52]	0.204789	0.223375	0.661130	0.842645

Table 4.2 Stable results of the temperature and density profiles for the half-space evaporation problem

DISTANCE	TEMPERATURE		DENSITY	
x	Converged Results	Exact[52]	Converged Results	Exact[52]
0.0	-0.204790	-0.204789	-0.661128	-0.661130
0.2	-0.206735	-0.206735	-0.745649	-0.745649
0.4	-0.209588	-0.209588	-0.776299	-0.776300
0.6	-0.211891	-0.211891	-0.794298	-0.794298
0.8	-0.213740	-0.213740	-0.806162	-0.816163
1.0	-0.215237	-0.215237	-0.814473	-0.814473
1.5	-0.217913	-0.217913	-0.826887	-0.826888
2.0	-0.219614	-0.219614	-0.833285	-0.833285
2.5	-0.220735	-0.220735	-0.836862	-0.836863
3.0	-0.221494	-0.221494	-0.838970	-0.838971
3.5	-0.222018	-0.222018	-0.840259	-0.840260
4.0	-0.222387	-0.222387	-0.841069	-0.841070
6.0	-0.223074	-0.223074	-0.842306	-0.842307
10.0	-0.223340	-	-0.842622	-
20.0	-0.223375	-0.223374	-0.842644	-0.842645
100.0	-0.223375	-	-0.842644	-
1000.0	-0.223375	-0.223375	-0.842644	-0.842645

Table 4.3 Convergence of the slip coefficients for the half-space heat transfer problem

N	TEMPERATURE		DENSITY	
	$x=0, \delta_2$	$x\to\infty, d_2$	$x=0, \gamma_2$	$x\to\infty, c_2$
4	0.853215	1.30249	0.396276	0.744059
6	0.853428	1.30266	0.396470	0.744214
8	0.853471	1.30269	0.396515	0.744246
10	0.853503	1.30271	0.396583	0.744286
12	0.853499	1.30270	0.396569	0.744279
14	0.853503	1.30270	0.396569	0.744278
16	0.853505	1.30271	0.396568	0.744277
18	0.853506	1.30271	0.396568	0.744278
20	0.853507	1.30271	0.396569	0.744278
22	0.853509	1.30271	0.396569	0.744278
24	0.853507	1.30271	0.396570	0.744278
26	0.853511	1.30271	0.396570	0.744279
28	0.853513	1.30272	0.396571	0.744279
30	0.853512	1.30272	0.396570	0.744278
Converged Results	0.853513	1.30272	0.396571	0.744279
Exact [52]	0.853515	1.30272	0.396572	0.744279

Table 4.4 Stable results of the temperature and density profiles for the half-space heat transfer problem

DISTANCE	TEMPERATURE		DENSITY	
x	Converged Results	Exact[52]	Converged Results	Exact[52]
0.0	0.853513	0.853515	-0.396571	-0.396572
0.2	1.20568	1.20568	-0.724405	-0.724406
0.4	1.47158	1.47158	-0.975507	-0.975508
0.6	1.71501	1.71501	-1.20817	-1.20817
0.8	1.94664	1.94665	-1.43152	-1.43152
1.0	2.17091	2.17091	-1.64921	-1.64921
1.5	2.23831	2.23831	-2.17910	-2.17910
2.0	3.23831	3.23831	-2.69757	-2.69757
2.5	3.75554	3.75555	-3.20985	-3.20985
3.0	4.26751	4.26751	-3.71840	-3.71840
3.5	4.77605	4.77605	-4.22454	-4.22454
4.0	5.28229	5.28229	-4.72904	-4.72904
6.0	7.29509	7.29509	-6.73843	-6.73843
10.0	11.3014	-	-10.7432	-
20.0	21.3027	21.3027	-20.7443	-20.7443
100.0	100.303	-	-100.744	-
1000.0	1000.30	-	-1000.74	-

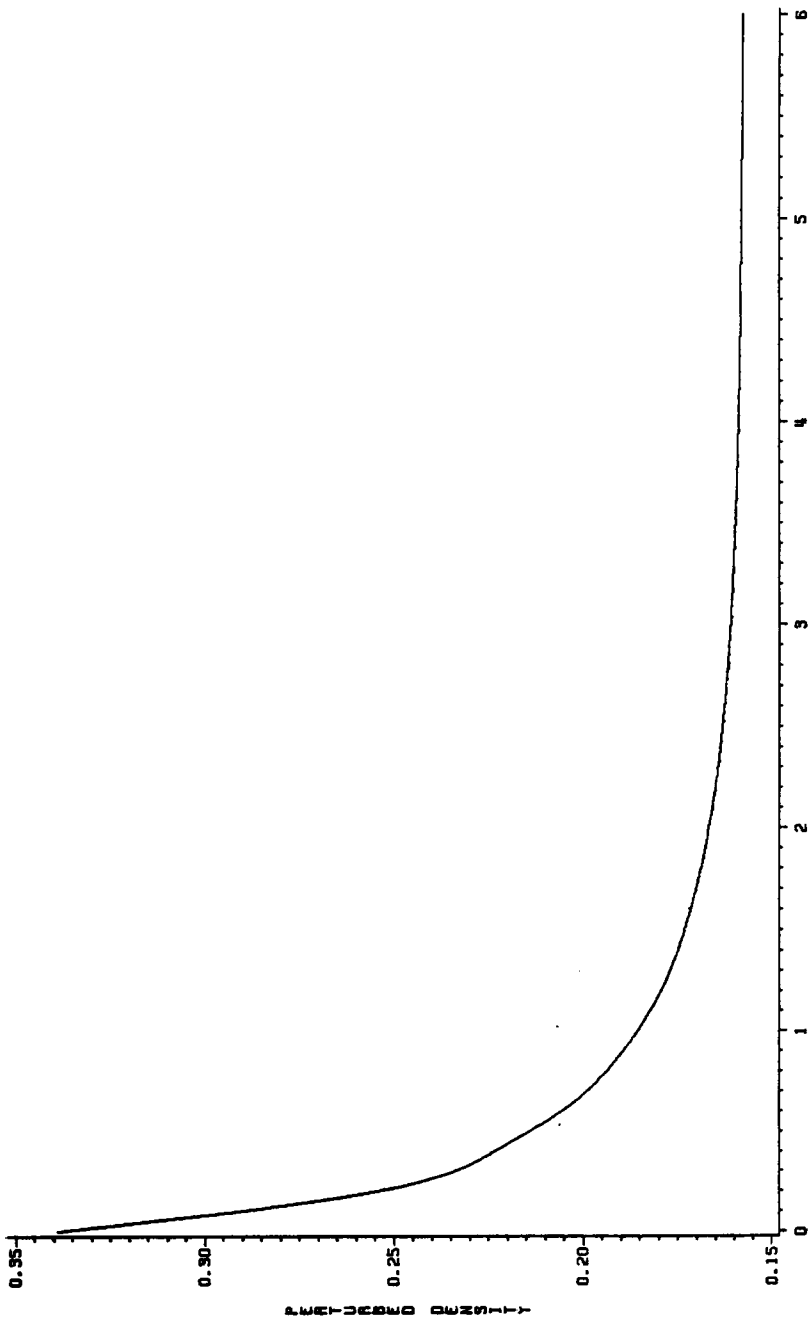

FIGURE 4.1 PROFILE OF THE DENSITY PERTURBATION FOR THE HALF-SPACE EVAPORATION PROBLEM

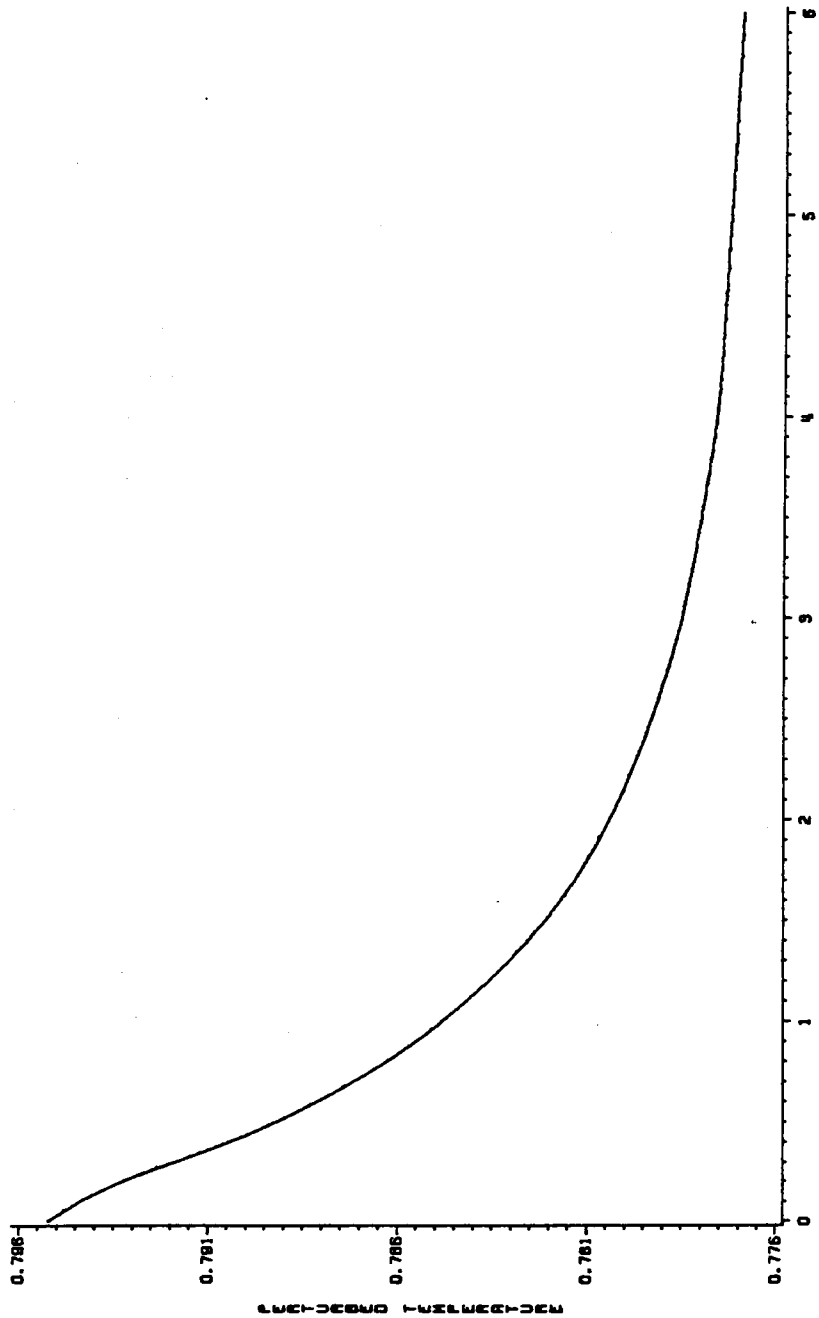

FIGURE 4.2 PROFILE OF THE TEMPERATURE PERTURBATION FOR THE HALF-SPACE EVAPORATION PROBLEM

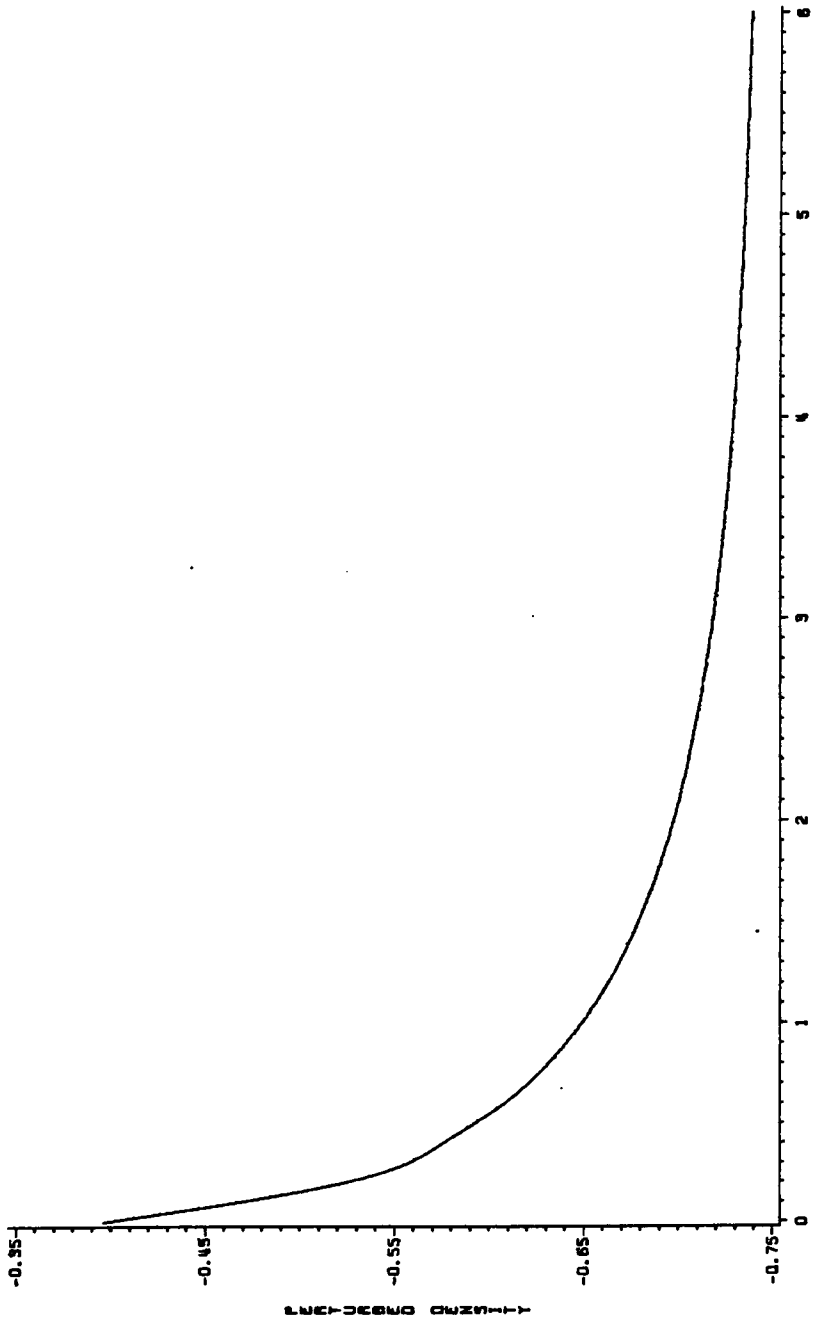

FIGURE 4.3 PROFILE OF THE DENSITY PERTURBATION FOR THE HALF-SPACE HEAT TRANSFER PROBLEM

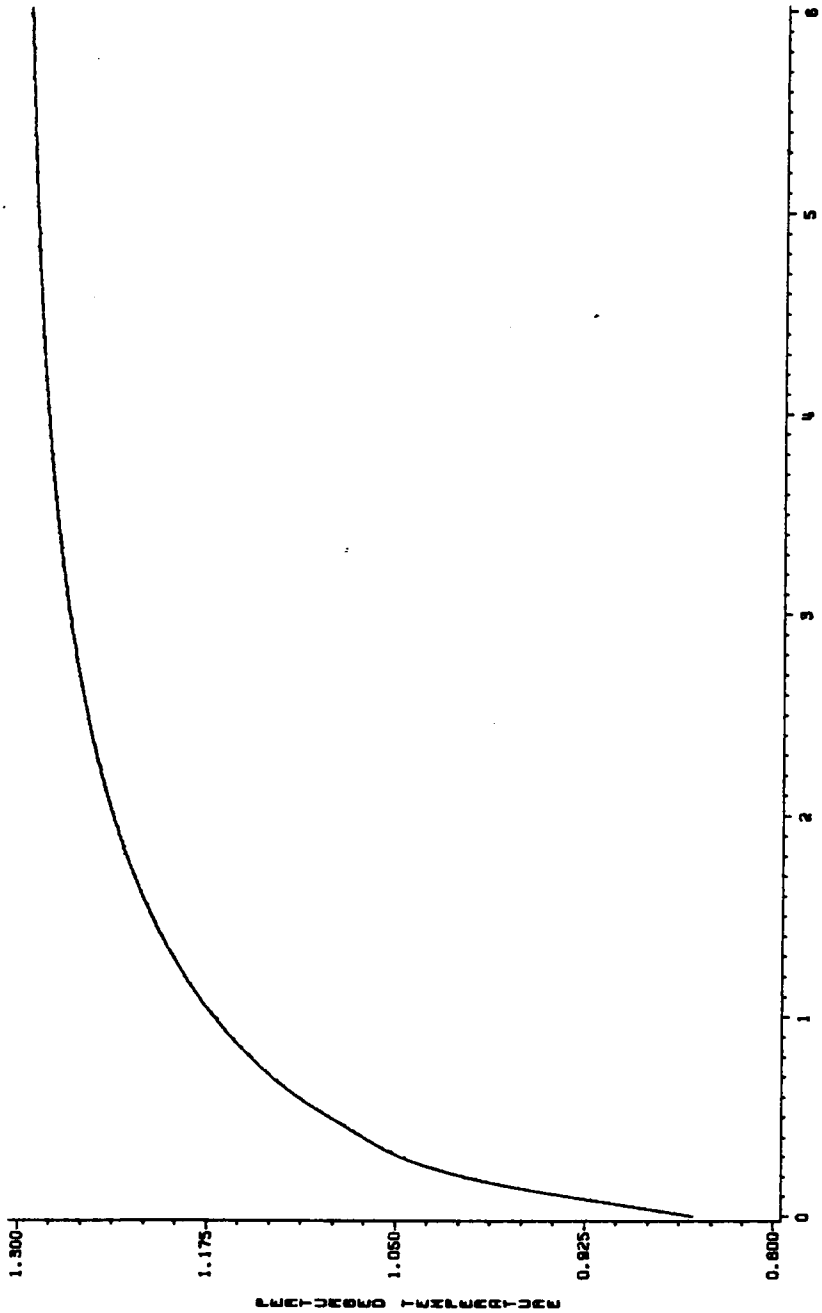

FIGURE 4.4 PROFILE OF THE TEMPERATURE PERTURBATION FOR THE HALF-SPACE HEAT TRANSFER PROBLEM

5. HEAT TRANSFER BETWEEN PARALLEL PLATES WITH UNEQUAL SURFACE ACCOMMODATION

5.1 Introduction

The problem of heat transfer between parallel plates has attracted considerable attention over the years from several authors [4,5,95,96,31,97,98,52,55,99]. The linearized problem has been formulated by Bassanini, et al., who applied a variational technique to the linearized BGK equation to compute the heat flux between the plates for purely diffuse reflection [31] and for arbitrary surface accommodation [97]. The variational results appeared to be quite accurate for the purely diffuse case, although such accuracy was not obtained for the more general case [97].

Kriese, et al. [51] reported a general solution of the vector transport equation describing temperature-density effects which arise after the linearized BGK equation is decomposed in the manner discussed by Cercignani [4]. Thomas [52] and Thomas, et al. [54] used the general analysis of Kriese, et al. and half range orthogonality to reduce the solution of the heat transfer problem between parallel plates with arbitrary accommodation coefficients to the solution of a coupled pair of Fredholm integral equations. They found that iterative solutions to these equations converge very rapidly and thus have computed the

solution correct up to six significant figures. Unlike the variational technique, their work yields accurate temperature and density profiles between the plates.

In the present chapter we use the F_N method to solve the same much-studied problem of heat transfer in a rarefied gas between two parallel plates with unequal surface accommodation. We have chosen a problem which has previously been solved [55] by relatively exact methods in order to have a basis of comparison. The objective is to demonstrate the efficiency of F_N method for providing solutions of benchmark accuracy to kinetic theory problems in finite media, as was done for half space problems in the previous chapter. We test the F_N method in finite geometry, since in other fields of application of this method, finite geometries have required different forms for the approximate solution. As it is presented later, that turns out to be the case here; an even simpler set of basis functions than those used in equations (4.22) and (4.43) provide best results. We rely on the tractable full-range orthogonality to derive singular integral equations for the distribution function, which then are solved by polynomial expansion and collocation. The total heat flux and temperature and density profiles are computed to high accuracy.

In addition we extend the use of the F_N method, using similar ideas, for interior reduced molecular distribution function calculations at any location in the slab. This

type of analysis was applied by Siewert and his co-workers in the fields of neutron-transport theory [78], radiative transfer [100] and plasma physics [101].

5.2 Physical Problem, General Solution and Boundary Conditions

We consider a two-surface problem of rarefied gas dynamics, that of heat transfer between parallel plates. The plates are taken to be in the planes x=0 and x=δ with

$$\delta = d\,\frac{\nu}{(2RT_1)^{\frac{1}{2}}}$$

to be the inverse Knudsen number. Here d is the physical distance between the plates, ν is the mean-free-collision frequency, R is the gas constant, and T_1 is the temperature of the plate at x=0. The temperature of the second plate at x=δ is T_2, such that $T_1 > T_2$, and as a result heat flows from left to right. We consider the case of a mixture of diffuse and specular reflection with a_1 and a_2 representing the arbitrary accommodation coefficients, or the fraction of the molecules which are diffusely reflected from the two plates at x=0 and x=δ respectively. By taking a_1 different from a_2 we destroy the anti-symmetry condition and generalize the problem.

In order to establish the required notation and formalism we again review and summarize briefly the

principal results of Thomas [55]. The temperature-density effects, which we are concerned with, are based on the pair of coupled equations written here in matrix notation as

$$\mu \frac{\partial}{\partial x} \underset{\sim}{\psi}(x,\mu) + \underset{\sim}{\psi}(x,\mu) = \frac{1}{\sqrt{\pi}} \underset{\sim}{Q}(\mu) \int_{-\infty}^{\infty} \underset{\sim}{\tilde{Q}}(\mu') \underset{\sim}{\psi}(x,\mu') e^{-\mu'^2} d\mu' , \qquad (5.1)$$

where $\underset{\sim}{\psi}(x,\mu)$ is a 2-vector related to perturbations in the density and temperature of the gas:

$$\Delta T(x) = \frac{2}{3\pi} \int_{-\infty}^{\infty} \begin{vmatrix} \mu^2 - \frac{1}{2} \\ 1 \end{vmatrix}^T \underset{\sim}{\psi}(x,\mu) e^{-\mu^2} d\mu \qquad (5.2)$$

and

$$\Delta N(x) = \frac{1}{\pi} \begin{vmatrix} 1 \\ 0 \end{vmatrix}^T \int_{-\infty}^{\infty} \underset{\sim}{\psi}(x,\mu) e^{-\mu^2} d\mu \quad . \qquad (5.3)$$

Similarly, the normalized heat flux q is related to $\underset{\sim}{\psi}(x,\mu)$ through

$$q = \frac{Q}{Q_{fm}} = - \frac{a_1 + a_2 - a_1 a_2}{a_1 a_2} \frac{1}{\sqrt{\pi}} \int_{-\infty}^{\infty} \begin{vmatrix} \mu^2 + 1 \\ 1 \end{vmatrix}^T \underset{\sim}{\psi}(x,\mu) \mu e^{-\mu^2} d\mu , \qquad (5.4)$$

where Q_{fm} represents the heat flux appropriate to free-molecular conditions and Q the actual heat flux. Kriese, et al. [51] have given the general solution of equation (5.1) in the form

$$\underset{\sim}{\psi}(x,\mu) = \sum_{\alpha=1}^{2} A_\alpha \underset{\sim}{\phi}_\alpha(\mu) + \sum_{\alpha=3}^{4} A_\alpha \underset{\sim}{\psi}_\alpha(x,\mu) + \sum_{\alpha=1}^{2} \int_{-\infty}^{\infty} A_\alpha(\eta) \underset{\sim}{\phi}_\alpha(\eta,\mu) e^{-\frac{x}{\eta}} d\eta , \qquad (5.5)$$

where the eigenvectors are given explicitly in equations (3.3) through (3.6). In this work we use the superscripts T or tilde to denote the transpose operation.

We use Maxwell's diffuse/specular boundary conditions to define the interaction of the molecules with the walls and write

$$f(0,\underset{\sim}{c}) = (1 - a_1)\, f(0,\underset{\sim}{c}^*) + a_1\, f_1(\underset{\sim}{c}) \quad , \quad c_1 > 0 \tag{5.6a}$$

and

$$f(\delta,\underset{\sim}{c}^*) = (1 - a_2)\, f(\delta,\underset{\sim}{c}) + a_2\, f_2(\underset{\sim}{c}) \quad , \quad c_1 > 0 \tag{5.6b}$$

where $\underset{\sim}{c}^* = (-c_1^*, c_2, c_3)$, f is the particle distribution function, a_1, a_2 are the accommodation coefficients and $f_1(\underset{\sim}{c})$, $f_2(\underset{\sim}{c})$ are the absolute Maxwellians based on temperatures T_1 and T_2 respectively. Linearizing the boundary conditions (5.6) about the same Maxwellian $f_1(\underset{\sim}{c})$ based on temperature T_1 and decomposing the resulting expressions in the same manner used to derive equation (5.1) we find that the boundary conditions at the two plates can be written as

$$\underset{\sim}{\psi}(0,\mu) = (1 - a_1)\, \underset{\sim}{\psi}(0,-\mu) \tag{5.7a}$$

and

$$\underset{\sim}{\psi}(\delta,-\mu) = (1 - a_2)\ \underset{\sim}{\psi}(\delta,\mu) + a_2\sqrt{\pi}\ \begin{vmatrix} \mu^2 + B \\ 1 \end{vmatrix} \quad , \tag{5.7b}$$

where B is to be determined by mass conservation. Further we note that since there must be no net flow in the x-direction we can write

$$\begin{vmatrix} 1 \\ 0 \end{vmatrix}^T \int_{-\infty}^{\infty} \underset{\sim}{\psi}(x,\mu)\ \mu e^{-\mu^2}\ d\mu = 0 \tag{5.8}$$

and thus B can be determined by satisfying the above condition of particle conservation at the boundary $x=\delta$.

5.3 The F_N Solution

The general solution (5.5) and the boundary conditions (5.7), along with the physical constraint (5.8) constitute the mathematical formulation of the problem we consider.

Operating on the general solution (5.5) and utilizing the full range orthogonality theorem proved by Kriese, et al. [51] we derive the singular integral equations

$$\int_{-\infty}^{\infty} \underset{\sim}{\tilde{X}}_{\alpha}(\mu)\ \underset{\sim}{\psi}(0,\mu)\ \mu e^{-\mu^2}\ d\mu = A_{\alpha} \quad , \quad \alpha = 1,2,3,4 \quad , \tag{5.9}$$

$$\int_{-\infty}^{\infty} \underset{\sim}{\tilde{X}}_{\alpha}(\eta,\mu)\ \underset{\sim}{\psi}(0,\mu)\ \mu e^{-\mu^2}\ d\mu = A_{\alpha}(\eta) \quad , \quad \alpha = 1,2 \quad , \tag{5.10}$$

and

$$\int_{-\infty}^{\infty} \tilde{\underset{\sim}{X}}_{\alpha}(-\eta,\mu)\ \underset{\sim}{\psi}(0,\mu)\ \mu e^{-\mu^2}\ d\mu = A_{\alpha}(-\eta) \quad , \quad \alpha = 1,2 \quad , \tag{5.11}$$

where $\underset{\sim}{\psi}(0,\mu)$ represents the general solution at x=0. A similar set of singular integral equations can be established at the second boundary of the problem. At $x=\delta$ we find

$$\int_{-\infty}^{\infty} \tilde{\underset{\sim}{X}}_{\alpha}(\mu)\ \underset{\sim}{\psi}(\delta,\mu)\ \mu e^{-\mu^2}\ d\mu = A_{\alpha} - \delta\ A_{\alpha+2} \quad , \quad \alpha = 1,2 \quad , \tag{5.12}$$

$$\int_{-\infty}^{\infty} \tilde{\underset{\sim}{X}}_{\alpha}(\mu)\ \underset{\sim}{\psi}(\delta,\mu)\ \mu e^{-\mu^2}\ d\mu = A_{\alpha} \quad , \quad \alpha = 3,4 \quad , \tag{5.13}$$

$$\int_{-\infty}^{\infty} \tilde{\underset{\sim}{X}}_{\alpha}(\eta,\mu)\ \underset{\sim}{\psi}(\delta,\mu)\ \mu e^{-\mu^2}\ d\mu = A_{\alpha}(\eta)\ e^{\frac{\delta}{\eta}} \quad , \quad \alpha = 1,2 \quad , \tag{5.14}$$

and

$$\int_{-\infty}^{\infty} \tilde{\underset{\sim}{X}}_{\alpha}(-\eta,\mu)\ \underset{\sim}{\psi}(\delta,\mu)\ \mu e^{-\mu^2}\ d\mu = A_{\alpha}(-\eta)\ e^{\frac{\delta}{\eta}} \quad , \quad \alpha = 1,2 \quad , \tag{5.15}$$

where $\underset{\sim}{\psi}(\delta,\mu)$ represents the general solution at the second boundary $x=\delta$. Eliminating by simple algebraic operations the expansion coefficients A_{α}, $\alpha=1,2,3,4$, $A_{\alpha}(\eta)$ and $A_{\alpha}(-\eta)$, $\alpha=1,2$ we find

$$\int_{-\infty}^{\infty} \tilde{\underset{\sim}{X}}_{\alpha}(\mu)\ \underset{\sim}{\psi}(\delta,\mu)\ \mu e^{-\mu^2}\ d\mu - \int_{-\infty}^{\infty} [\tilde{\underset{\sim}{X}}_{\alpha}(\mu) - \delta\ \tilde{\underset{\sim}{X}}_{\alpha+2}(\mu)]\ \underset{\sim}{\psi}(0,\mu)\ \mu e^{-\mu^2}\ d\mu = 0 \ , \quad \alpha = 1,2 \quad , \tag{5.16}$$

$$\int_{-\infty}^{\infty} \tilde{\underset{\sim}{X}}_{\alpha}(\mu)\ \underset{\sim}{\psi}(\delta,\mu)\ \mu e^{-\mu^2}\ d\mu - \int_{-\infty}^{\infty} \tilde{\underset{\sim}{X}}_{\alpha}(\mu)\ \underset{\sim}{\psi}(0,\mu)\ \mu e^{-\mu^2}\ d\mu = 0 \ , \quad \alpha = 3,4 \quad , \tag{5.17}$$

$$\int_{-\infty}^{\infty} \tilde{\underset{\sim}{X}}_{\alpha}(\eta,\mu)\ \underset{\sim}{\psi}(\delta,\mu)\ \mu e^{-\mu^2}\ d\mu - e^{-\frac{\delta}{\eta}} \int_{-\infty}^{\infty} \tilde{\underset{\sim}{X}}_{\alpha}(\eta,\mu)\ \underset{\sim}{\psi}(0,\mu)\ \mu e^{-\mu^2}\ d\mu = 0 \quad , \qquad \alpha = 1,2 \quad , \tag{5.18}$$

and

$$e^{-\frac{\delta}{\eta}} \int_{-\infty}^{\infty} \tilde{\underset{\sim}{X}}_{\alpha}(-\eta,\mu)\ \psi(\delta,\mu)\ \mu e^{-\mu^2}\ d\mu - \int_{-\infty}^{\infty} \tilde{\underset{\sim}{X}}_{\alpha}(-\eta,\mu)\ \underset{\sim}{\psi}(0,\mu)\ \mu e^{-\mu^2}\ d\mu = 0 \quad , \qquad \alpha = 1,2 \quad . \tag{5.19}$$

Here $\underset{\sim}{X}_{\alpha}(\mu)$, $\underset{\sim}{X}_{\alpha}(\eta,\mu)$ are the full-range adjoint vectors given explicitly in section 3.2.

Since $\underset{\sim}{\psi}(0,\mu)$ and $\underset{\sim}{\psi}(\delta,-\mu)$ are known only for $\mu>0$ from the boundary conditions (5.7), for reasons given in the section (9.3) of the appendices, we substitute the simple polynomial approximations

$$\underset{\sim}{\psi}(0,-\mu) = \sum_{m=0}^{N} \underset{\sim}{A}_m\ \mu^m \quad , \quad \mu > 0 \tag{5.20}$$

and

$$\underset{\sim}{\psi}(\delta,\mu) = \sum_{m=0}^{N} \underset{\sim}{B}_m\ \mu^m \quad , \quad \mu > 0 \tag{5.21}$$

where $\{A_m\}$, $\{B_m\}$ are two 2-vectors to be determined and μ^{α} the basis functions, along with the boundary conditions (5.7), into equations (5.17) through (5.20) to obtain

$$\sum_{m=0}^{N} \{[(2-a_1)\ \tilde{\underset{\sim}{C}}_{m+2} + a_1\,\delta\,\tilde{\underset{\sim}{C}}_{m+1}]\underset{\sim}{A}_m - (2-a_2)\ \tilde{\underset{\sim}{C}}_{m+2}\ \underset{\sim}{B}_m\} = a_2\ \frac{\sqrt{6\pi}}{4} \quad , \tag{5.22}$$

$$\sum_{m=0}^{N} \{[(2-a_1)\ \tilde{\underset{\sim}{D}}_{m+2} + a_1\,\delta\,\tilde{\underset{\sim}{D}}_{m+1}]\underset{\sim}{A} - (2-a_2)\ \tilde{\underset{\sim}{D}}_{m+2}\ \underset{\sim}{B}_m\} = a_2\ \frac{\sqrt{\pi}}{2}\left(B + \frac{1}{2}\right) \quad , \tag{5.23}$$

$$\sum_{m=0}^{N} \{\tilde{\underset{\sim}{C}}_{m+1}\ \underset{\sim}{A}_m + \tilde{\underset{\sim}{C}}_{m+2}\ \underset{\sim}{B}_m\} = \frac{\sqrt{6}}{10}\ (3 - B) \quad , \tag{5.24}$$

$$\sum_{m=0}^{N} \{\tilde{\underset{\sim}{D}}_{m+1}\ \underset{\sim}{A}_m + \tilde{\underset{\sim}{D}}_{m+1}\ \underset{\sim}{B}_m\} = \frac{2}{5}\ (1 + 3B) \quad , \tag{5.25}$$

$$\sum_{m=0}^{N} \{[(1-a_1)\ \tilde{\underset{\sim}{S}}_m(\eta) - \tilde{\underset{\sim}{R}}_m(\eta)]\ \underset{\sim}{A}_m + e^{-\frac{\delta}{\eta}}\ [(1-a_2)\ \tilde{\underset{\sim}{R}}_m(\eta) - \tilde{\underset{\sim}{S}}_m(\eta)]\ \underset{\sim}{B}_m$$

$$= - a_2\ \sqrt{\pi}\ e^{-\frac{\delta}{\eta}}\ W_1(\eta) \quad , \tag{5.26}$$

$$\sum_{m=0}^{N} \{[(1-a_1)\ \tilde{\underset{\sim}{T}}_m(\eta) - \tilde{\underset{\sim}{P}}_m(\eta)]\ \underset{\sim}{A}_m + e^{-\frac{\delta}{\eta}}\ [(1-a_2)\ \tilde{\underset{\sim}{P}}_m(\eta) - \tilde{\underset{\sim}{T}}_m(\eta)]\ \underset{\sim}{B}_m\}$$

$$= - a_2\ \sqrt{\pi}\ e^{-\frac{\delta}{\eta}}\ W_2(\eta) \quad , \tag{5.27}$$

$$e^{-\frac{\delta}{\eta}} \sum_{m=0}^{N} \{[(1-a_1)\ \tilde{\underset{\sim}{R}}_m(\eta) - \tilde{\underset{\sim}{S}}_m]\ \underset{\sim}{A}_m + [(1-a_2)\ \tilde{\underset{\sim}{S}}_m(\eta) - \tilde{\underset{\sim}{R}}_m(\eta)]\ \underset{\sim}{B}_m\}$$

$$= - a_2\ \sqrt{\pi}\ W_1(\eta) \quad , \tag{5.28}$$

and

$$e^{-\frac{\delta}{\eta}} \sum_{m=0}^{N} \{[(1-a_1)\ \tilde{\underset{\sim}{P}}_m(\eta) - \tilde{\underset{\sim}{T}}_m(\eta)]\ \underset{\sim}{A}_m + [(1-a_2)\ \tilde{\underset{\sim}{T}}_m(\eta) - \tilde{\underset{\sim}{P}}_m(\eta)\ ]\ \underset{\sim}{B}_m\}$$

$$= - a_2\ \sqrt{\pi}\ W_2(\eta) \quad . \tag{5.29}$$

Here we have used the definitions

$$\underset{\sim}{C}_m = \int_0^\infty \underset{\sim}{X}_3(\mu)\, \mu^m\, e^{-\mu^2}\, d\mu \quad , \tag{5.30}$$

$$\underset{\sim}{D}_m = \int_0^\infty \underset{\sim}{X}_4(\mu)\, \mu^m\, e^{-\mu^2}\, d\mu \quad , \tag{5.31}$$

$$\underset{\sim}{S}_m(\eta) = \int_0^\infty \underset{\sim}{X}_1(\eta,-\mu)\, \mu^{m+1}\, e^{-\mu^2}\, d\mu \quad , \tag{5.32}$$

$$\underset{\sim}{T}_m(\eta) = \int_0^\infty \underset{\sim}{X}_2(\eta,-\mu)\, \mu^{m+1}\, e^{-\mu^2}\, d\mu \quad , \tag{5.33}$$

$$\underset{\sim}{R}_m(\eta) = \int_0^\infty \underset{\sim}{X}_1(\eta,\mu)\, \mu^{m+1}\, e^{-\mu^2}\, d\mu \quad , \tag{5.34}$$

$$\underset{\sim}{P}_m(\eta) = \int_0^\infty \underset{\sim}{X}_2(\eta,\mu)\, \mu^{m+1}\, e^{-\mu^2}\, d\mu \quad , \tag{5.35}$$

$$W_1(\eta) = \int_0^\infty \underset{\sim}{\tilde{X}}_1(\eta,\pm\mu) \begin{vmatrix} \mu^2 + B \\ 1 \end{vmatrix} \mu e^{-\mu^2}\, d\mu \quad , \tag{5.36}$$

and

$$W_2(\eta) = \int_0^\infty \underset{\sim}{\tilde{X}}_2(\eta,\pm\mu) \begin{vmatrix} \mu^2 + B \\ 1 \end{vmatrix} \mu e^{-\mu^2}\, d\mu \quad . \tag{5.37}$$

The physical constraint (5.8) can be used to express the constant B in terms of the unknown F_N coefficients $\{B_m\}$:

$$B = -1 + \frac{2}{\sqrt{\pi}} \begin{vmatrix} 1 \\ 0 \end{vmatrix}^T \sum_{m=0}^{N} \underset{\sim}{B}_m \int_0^\infty \mu^{m+1}\, e^{-\mu^2}\, d\mu \tag{5.38}$$

It is clear that an approximation N involves N+1 unknown vectors $\{A_m\}$ and $\{B_m\}$ for a total of 4N+4 unknowns. When the full-range adjoints $\underset{\sim}{X}_\alpha(\mu)$ and $\underset{\sim}{X}_\alpha(\eta,\mu)$ are introduced explicitly into equations (5.22) through (5.29) it is found, as is shown in section 9.4 of the appendices, that all integrals can be reduced to combinations of the basic integral

$$I(\eta) = \int_0^\infty \frac{e^{-\mu^2}}{\mu+\eta}\, d\mu \tag{5.39}$$

which we evaluate numerically using Gaussian quadrature.

Evaluation of equations (5.26) through (5.29) at N discrete values of $0<\eta<\infty$, along with equations (5.22) through (5.25), leads to a system of 4N+4 linear algebraic equations that can be solved to yield the desired 4N+4 unknowns $\{A_\alpha\}$ and $\{B_\alpha\}$. If we presume now that the system of linear equations is solved, then the F_N coefficients are used to establish the distribution at the boundaries and as a result quantities like the heat flux and the microscopic temperature and density jumps at the two boundaries follow immediately from equations (5.4), (5.2) and (5.3), respectively. Inserting the general solution (5.5) into equations (5.2), (5.3) and (5.4) yields

$$\Delta T(x) = \sqrt{\frac{2}{3\pi}}\,(A_1 - A_3 x) + \frac{1}{\pi}\int_0^\infty [A_1(\eta)\, e^{-\frac{x}{\eta}} + A_1(-\eta)\, e^{\frac{x}{\eta}}]\, d\eta \quad , \tag{5.40}$$

$$\Delta N(x) = \frac{1}{\sqrt{\pi}} (A_2 - A_4 x) + \frac{1}{\pi} \int_0^\infty [A_2(\eta)\, e^{-\frac{x}{\eta}} + A_2(-\eta)\, e^{\frac{x}{\eta}}]d\eta \quad , \tag{5.41}$$

and

$$q = -\frac{a_1 + a_2 - a_1 a_2}{a_1 a_2} \frac{5}{8} \sqrt{\frac{2}{3}}\, A_3 \tag{5.42}$$

where the A_α and $A_\alpha(\eta)$ are the expansion coefficients and can be determined through expressions (5.9), (5.10) and (5.11), which can be evaluated in term of the known F_N coefficients as

$$A_\alpha = (2-a_1) \int_0^\infty \tilde{\underset{\sim}{X}}_\alpha(\mu) \sum_{m=0}^{N} \underset{\sim}{A}_m \mu^{m+2} e^{-\mu^2} d\mu \quad , \quad \alpha = 1,2 \ , \tag{5.43}$$

$$A_\alpha = - a_1 \int_0^\infty \tilde{\underset{\sim}{X}}_\alpha(\mu) \sum_{m=0}^{N} \underset{\sim}{A}_m \mu^{m+1} e^{-\mu^2} d\mu \quad , \quad \alpha = 3,4 \ , \tag{5.44}$$

$$A_\alpha(\eta) = \int_0^\infty [(1-a_1)\, \tilde{\underset{\sim}{X}}_\alpha(\eta,\mu) - \tilde{\underset{\sim}{X}}_\alpha(\eta,-\mu)] \sum_{m=0}^{N} \underset{\sim}{A}_m \mu^{m+1} e^{-\mu^2} d\mu \quad ,$$

$$\alpha = 1,2 \tag{5.45}$$

and

$$A_\alpha(-\eta) = e^{-\frac{\delta}{\eta}} \int_0^\infty [(1-a_2)\, \tilde{\underset{\sim}{X}}_\alpha(\eta,\mu) - \tilde{\underset{\sim}{X}}_\alpha(\eta,-\mu)] \sum_{m=0}^{N} \underset{\sim}{B}_m \mu^{m+1} e^{-\mu^2} d\mu$$

$$+ a_2\sqrt{\pi} \int_0^\infty \tilde{\underset{\sim}{X}}_\alpha(\eta,\mu) \begin{vmatrix} \mu^2 + B \\ 1 \end{vmatrix} \mu e^{-\mu^2} d\mu \quad , \quad \alpha = 1,2 \ . \tag{5.46}$$

Consequently the temperature and density profiles between the plates follow immediately through a double integration

scheme over μ and η from zero to infinity.

5.4 Position-Dependent F_N Approximation

We prefer to use a different approach [78,101,102] which gives the temperature and density profiles directly through equations (5.2) and (5.3), as well as the interior molecular distribution function.

Through a procedure analogous to that used in deriving equations (5.12-5.15) we find for any $0<x<\delta$

$$\int_{-\infty}^{\infty} \tilde{\underset{\sim}{X}}_{\alpha}(\mu)\, \underset{\sim}{\psi}(x,\mu)\, \mu e^{-\mu^2}\, d\mu = A_{\alpha} - xA_{\alpha+2} \quad , \quad \alpha = 1,2 \quad , \tag{5.47}$$

$$\int_{-\infty}^{\infty} \tilde{\underset{\sim}{X}}_{\alpha}(\mu)\, \underset{\sim}{\psi}(x,\mu)\, \mu e^{-\mu^2}\, d\mu = A_{\alpha} \quad , \quad \alpha = 3,4 \quad , \tag{5.48}$$

$$\int_{-\infty}^{\infty} \tilde{\underset{\sim}{X}}_{\alpha}(\eta,\mu)\, \underset{\sim}{\psi}(x,\mu)\, \mu e^{-\mu^2}\, d\mu = A_{\alpha}(\eta)\, e^{-\frac{x}{\eta}} \quad , \quad \alpha = 1,2 \tag{5.49}$$

and

$$\int_{-\infty}^{\infty} \tilde{\underset{\sim}{X}}_{\alpha}(-\eta,\mu)\, \underset{\sim}{\psi}(x,\mu)\, \mu e^{-\mu^2}\, d\mu = A_{\alpha}(-\eta)\, e^{\frac{x}{\eta}} \quad , \quad \alpha = 1,2 \tag{5.50}$$

where $\underset{\sim}{\psi}(x,\mu)$ is given by equation (5.5). The unknowns A_{α}, $\alpha=1,2,3,4$, $A_{\alpha}(\eta)$ and $A_{\alpha}(-\eta)$, $\alpha=1,2$, $\eta>0$, can be eliminated from the above set of equations by considering the same equations for $x=0$. In this way we develop the equations

$$\int_{-\infty}^{\infty} \tilde{\underset{\sim}{X}}_{\alpha}(\mu)\ \underset{\sim}{\psi}(x,\mu)\ \mu e^{-\mu^2}\ d\mu - \int_{-\infty}^{\infty} [\tilde{\underset{\sim}{X}}_{\alpha}(\mu) - x\ \tilde{\underset{\sim}{X}}_{\alpha+2}(\mu)]\ \underset{\sim}{\psi}(0,\mu)\ \mu e^{-\mu^2}\ d\mu = 0\ ,$$

$$\alpha = 1,2\ , \qquad (5.51)$$

$$\int_{-\infty}^{\infty} \tilde{\underset{\sim}{X}}_{\alpha}(\mu)\ \underset{\sim}{\psi}(x,\mu)\ \mu e^{-\mu^2}\ d\mu - \int_{-\infty}^{\infty} \tilde{\underset{\sim}{X}}_{\alpha}(\mu)\ \psi(0,\mu)\ \mu e^{-\mu^2}\ d\mu\ ,\quad \alpha = 3,4 \qquad (5.52)$$

$$\int_{-\infty}^{\infty} \tilde{\underset{\sim}{X}}_{\alpha}(\eta,\mu)\ \underset{\sim}{\psi}(x,\mu)\ \mu e^{-\mu^2}\ d\mu - e^{-\frac{x}{\eta}} \int_{-\infty}^{\infty} \tilde{\underset{\sim}{X}}_{\alpha}(-\eta,\mu)\ \underset{\sim}{\psi}(0,\mu)\ \mu e^{-\mu^2}\ d\mu = 0\ ,$$

$$\alpha = 1,2\ , \qquad (5.53)$$

and

$$e^{-\frac{x}{\eta}} \int_{-\infty}^{\infty} \tilde{\underset{\sim}{X}}_{\alpha}(-\eta,\mu)\ \underset{\sim}{\psi}(x,\mu)\ \mu e^{-\mu^2}\ d\mu - \int_{-\infty}^{\infty} \tilde{\underset{\sim}{X}}_{\alpha}(-\eta,\mu)\ \psi(0,\mu)\ \mu e^{-\mu^2}\ d\mu = 0\ ,$$

$$\alpha = 1,2\ , \qquad (5.54)$$

that are the desired generalizations of (5.16-5.19). We now approximate for $\mu>0$

$$\underset{\sim}{\psi}(x,\mu) = \sum_{m=0}^{N} \underset{\sim}{F}_m(x)\ \mu^{\alpha} \qquad (5.55)$$

and

$$\underset{\sim}{\psi}(x,-\mu) = \sum_{m=0}^{N} \underset{\sim}{G}_m(x)\ \mu^{\alpha} \qquad (5.56)$$

where $\{F_m\}$ and $\{G_m\}$ are two 2-vectors to be determined. On substituting (5.55) and (5.56) into equations (5.51-5.54), after invoking the fact that $\underset{\sim}{\psi}(0,\mu)$ is known for $-\infty<\mu<\infty$ and considering the resulting equations at N values of η, we find the system of linear algebraic equations

$$\sum_{m=0}^{N} \{\tilde{C}_{m+2} \underset{\sim}{F}_m(x) + \tilde{C}_{m+2} \underset{\sim}{G}_m(x)\} = \sum_{m=0}^{N} [(2-a_1) \tilde{C}_{m+2} + a_1 \times \tilde{C}_{m+1}] \underset{\sim}{A}_m \quad , \tag{5.57}$$

$$\sum_{m=0}^{N} \{\tilde{D}_{m+2} \underset{\sim}{F}_m(x) + \tilde{D}_{m+2} \underset{\sim}{G}_m(x)\} = \sum_{m=0}^{N} [(2-a_1) \tilde{D}_{m+2} + a_1 \times \tilde{D}_{m+1}] \underset{\sim}{A}_m \quad , \tag{5.58}$$

$$\sum_{m=0}^{N} \{\tilde{C}_{m+2} \underset{\sim}{F}_m(x) - \tilde{C}_{m+1} \underset{\sim}{G}_m(x) = - a_1 \sum_{m=0}^{N} \tilde{C}_{m+1} \underset{\sim}{A}_m \quad , \tag{5.59}$$

$$\sum_{m=0}^{N} \{\tilde{D}_{m+1} \underset{\sim}{F}_m(x) - \tilde{D}_{m+1} \underset{\sim}{G}_m(x)\} = - a_1 \sum_{m=0}^{N} \tilde{D}_{m+1} \underset{\sim}{A}_m \quad , \tag{5.60}$$

$$\sum_{m=0}^{N} \{\tilde{R}_m(\eta) \underset{\sim}{F}_m(x) - \tilde{S}_m(\eta) \underset{\sim}{G}_m(x)\} = e^{-\frac{x}{\eta}} \sum_{m=0}^{N} [(1-a_1) \tilde{R}_m(\eta) - \tilde{S}_m(\eta)] \underset{\sim}{A}_m \quad , \tag{5.61}$$

$$\sum_{m=0}^{N} \{\tilde{P}_m(\eta) \underset{\sim}{F}_m(x) - \tilde{S}_m(\eta) \underset{\sim}{G}_m(x)\} = e^{-\frac{x}{\eta}} \sum_{m=0}^{N} [(1-a_1) \tilde{P}_m(\eta) - \tilde{T}_m(\eta)] \underset{\sim}{A}_m \quad , \tag{5.62}$$

$$\sum_{m=0}^{N} \{\tilde{S}_m(\eta) \underset{\sim}{F}_m(x) - \tilde{R}_m(\eta) \underset{\sim}{G}_m(x)\} = e^{\frac{x}{\eta}} \sum_{m=0}^{N} [(1-a_1) \tilde{S}_m(\eta) - \tilde{R}_m(\eta)] \underset{\sim}{A}_m \, , \tag{5.63}$$

and

$$\sum_{m=0}^{N} \{\tilde{T}_m(\eta) \underset{\sim}{F}_m(x) - \tilde{P}_m(\eta) \underset{\sim}{G}_m(x)\} = e^{\frac{x}{\eta}} \sum_{m=0}^{N} [(1-a_1) \tilde{T}_m(\eta) - \tilde{P}_m(\eta)] \underset{\sim}{A}_m \, , \tag{5.64}$$

to be solved. We observe that the two element vectors $\underset{\sim}{C}_m$, $\underset{\sim}{D}_m$, $\underset{\sim}{S}_m(\eta)$, $\underset{\sim}{T}_m(\eta)$, $\underset{\sim}{R}_m(\eta)$ and $\underset{\sim}{P}_m(\eta)$ appearing in equations

(5.57-5.64) are the same as used in (5.22-5.29) and thus no new quantities need to be evaluated. Finally we note that the matrix of coefficients in (5.57-5.64) is independent of x. The solution of these equations for many values of x can thus be achieved at modest computational cost, since one matrix inversion is sufficient for all $0<x<\delta$. We evaluate equations (5.61-5.64) at N values of $0<\eta<\infty$ to achieve along with equations (5.57-5.60) a total of 4N+4 equations for the 4N+4 unknowns $\{F_m(x)\}$ and $\{G_m(x)\}$. This system of equations is then solved for $\{F_m(x)\}$ and $\{G_m(x)\}$ at each value of x of interest. With the F_N expansion coefficients known at each x the perturbed particle distribution $\psi(x,\mu)$ at each x can be estimated directly through (5.55) and (5.56) and as a result the heat flux and the temperature and density profiles follow immediately from equations (5.4), (5.2) and (5.3).

Although the detailed behavior of the distribution function is very difficult to be predicted, this approach allows us to calculate the reduced distribution function

$$\phi(x,\xi_1) \triangleq \int_{-\infty}^{\infty}\int_{-\infty}^{\infty} f(x,\xi)\, d\xi_2\, d\xi_3 \quad , \tag{5.65}$$

where $f(x,\mu)$ is the molecular distribution function at location x and velocity $\xi=(\xi_1,\xi_2,\xi_3)$. It is shown in section 9.5 of the appendices that

$$\phi(x,\mu) = \frac{\rho_1}{(2\pi RT_1)^{\frac{1}{2}}} \left\{ 1 + \frac{\Delta T}{\sqrt{\pi}\, T_1} \left| \begin{matrix} 1 \\ 0 \end{matrix} \right|^{T} \underset{\sim}{\psi}(x,\mu) \right\} e^{-\mu^2} \tag{5.66}$$

and

$$\phi_M(x,\mu) = \frac{\rho_1}{(2\pi RT_1)^{\frac{1}{2}}} \left\{ 1 + \frac{x}{\delta} \frac{\Delta T}{T_1} \left(\mu^2 - \frac{3}{2} \right) \right\} e^{-\mu^2} \quad , \tag{5.67}$$

where $\Delta T = T_2 - T_1$, $\mu = \xi_1/(2RT_1)^{1/2}$, $\phi(x,\mu)$ is the reduced molecular distribution function and $\phi_M(x,\mu)$ denotes the reduced Maxwellian at each location in the slab.

5.5 Numerical Results

First of all we have used an elementary transformation to map the interval $(0,\infty)$ into $(0,1)$ and subsequently used a Gaussian quadrature integration procedure in the same manner used for the two half space problems to evaluate the required integrals. In solving the system of linear algebraic equations given by (5.22-5.29) and (5.57-5.64) we have used for various orders of the F_N approximation the roots of the Hermite polynomial as the collocation points. As noted in the foregoing discussion we now have available a complete formalism that yields the distribution $\underset{\sim}{\psi}(x,\mu)$ for all $-\infty<\mu<\infty$ and all $0<x<\delta$. It is seen that the desired results for the heat flux and the temperature and density profiles can be evaluated by estimating the expansion coefficients A_α, $\alpha=1,2,3,4$ and $A_\alpha(\eta)$, $\alpha=1,2$, $-\infty<\eta<\infty$, or

directly through equations (5.2), (5.3) and (5.4).

In Tables 5.1 and 5.2 we illustrate the convergence of the F_N method by tabulating values of the normalized heat flux q as computed from equations (5.4) or (5.42) vs. the order of the approximation N. We also show the exact results based on half-range analysis [102]. It is seen that we were able to obtain $q(\delta)$ for $18<N<26$ accurate to five or six significant figures for inverse Knudsen number $\delta>1.0$ and $\delta<0.01$. In fact, only a fourth-order approximation is adequate to give results correct to four significant figures, while for the special case of $\delta=0$ the correct value of unity was achieved to ten significant figures.

However, for $0.01<\delta<1.0$ four significant figures seem to be the limit for the approximation of the form shown in equations (5.20) and (5.21). Although the convergence of the generated numerical results is evident, a 24th order approximation, which leads to a system of 100 linear algebraic equations, is not high enough to give better accuracy. Larger values of N than those in Tables 5.1 lead to a numerically ill-conditioned matrix with respect to inversion and consequently to numerical difficulties. It is possible that some modification of the basis function of the F_N approximations only for the case of $0.01<\delta<1.0$ could lead to improved numerical results. However, the complexity of equation (9.22) does not allow, for reasons given in section 9.3 of the appendices, any suggestions for better

formulation of the basis function and only unjustified guesses can be made. As an alternative scheme of basis functions, based on equation (9.22), we recommend the approximation

$$\underset{\sim}{\psi}\left(-\frac{\delta}{2}, \mu\right) = \underset{\sim}{Q}(\mu) \sum_{\alpha=0}^{N} \underset{\sim}{A}_{\alpha}[1 - (-1)^{\alpha} e^{-\frac{\delta}{\mu}}] \mu^{\alpha} \tag{5.68}$$

which might lead to more rapidly converging numerical results.

To attempt to establish confidence in our calculations a number of additional calculations were performed. For example we have satisfied equation (5.8) by a difference of less than one part in 10^{11}, using the two F_N expansions given by equations (5.55) and (5.56) to approximate the distribution function at each x. We have computed the heat flux q at each x in the slab, based on the expressions (5.55), (5.56) and (5.4), and agreement with the value of q based on equation (5.42) was achieved to eight significant figures. Finally, the number of nodal points in the quadrature scheme was increased until such calculations failed to alter the reported values of the heat flux and temperature and density profiles.

We list converged results for the heat flux by comparison to references [55,103] in Table 5.3 for several different values of the accommodation coefficients and for δ=5.0. At least five significant figure accuracy was obtained for all values of a tested.

Temperature and density profiles are shown in Tables 5.4 and 5.5 as computed from equations (5.2) and (5.3), using the x-dependent approximation, for representative values of a and δ. For most cases five or six significant figures are correct.

In figures 5.1 and 5.2 we show the temperature and density profiles for the anti-symmetric case $a_1=a_2=1.0$ and in figures 5.3 and 5.4 the same profiles for the more general case of $a_1=0.7$ and $a_2=0.3$, for different values of δ. In the last two figures the magnitude of the temperature and density jump at $x=\delta$ is larger than at $x=0$ since $a_1>a_2$. It is evident that the kinetic theory solution is valid through the whole range of the Knudsen number, which predicts three regimes. The first regime ($\delta<0.1$) is devoted to free molecular conduction and the flat temperature and density profiles between the plates are due to the highly rarefied conditions. Conduction in gases in the second regime ($\delta>10$) is characterized by the temperature and density jump and the linear temperature and density profiles as $\delta\to\infty$ are predicted by Fourier's law and the law of ideal gases at equilibrium. Finally, the third section shows how the connection between the two preceding regimes can be made in what we call the transition regime ($0.1<\delta<10$).

In figures 5.5 and 5.6 we show the dependence of the normalized heat flux q on the distance δ, and the accommodation coefficients a_1, a_2 respectively.

The reduced distribution function given by equation (5.66) is shown in figure 5.7 at $x=0$ and $x=\delta$. We also show the local Maxwellian distribution at the same locations for comparison. Although the increased departure from equilibrium at the right boundary $x=\delta$ is evident, the perturbation in the distribution function is still small enough to justify a linear analysis.

Finally in figure 5.8 the reduced distribution function is plotted with respect to x with μ as a parameter. The similarity of these plots with the density profiles shown in figures 5.2 and 5.4 is obvious and can be explained easily considering the fact that integration of the reduced distribution function over all μ leads directly to the definition of density. We note that explicit information about the distribution function can only be obtained through the position-dependent analysis based on the two F_N approximations given by equations (5.55) and (5.56).

Table 5.1 Convergence of the Normalized Heat Flux for $a_1 = 0.7$ and $a_2 = 0.3$

Distance Between Plates	Order of the Approximation							
	4	8	12	16	18	20	22	24
0.0	1.000000	1.000000						
0.001	0.999815	0.999810	0.999807	0.999806	0.999805	0.999804	0.999804	0.999803
0.01	0.998157	0.998105	0.998080	0.998064	0.998057	0.998053	0.998049	0.998046
0.5	0.921005	0.920651	0.920647	0.920696	0.920723	0.920745	0.920769	0.920778
1.0	0.861922	0.862139	0.862257	0.862297	0.862302	0.862297	0.862291	0.862289
2.0	0.772297	0.772374	0.772335	0.772303	0.772293	0.772293		
3.0	0.703051	0.703017	0.702982	0.702977	0.702979	0.702979		
4.0	0.646558	0.646515	0.646503	0.646506	0.646507	0.646506	0.646505	0.646505
5.0	0.599104	0.599068	0.599065	0.599065	0.599064	0.599063	0.599062	0.599062
7.0	0.523124	0.523010	0.523097	0.523094	0.523093	0.523093	0.523092	0.523092
10.0	0.439993	0.439978	0.439975	0.439973	0.439972	0.439972	0.439971	0.439971
100.0	0.0765027	0.0765023	0.0765022	0.0765022	0.0765022	0.0765021	0.0765021	

Table 5.1 (cont.) Convergence of normalized heat flux for $a_1 = 0.7$ and $a_2 = 0.3$

Distance Between Plates	Converged Results	Exact[102]
0.0	1.000000	1.000000
0.001	0.999802	0.999794
0.01	0.99804	0.997966
0.5	0.9208	0.920840
1.0	0.86229	0.862238
2.0	0.772293	0.772293
3.0	0.702979	0.702979
4.0	0.646504	0.646500
5.0	0.599062	0.599058
7.0	0.523092	0.523090
10.0	0.439971	0.439970
100.0	0.0765021	0.0765021

Table 5.2 Convergence of the normalized heat flux for $a_1 = 1.0$ and $a_2 = 1.0$

Distance Between Plates	Order of the Approximation							
	4	8	12	16	18	20	22	24
0.0	1.000000	1.000000						
0.001	0.999305	0.999286	0.999276	0.999270	0.999267	0.999266	0.999264	0.999263
0.01	0.993121	0.992937	0.992846	0.992789	0.992768	0.992753	0.992742	0.992735
0.1	0.937236	0.936212	0.935786	0.935558	0.935478	0.935425	0.935382	0.935340
1.0	0.640556	0.640797	0.640883	0.640903	0.640903	0.640898	0.640893	0.640889
2.0	0.489212	0.489249	0.489224	0.489207	0.489202	0.489203	0.489203	
3.0	0.398359	0.398339	0.398325	0.398323	0.398324	0.398324		
4.0	0.336746	0.336729	0.336725	0.336726	0.336726	0.336726	0.336726	0.336725
5.0	0.291933	0.291921	0.291920	0.291920	0.291920	0.291920	0.291919	0.291919
7.0	0.230819	0.230812	0.230812	0.230811	0.230811	0.230811	0.230810	0.230810
10.0	0.175793	0.175790	0.175789	0.175789	0.175788	0.175788		
100.0	0.0215931	0.0215931						

Table 5.2 (cont.) Convergence of normalized heat flux for $a_1 = 1.0$ and $a_2 = 1.0$

Distance Between Plates	Converged Results	Exact[102]
0.0	1.000000	1.000000
0.001	0.99926	0.999231
0.01	0.9927	0.992484
0.1	0.9353	0.935159
1.0	0.64090	0.640853
2.0	0.489203	0.489203
3.0	0.398324	0.398324
4.0	0.336725	0.336724
5.0	0.291919	0.291919
7.0	0.230810	0.230810
10.0	0.175788	0.175788
100.0	0.0215931	0.0215931

Table 5.3 Normalized heat flux for δ=5.0

a_1	a_2	Converged Results	Exact[55,102]
0.7	0.9	0.384792	0.384790
0.7	0.7	0.428231	0.428228
0.7	0.5	0.492920	0.492918
0.7	0.3	0.599062	0.599058
0.7	0.1	0.804266	0.804263
1.0	0.9	0.313373	0.313371
1.0	0.8	0.338420	0.338418
1.0	0.7	0.368048	0.368046
1.0	0.6	0.403647	0.403645
1.0	0.5	0.447229	0.447227

Table 5.4 Stable results of the temperature and density profiles for δ=2.0, a_1=0.7, a_2=0.3

DISTANCE	TEMPERATURE		DENSITY	
x	Converged Results	Exact[102]	Converged Results	Exact[102]
0.00	0.167208	0.162708	-0.077030	-0.077013
0.05	0.185460	0.185460	-0.097828	-0.097827
0.10	0.201816	0.201815	-0.112758	-0.112759
0.15	0.216388	0.216387	-0.126138	-0.126138
0.20	0.230009	0.230008	-0.138712	-0.138712
0.25	0.243045	0.243044	-0.150799	-0.150798
0.30	0.255699	0.255698	-0.162572	-0.162571
0.35	0.268104	0.268103	-0.174142	-0.174141
0.40	0.280355	0.280354	-0.185587	-0.185586
0.45	0.292528	0.292526	-0.196967	-0.196967
0.50	0.304688	0.304687	-0.208338	-0.208337
0.55	0.316899	0.316897	-0.219747	-0.219746
0.60	0.329226	0.329224	-0.231246	-0.231245
0.65	0.341742	0.341740	-0.242895	-0.242894
0.70	0.354539	0.354537	-0.254767	-0.254767
0.75	0.367735	0.367733	-0.266963	-0.266962
0.80	0.381505	0.381502	-0.279627	-0.279626
0.85	0.396120	0.396117	-0.292994	-0.292992
0.90	0.412078	0.412076	-0.307500	-0.307498
0.95	0.430531	0.430529	-0.324181	-0.324184
1.00	0.457969	0.457966	-0.349100	-0.349189

Table 5.5 Stable results of the temperature and density profiles for δ=5.0, a_1=1.0, a_2=0.5

DISTANCE	TEMPERATURE		DENSITY	
x	Converged Results	Exact[102]	Converged Results	Exact[102]
0.00	0.086631	0.086636	-0.040202	-0.040212
0.05	0.129544	0.129546	-0.080152	-0.080157
0.10	0.162129	0.162130	-0.111004	-0.111008
0.15	0.192182	0.192183	-0.139812	-0.139816
0.20	0.220969	0.220970	-0.167637	-0.167640
0.25	0.249012	0.249013	-0.194899	-0.194902
0.30	0.276591	0.276591	-0.221814	-0.221817
0.35	0.303875	0.303875	-0.248514	-0.248517
0.40	0.330985	0.330985	-0.275087	-0.275089
0.45	0.358011	0.358011	-0.301599	-0.301601
0.50	0.385032	0.385032	-0.328106	-0.328108
0.55	0.412125	0.412124	-0.354664	-0.354666
0.60	0.439368	0.439367	-0.381329	-0.381331
0.65	0.466856	0.466855	-0.408171	-0.408173
0.70	0.494712	0.494711	-0.435279	-0.435280
0.75	0.523105	0.523103	-0.462779	-0.462780
0.80	0.552291	0.552289	-0.490869	-0.490870
0.85	0.582700	0.582698	-0.519885	-0.519885
0.90	0.615159	0.615156	-0.550494	-0.550494
0.95	0.651696	0.651693	-0.584409	-0.584408
1.00	0.705115	0.705149	-0.633270	-0.633331

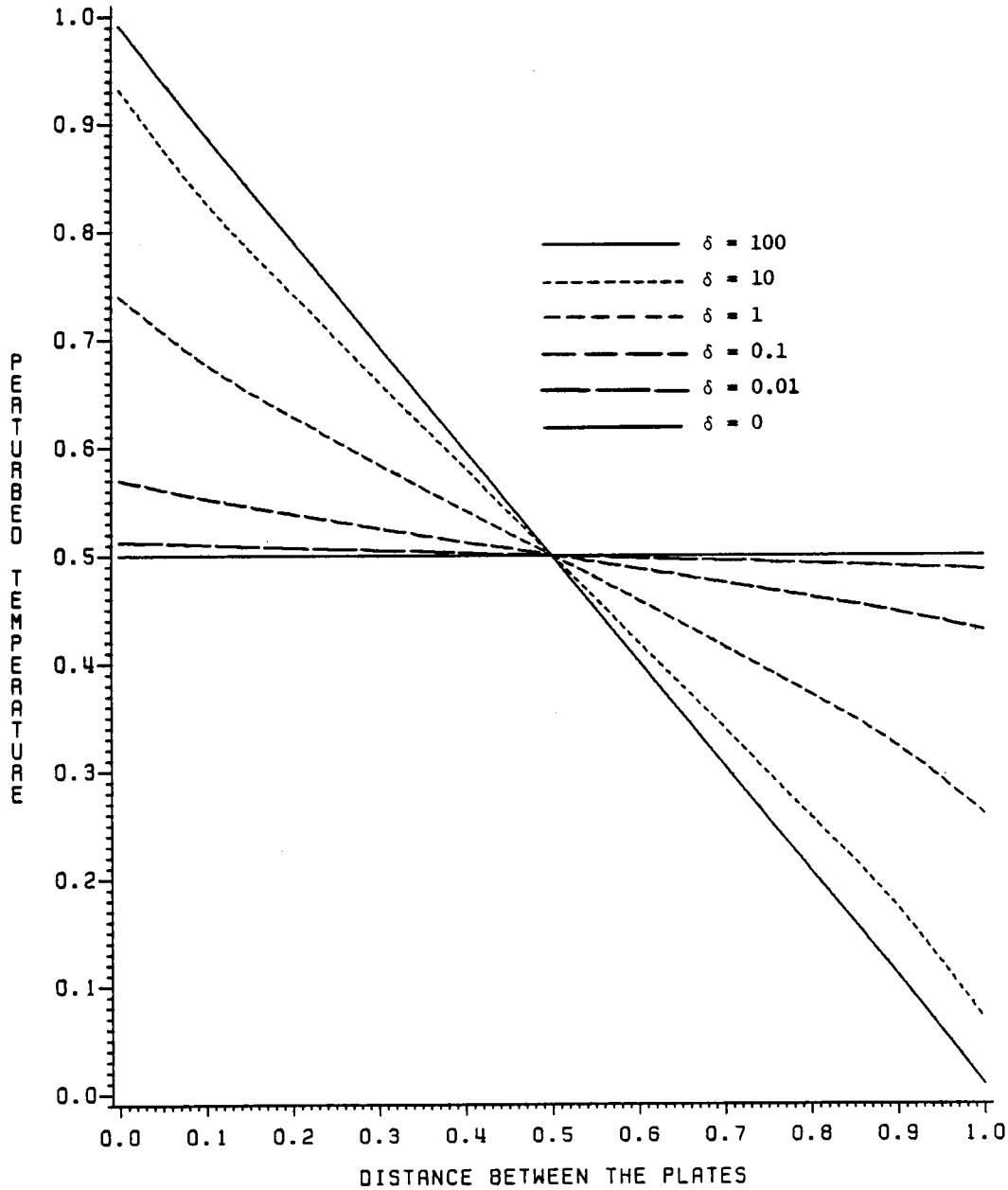

FIGURE 5.1 TEMPERATURE PROFILE BETWEEN THE TWO PARALLEL PLATES FOR A1=A2=1.0

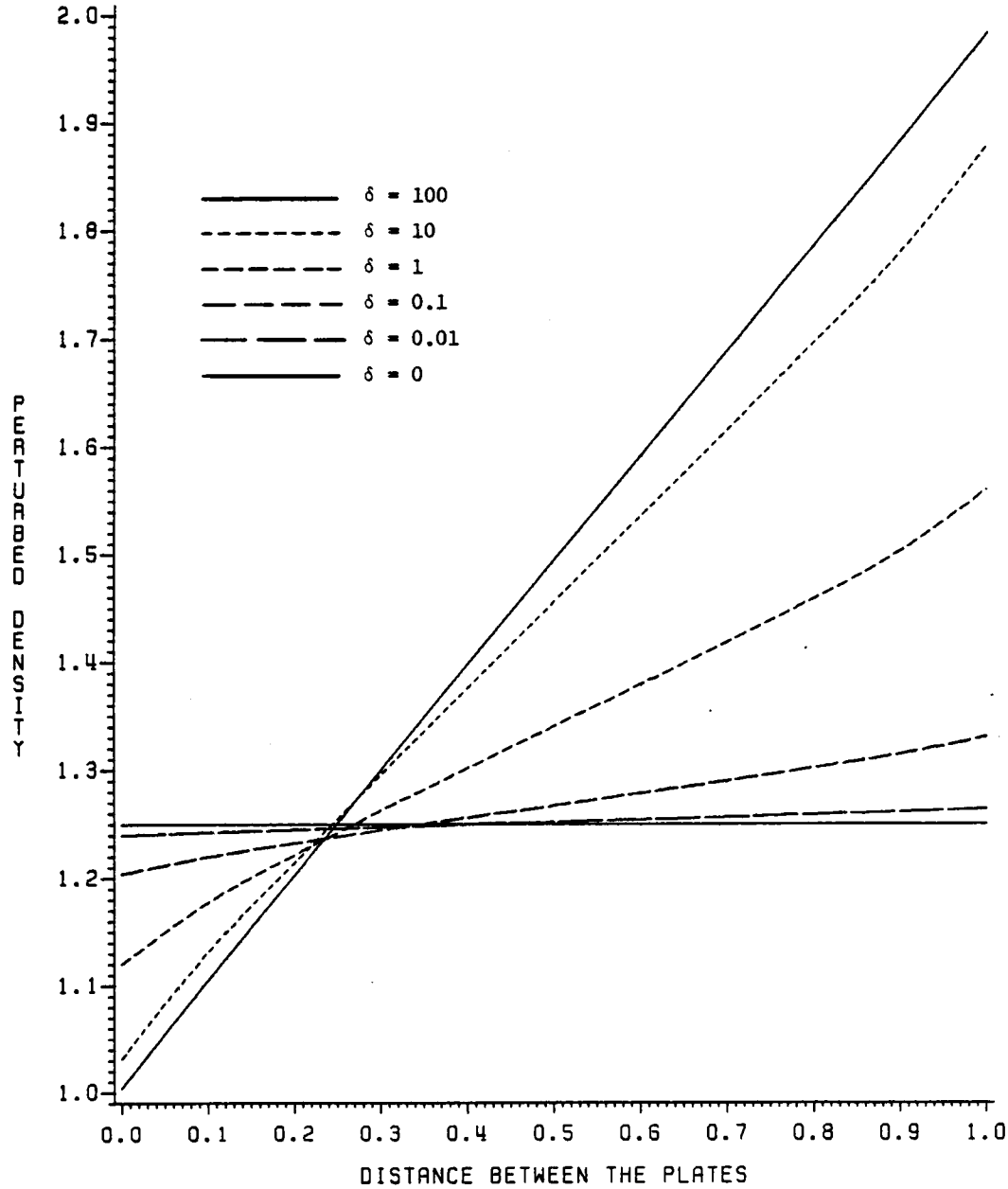

FIGURE 5.2 DENSITY PROFILE BETWEEN THE TWO PARALLEL PLATES FOR A1=A2=1.0

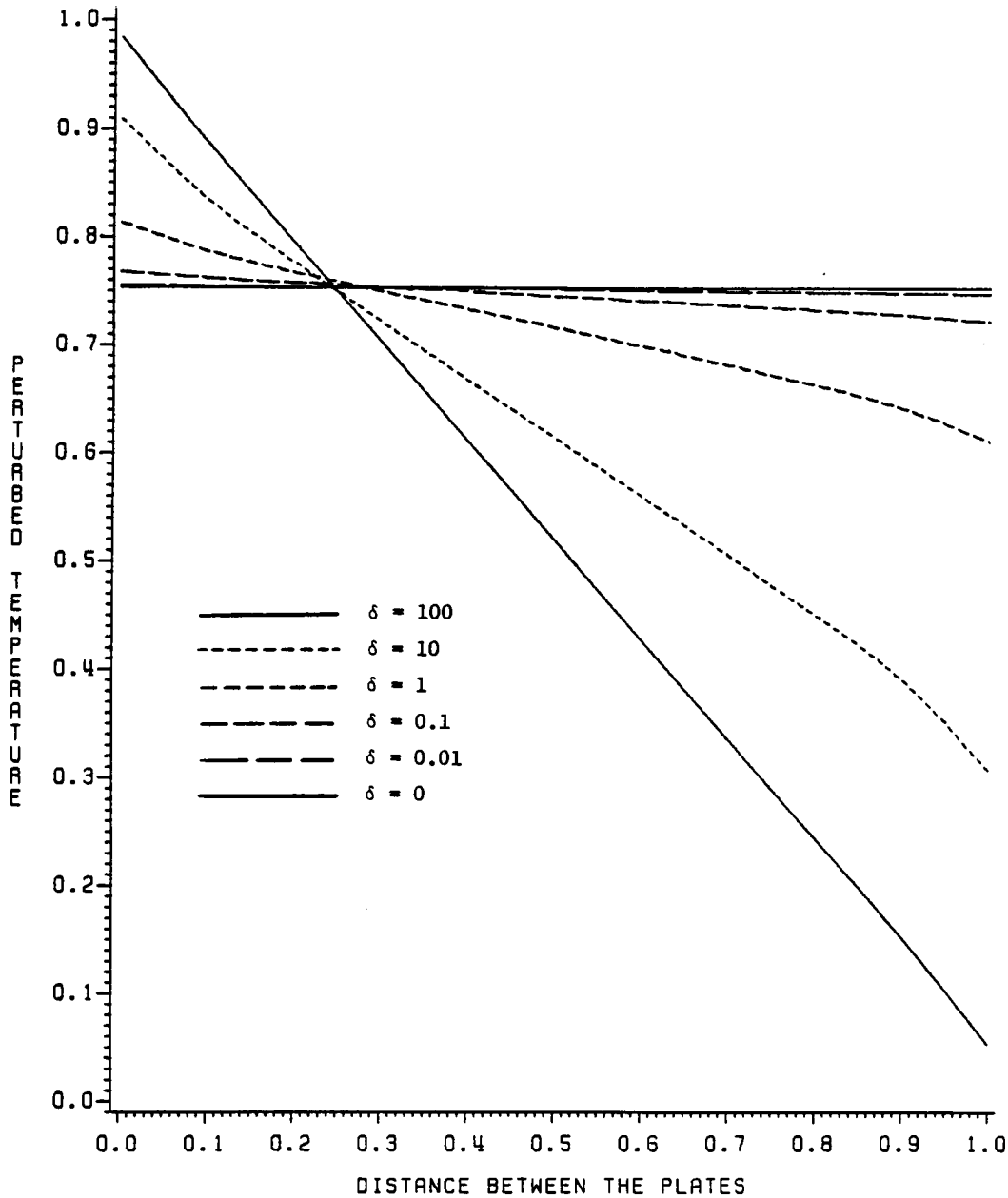

FIGURE 5.3 TEMPERATURE PROFILE BETWEEN THE TWO PARALLEL PLATES FOR A1=0.7, A2=0.3

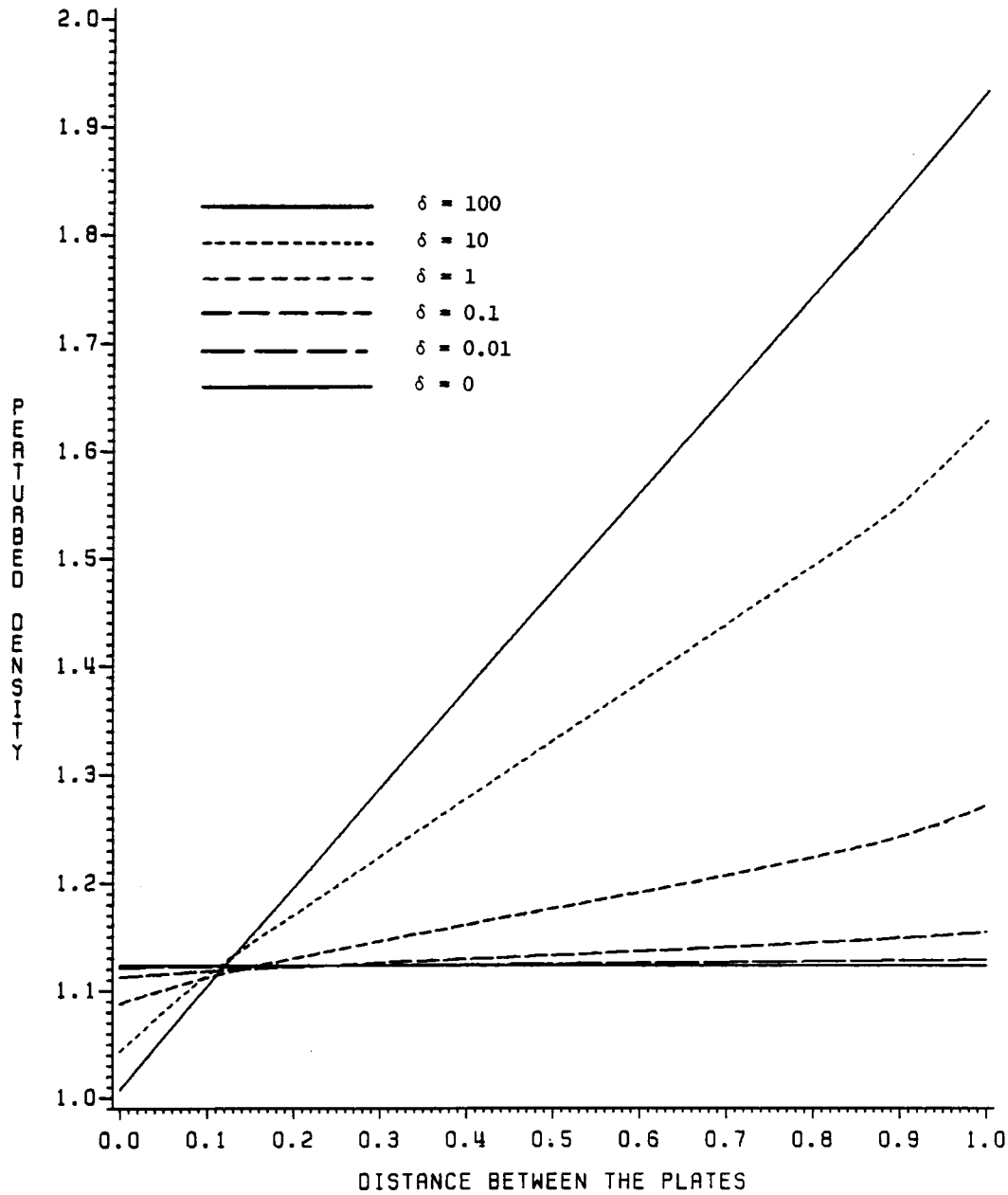

FIGURE 5.4 DENSITY PROFILE BETWEEN THE TWO PARALLEL PLATES FOR A1=0.7, A2=0.3

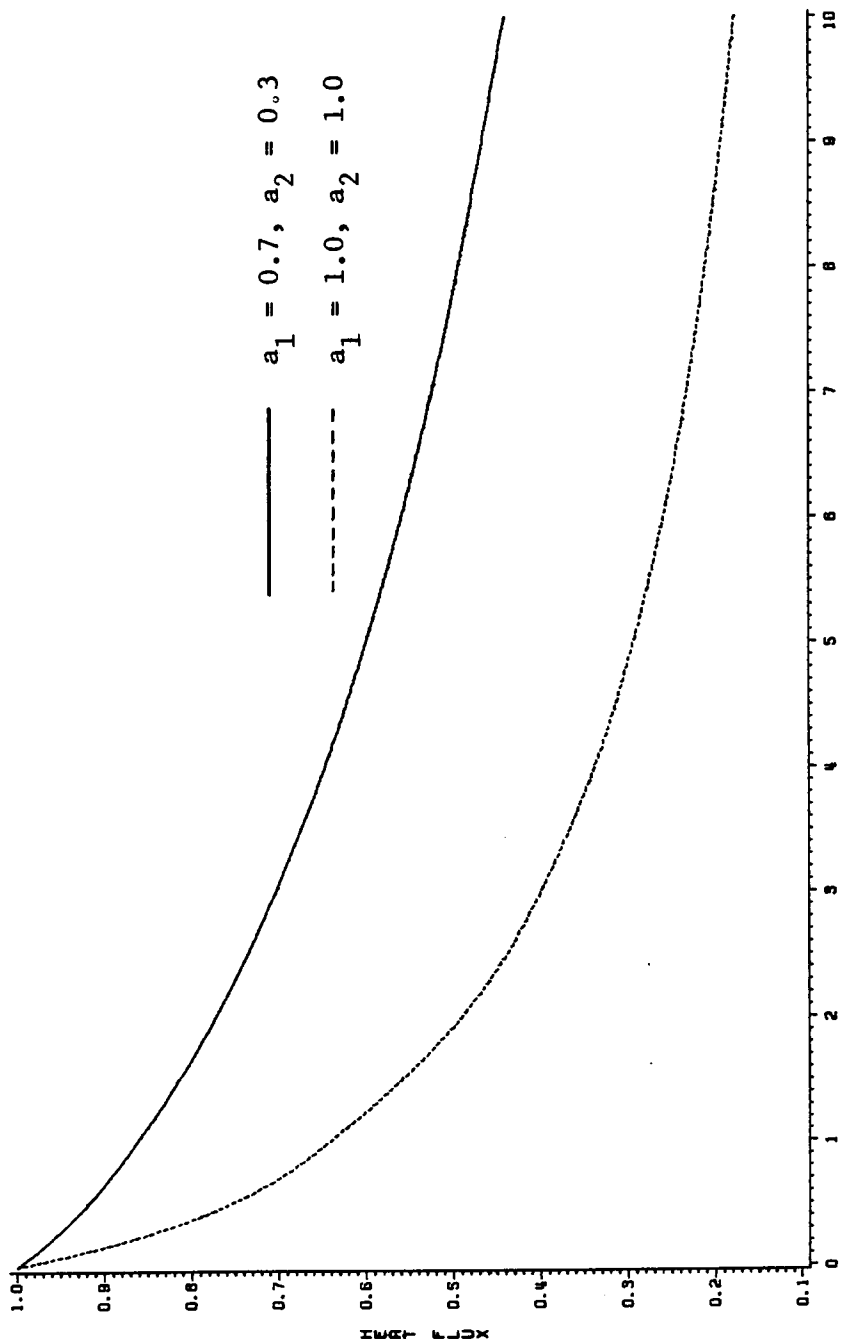

FIGURE 5.5 NORMALIZED HEAT FLUX VERSUS INVERSE KNUDSEN NUMBER

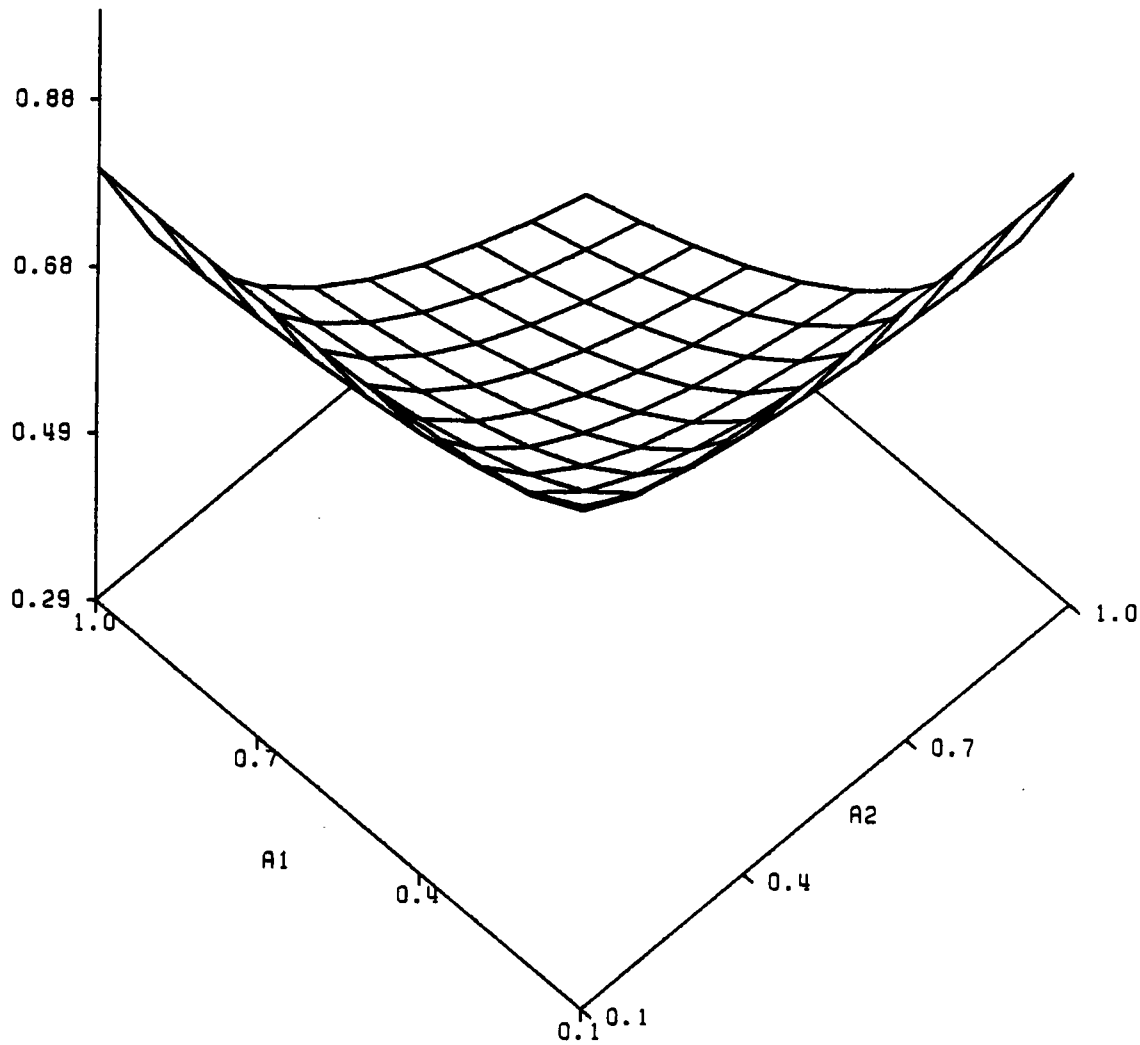

FIGURE 5.6 NORMALIZED HEAT FLUX FOR D=5.0 AND VARIABLE ACCOMMODATION COEFFICIENTS

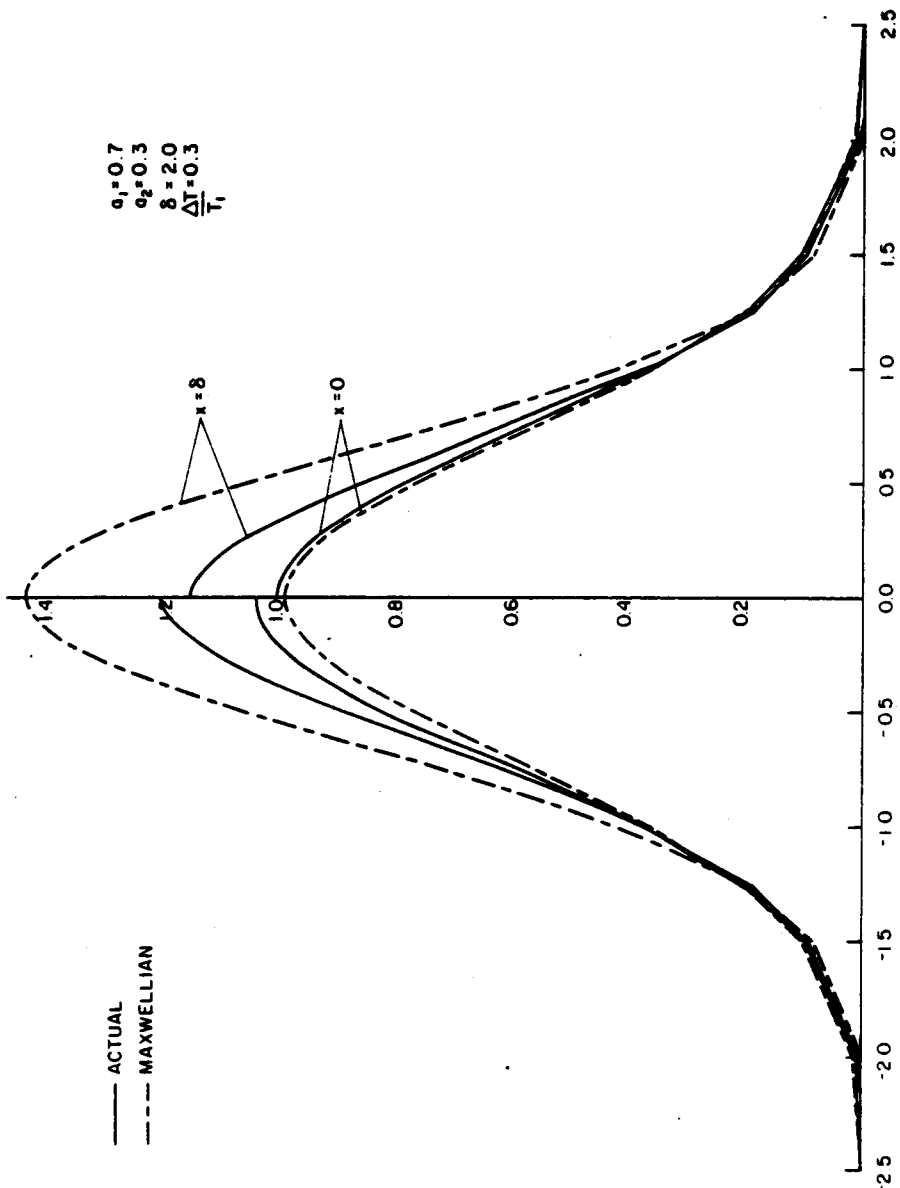

FIGURE 5.7 REDUCED DISTRIBUTION FUNCTION, EQ. (5.67), VERSUS THE X-COMPONENT OF VELOCITY

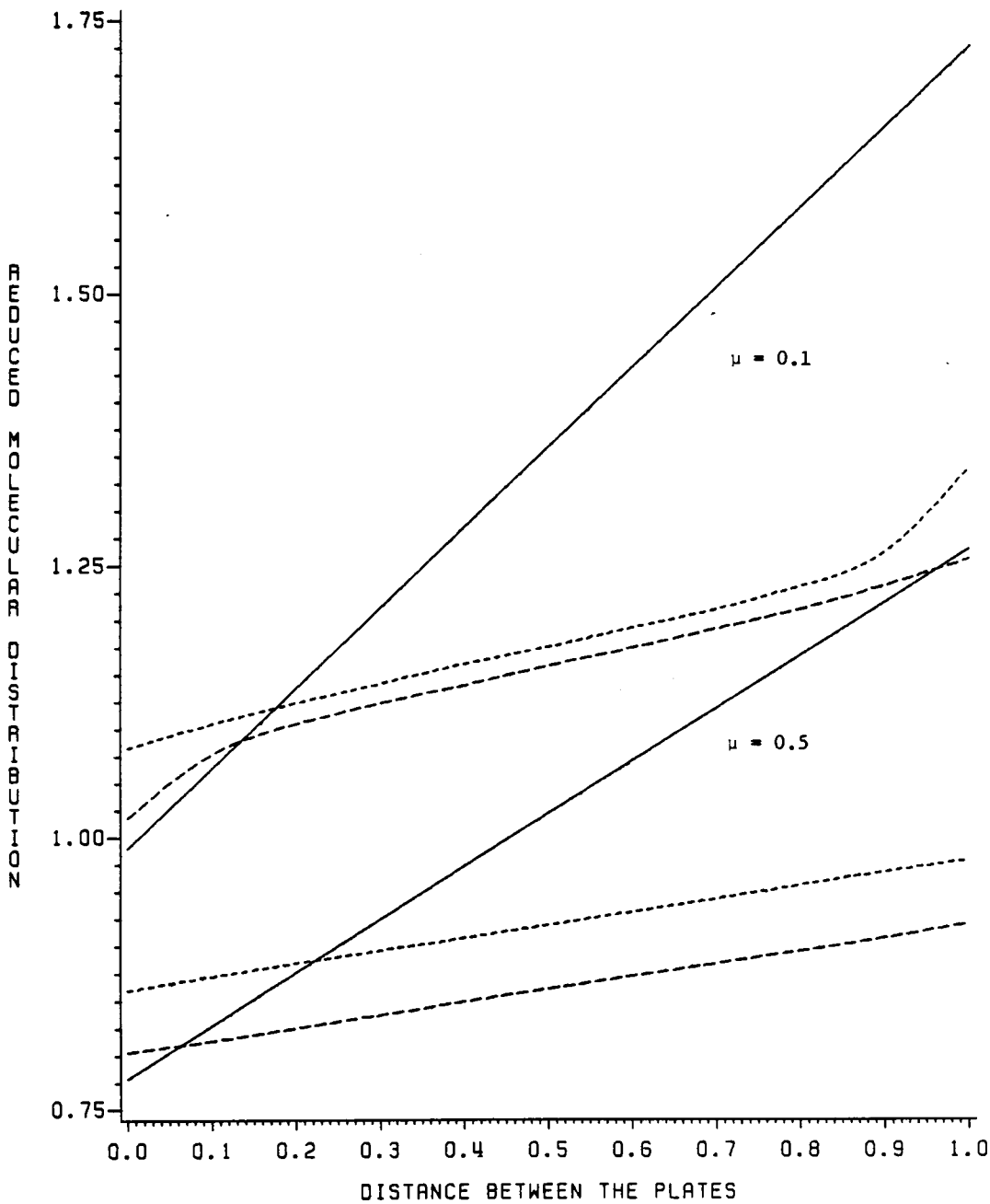

FIGURE 5.8 REDUCED MOLECULAR DISTRIBUTION FUNCTION PROFILE BETWEEN THE PLATES FOR D=2.0, A1=0.7 AND A2=0.3

6. POISEUILLE AND THERMAL CREEP FLOW OF A RAREFIED GAS IN A CYLINDRICAL TUBE

6.1 Introduction

Exact analysis of slip-flow problems in kinetic theory was originated by Cercignani [44,45,46,47], who adapted the method of elementary solutions [44], originated in neutron transport theory, to solve the Kramers problem [45], and the problems of plane Couette [46] and Poiseuille [47] flow. Cercignani later considered cylindrical Poiseuille flow and presented results computed by a direct numerical approach to the integral form of the BGK model [31]. Ferziger used the earlier work by Mitsis [49], who established the method of elementary solutions in cylindrical geometry, to derive analytical results for the cylindrical Poiseuille problem in the near free-molecule and near continuum regimes [48]. Loyalka [50] extended Ferziger's work to the thermal creep problem in a cylindrical tube and corrected earlier results of Sone and Yamamoto [103]. The accuracy of these results was improved in further work by Loyalka [37], who solved the Poiseuille and thermal creep problems for the case of diffuse-specular reflection in plane and cylindrical geometry, through numerical solution of the integral form of the BGK equation. Loyalka [37], who reported his results up to five significant figures, found that previously reported

results for the flow rate were in error by 10-15%. Finally, Loyalka, Petrellis and Storvick [60] used the method of elementary solutions to derive Fredholm integral equations for the plane Couette, Poiseuille, and thermal creep flow problems with the Maxwell diffuse-specular boundary condition. By iterating these equations, they provided highly accurate numerical results in plane geometry only, finding agreement with Loyalka's earlier results [37] to within 1%. Motivated by the success of their work, they encouraged further exploration of the numerical aspects of the method of elementary solutions. In our knowledge, no similarly accurate results were reported for the cylindrical case.

Quite recently, Siewert, Garcia, and Grandjean [80] used the F_N method [7,8] to compute highly accurate flow rates for Poiseuille flow in a plane channel. These results agreed with those of Loyalka, Petrellis and Storvick to five significant figures even though they were computed with a low-order approximation. The F_N method has been extended to cylindrical geometry for neutron transport problems by Thomas, Southers, and Siewert [71], and Siewert and Thomas [104,72].

In this chapter the F_N method is tested for the first time in cylindrical geometry in kinetic theory by developing a complete solution for the cylindrical Poiseuille flow and thermal creep problems, based on the linearized BGK model.

Highly accurate numerical results are presented for flow rates and velocity profiles throughout the complete Knudsen number range. In particular our numerical results, which we believe to be accurate to at least four significant figures, are in agreement with those of Loyalka [37] to within two to four significant figures.

Let us consider a gas flowing in a circular pipe of radius R, with the flow resulting from a density gradient which is supported by a pressure gradient (Poiseuille flow) or a temperature gradient (thermal creep flow). We assume that the walls re-emit the molecules with a Maxwellian distribution f_0 with constant temperature and an unknown density $\rho=\rho(z)$ where z is the coordinate parallel to the flow and R the inverse Knudsen number. Since we are considering a steady situation the corresponding linearized equations, following the formulation by Loyalka [50], can be written as

$$c_\perp\left(\cos\phi\,\frac{\partial h_P}{\partial r}-\frac{\sin\phi}{r}\,\frac{\partial h_P}{\partial\phi}\right)+h_P=\frac{2}{\pi^{3/2}}\,c_z\int c_z'\,h_P(r,c')\,e^{-c'^2}\,d^3c'+c_z, \tag{6.1}$$

for the Poiseuille (P) flow problem, subject to the boundary condition

$$h_P(R,c)=0\quad,\quad c_r<0\quad, \tag{6.2}$$

and

$$c_\perp \left(\cos\phi \frac{\partial h_{PT}}{\partial r} - \frac{\sin\phi}{r} \frac{\partial h_{PT}}{\partial \phi} \right) + h_{PT}$$

$$= \frac{2}{\pi^{3/2}} c_z \int c'_z \, h_{PT}(r,c') \, e^{-c'^2} \, d^3c' + c_z \left(c^2 - \frac{3}{2} \right) \quad , \tag{6.3}$$

for the (PT) problem, subject to the boundary condition

$$h_{PT}(R,c) = 0 \quad , \quad c_r < 0 \quad . \tag{6.4}$$

We will refer to the (PT) problem as the pseudo thermal creep problem, since $h_T = h_P - h_{PT}$. Here, h is a measure of the perturbation in the distribution $f = f_0(1+h)$ from the Maxwellian f_0, r is a radial coordinate measured in units of mean free paths, ϕ the angle coordinate, c the molecular velocity having components c_z, c_r, c_ϕ and $c_\perp^2 = c_r^2 + c_\phi^2$. Now both equations (6.1) and (6.3) can be transformed into the more convenient form of the integral equation [48]

$$Z(r) = \frac{2}{\sqrt{\pi}} \int_0^\infty \frac{e^{-\mu^2}}{\mu^2} d\mu \left[\int_0^r tZ(t) \, K_0(r/\mu) \, I_0(t/\mu) \, dt \right.$$

$$\left. + \int_r^R tZ(t) \, K_0(t/\mu) \, I_0(r/\mu) \, dt \right] + Y(r) \quad , \tag{6.5}$$

where I_0 and K_0 represent modified Bessel functions of the first and second kind, respectively. The function Z(r) is related to the velocity profiles in the Poiseuille and thermal creep problems through [50]

$$Z_p(r) = \sqrt{\pi} \; V_p(r) + \frac{1}{2} \quad , \tag{6.6}$$

and

$$Z_{PT}(r) = \sqrt{\pi}\ V_{PT}(r) + \frac{1}{4} \quad , \tag{6.7}$$

where

$$V_T(r) = V_p(r) - V_{PT}(r) \ . \tag{6.8}$$

In equation (6.5)

$$V_p(r) = \frac{\sqrt{\pi}}{2} \quad , \tag{6.9}$$

while

$$Y_{PT}(r) = \frac{\sqrt{\pi}}{4} + \int_0^\infty e^{-\mu^2}\, d\mu \left[\int_0^r t\, K_o(r/\mu)\, I_o(t/\mu)\, dt + \int_r^R t\, K_o(t/\mu)\, I_o(r/\mu)\, dt \right] \ . \tag{6.10}$$

6.2 Mathematical Formulation and General Solution of the Poiseuille Flow and Thermal Creep Problems.

In order to apply the F_N method for treating problems in cylindrical geometry relative to shear effects it is important to develop the governing integro-differential equation, analogous to the vector integro-differential equations (3.1) derived by Kriese, et al. to determine temperature and density effects in half-space and plane-

parallel media. Following Mitsis [49] if we define

$$\phi(r,\mu) = K_o(r/\mu) \int_0^r tZ(t)\, I_o(t/\mu)\, dt + I_o(r/\mu) \int_r^R tZ(t)\, K_o(t/\mu)\, dt \quad , \tag{6.11}$$

and differentiate twice invoking Leibnitz's integral formula, we find that $\phi(r,\mu)$ for $0<\mu<\infty$ and $0<r<R$ must satisfy the integro-differential equations

$$(B\phi_P)(r,\mu) = - Y_P(r) \quad , \tag{6.12}$$

and

$$(B\phi_{PT})(r,\mu) = - Y_{PT}(r) \quad , \tag{6.13}$$

where $Y_P(r)$ and $Y_{PT}(r)$ are given explicitly by (6.9) and (6.10) respectively. Here the subscripts P and PT have the same meanings as in equations (6.1) and (6.3), and the operator B is defined as

$$(Bf)(r,\mu) = \left(\frac{\partial^2}{\partial r^2} + \frac{1}{r}\frac{\partial}{\partial r} - \frac{1}{\mu^2}\right) f(r,\mu) + \frac{2}{\sqrt{\pi}} \int_0^\infty f(r,\mu)\, e^{-\mu^2}\, \frac{d\mu}{\mu^2} \quad . \tag{6.14}$$

Performing the integration over t in equation (6.10) and using the Wronskian relation [107]

$$z[I_o(z)\, K_1(z) + I_1(z)\, K_o(z)] = 1 \quad , \tag{6.15}$$

equation (6.10) can be written as

$$Y_{PT}(r) = \frac{\sqrt{\pi}}{2} - R \int_0^\infty \mu\, I_o(r/\mu)\, K_1(R/\mu)\, e^{-\mu^2}\, d\mu \quad . \tag{6.16}$$

Substituting equation (6.9) and (6.16) into equation (6.12) and (6.13) we find

$$(B\phi_P)(r,\mu) = -\frac{\sqrt{\pi}}{2} \quad , \tag{6.17}$$

and

$$(B\phi_{PT})(r,\mu) = -\frac{\sqrt{\pi}}{2} + R \int_0^\infty \mu\, I_o(r/\mu)\, K_1(R/\mu)\, e^{-\mu^2}\, d\mu \quad , \tag{6.18}$$

which are the governing equations to be solved for the Poiseuille and pseudo thermal creep flow problems respectively, subject to the common boundary conditions that $\phi(0,\mu)$ is bounded and

$$K_1(R/\mu)\, \phi(R,\mu) + \mu\, K_o(R/\mu)\, \frac{\partial}{\partial r}\, \phi(r,\mu)\Big|_{r=R} = 0 \quad , \quad \mu > 0 \quad . \tag{6.19}$$

It is important to note that equation (6.19) is a reduced boundary condition derived through mathematical manipulation of equation (6.11) while the physical Maxwellian boundary conditions (6.2) and (6.4) have been employed in the derivation of the integro-differential equations (6.17) and (6.18) respectively.

Proceeding, we find it convenient to modify slightly the pseudo thermal creep problem by introducing

$$X(r,\mu) = \phi_{PT}(r,\mu) - \frac{\sqrt{\pi}}{2} R \mu^3 K_1(R/\mu) I_o(r/\mu) \quad , \tag{6.20}$$

so that $X(r,\mu)$ is the solution of

$$(BX)(r,\mu) = -\frac{\sqrt{\pi}}{2} \quad , \tag{6.21}$$

which is analogous to equation (6.17), subject to the modified boundary condition

$$K_1(R/\mu) X(r,\mu) + \mu K_o(R/\mu) \left.\frac{\partial X(r,\mu)}{\partial r}\right|_{r=R} = -\frac{\sqrt{\pi}}{2} \mu^4 K_1(R/\mu) \quad , \quad \mu > 0 \quad . \tag{6.22}$$

It is seen at once that both the Poiseuille and pseudo thermal creep flow problems have been reduced to the problem of solving the same integro-differential equation subject to different boundary conditions.

The desired general solution of equation (6.17) or (6.21) can be expressed, as is shown in section 9.6 of the appendices, in terms of the elementary solutions [44] as

$$Y(r,\mu) = \mu^2 \left\{ C_o f_\infty + C_1 \ell\eta(r) + \int_0^\infty C(\xi) [f(\xi,\mu) + f(-\xi,\mu)] I_o(r/\xi) \, d\xi \right\} + g(r,\mu) \quad , \tag{6.23}$$

where $Y(r,\mu)$ represents $\phi_P(r,\mu)$ or $X(r,\mu)$, C_o, C_1 and $C(\xi)$ are the expansion coefficients to be determined by the boundary conditions (6.19) and (6.22), f_∞=1 and

$$f(\xi,\mu) = Pv\left(\frac{\xi}{\xi-\mu}\right) + \lambda(\xi)\ \delta(\xi-\mu) \quad , \tag{6.24}$$

with

$$\lambda(\xi) = e^{\xi^2}\left[\sqrt{\pi} + \int_{-\infty}^{\infty} Pv\left(\frac{\xi}{t-\xi}\right) e^{-t^2}\, dt\right] \quad . \tag{6.25}$$

In equation (6.24) $\delta(x)$ represents the Dirac delta functional and the Pv indicates that integrals are to be interpreted in the Cauchy principal-value sense. The eigenfunctions f_∞ and $f(\xi,\mu)$ are identical to the eigenfunctions given by Cercignani [44], who proved the full-range orthogonality and completeness theorems for the developed normal modes. He showed with usual techniques that the required orthogonality relations among eigenfunctions corresponding to different eigenvalues, and among continuous and discrete eigenfunctions are

$$\int_{-\infty}^{\infty} f(\xi,\mu)\ f(\xi',\mu)\ \mu e^{-\mu^2}\, d\mu = N(\xi)\ \delta(\xi-\xi') \quad , \tag{6.26}$$

$$\int_{-\infty}^{\infty} f(\xi,\mu)\ \mu e^{-\mu^2}\, d\mu = 0 \quad , \tag{6.27}$$

$$\int_{-\infty}^{\infty} f(\xi,\mu)\ \mu^2 e^{-\mu^2}\, d\mu = 0 \quad , \tag{6.28}$$

and

$$\int_{-\infty}^{\infty} f_\infty\ \mu\ e^{-\mu^2}\, d\mu = \int_{-\infty}^{\infty} \mu\, e^{-\mu^2}\, d\mu = 0 \quad , \tag{6.29}$$

where

$$N(\xi) = \xi e^{\xi^2} \left[\pi \lambda^2(\xi) + \pi \xi^2 e^{-2\xi^2}\right] \quad . \tag{6.30}$$

Finally we note that for the two particular problems under consideration $C_1=0$ since the solution must be bounded at $r=0$, while the particular solution

$$g(r,\mu) = -\frac{\sqrt{\pi}}{4} \mu^2(r^2 - R^2 + 4\mu^2) \quad , \tag{6.31}$$

may be verified by direct substitution into equations (6.17) or (6.21).

To proceed with the method of elementary solutions we would substitute equation (6.23) into (6.19) and (6.22) and use half-range orthogonality to obtain Fredholm-type integral equations for $C(\xi)$ for the Poiseuille flow and pseudo thermal creep problems respectively. However, instead of pursuing the method of elementary solutions, we prefer to establish $\phi_P(R,\mu)$ and $X(R,\mu)$ by introducing the F_N method.

6.3 The F_N Approximation

We start our approach by using the full-range orthogonality conditions (6.26) and (6.28) along with the reciprocity condition $Y(r,\mu)=Y(r,-\mu)$ to deduce from equation

(6.23) that

$$\int_0^\infty [f(\xi,\mu) - f(-\xi,\mu)]\, Y(r,\mu) e^{-\mu^2} \frac{d\mu}{\mu} = C(\xi)\, I_o(r/\xi)\, N(\xi)$$

$$- \frac{\sqrt{\pi}}{4} \int_0^\infty \mu[f(\xi,\mu) - f(\xi,-\mu)]\, (r^2 - R^2 + 4\mu^2)\, e^{-\mu^2}\, d\mu \quad , \qquad (6.32)$$

$$\int_0^\infty [f(\xi,\mu) - f(-\xi,\mu)]\, \frac{\partial Y}{\partial r}\, e^{-\mu^2} \frac{d\mu}{\mu} = C(\xi)\, I_1(r/\xi)\, \frac{N(\xi)}{\xi}$$

$$- \frac{\sqrt{\pi}}{2} r \int_0^\infty \mu[f(\xi,\mu) - f(\xi,-\mu)]\, e^{-\mu^2}\, d\mu \quad , \qquad (6.33)$$

$$\int_0^\infty Y(r,\mu)\, e^{-\mu^2}\, d\mu = \frac{\sqrt{\pi}}{4} C_o - \frac{\sqrt{\pi}}{4} \left[\frac{\sqrt{\pi}}{4} (r^2 - R^2) + \frac{3\sqrt{\pi}}{2}\right] \qquad (6.34)$$

and

$$\int_0^\infty \frac{\partial Y}{\partial r}\, (r,\mu)\, e^{-\mu^2}\, d\mu = - \frac{\pi}{8} r \qquad (6.35)$$

where

$$\frac{\partial Y(r,\mu)}{\partial r} = \mu^2 \left\{ \int_0^\infty C(\xi)\, [f(\xi,\mu) + f(-\xi,\mu)]\, I_1(r/\xi)\, \frac{d\xi}{\xi} - \frac{\sqrt{\pi}}{2} r \right\} \quad . \qquad (6.36)$$

We can eliminate the normalization factor $N(\xi)$ from equations (6.32) and (6.33) to obtain for $0<\xi<\infty$

$$\int_0^\infty [f(\xi,\mu) - f(\xi,-\mu)] \left[Y(r,\mu) - \xi \frac{I_o(r/\xi)}{I_1(r/\xi)} \frac{\partial Y(r,\mu)}{\partial r}\right] e^{-\mu^2} \frac{d\mu}{\mu}$$

$$= - \frac{\sqrt{\pi}}{4} \int_0^\infty [f(\xi,\mu) - f(\xi,-\mu)] \left[r^2 - R^2 + 4\mu^2 - 2r\xi \frac{I_o(r/\xi)}{I_1(r/\xi)}\right] \mu\, e^{-\mu^2}\, d\mu \quad . \qquad (6.37)$$

By setting r=R in equations (6.37) and (6.35) and using the boundary conditions (6.19) and (6.22) in the manner explained by Thomas, et al. [71] we deduce the singular integral equations

$$\int_0^\infty [f(\xi,\mu) - f(\xi,-\mu)][\mu + \xi \equiv (R;\xi,\mu)]\, \phi_p(R,\mu)\, e^{-\mu^2}\, \frac{d\mu}{\mu^2} = \frac{\pi\xi}{2} \quad , \tag{6.38}$$

and

$$\int_0^\infty \frac{K_1(R/\mu)}{K_o(R/\mu)}\, \phi_p(R,\mu)\, e^{-\mu^2}\, \frac{d\mu}{\mu} = \frac{\pi R}{8} \quad , \tag{6.39}$$

for the Poiseuille flow problem and similarly

$$\int_0^\infty [f(\xi,\mu) - f(\xi,-\mu)][\mu + \xi \equiv (R;\xi,\mu)]\, X(R,\mu)\, e^{-\mu^2}\, \frac{d\mu}{\mu^2} = \frac{\pi\xi}{2}$$

$$- \frac{\sqrt{\pi}}{2}\, \xi \int_0^\infty [f(\xi,\mu) - f(\xi,-\mu)] \equiv (R;\xi,\mu)\, \mu^2\, e^{-\mu^2}\, d\mu \quad , \tag{6.40}$$

and

$$\int_0^\infty \frac{K_1(R/\mu)}{K_o(R/\mu)}\, X(R,\mu)\, e^{-\mu^2}\, \frac{d\mu}{\mu} = \frac{\pi R}{8} - \frac{\sqrt{\pi}}{2} \int_0^\infty \frac{K_1(R/\mu)}{K_o(R/\mu)}\, \mu^3\, e^{-\mu^2}\, d\mu \tag{6.41}$$

for the "PT" problem, where

$$\equiv (R;\xi,\mu) = \frac{I_o(R/\xi) \cdot K_1(R/\mu)}{I_1(R/\xi) \cdot K_o(R/\mu)} \tag{6.42}$$

It is seen that equations (6.38-6.41), which have been derived without any approximation, represent two sets of singular integral equations each to be solved for the unknown surface functions $\phi_p(R,\mu)$ and $X(R,\mu)$.

At this point we introduce the F_N method to construct a concise approximate solution. We substitute the two F_N approximations, which have been formulated by the method shown in appendix 9.7,

$$\phi_p(R,\mu) = \left\{\frac{1}{\mu} K_o(R/\mu)\ I_1(R/\mu)\right\}^{w(R)} \sum_{\alpha=0}^{N} A_\alpha\ \mu^{\alpha+2} \tag{6.43}$$

and

$$X(R,\mu) = -\frac{\sqrt{\pi}}{2}\mu^4\ w(R) + \left\{\frac{1}{\mu} K_o(R/\mu)\ I_1(R/\mu)\right\}^{w(R)} \sum_{\alpha=0}^{N} B_\alpha\ \mu^{\alpha+2} \quad , \tag{6.44}$$

where $\{\mu^\alpha\}$ is the set of the basis functions and the constants $\{A_\alpha\}$ and $\{B_\alpha\}$ are to be determined, into the two sets of equations (6.37), (6.38) and (6.39), (6.40). By setting $w(R)=1$ we obtain

$$\sum_{\alpha=0}^{N} \left[E_\alpha(\xi) + \xi \frac{I_o(R/\xi)}{I_1(R/\xi)} D_\alpha(\xi)\right] A_\alpha = \frac{\pi\xi}{2} \quad , \tag{6.45}$$

$$\sum_{\alpha=0}^{N} S_\alpha\ A_\alpha = \frac{\pi R}{8} \quad , \tag{6.46}$$

$$\sum_{\alpha=0}^{N} \left[E_\alpha(\xi) + \xi \frac{I_o(R/\xi)}{I_1(R/\xi)} D_\alpha(\xi)\right] B_\alpha = \frac{\pi\xi}{4} \quad , \tag{6.47}$$

and

$$\sum_{\alpha=0}^{N} S_\alpha\ B_\alpha = \frac{\pi R}{8} \quad . \tag{6.48}$$

Here we have used the definitions

$$E_\alpha(\xi) = \int_0^\infty [f(\xi,\mu) - f(\xi,-\mu)]\, K_o(R/\mu)\, I_1(R/\mu)\, \mu^\alpha\, e^{-\mu^2}\, d\mu \quad , \tag{6.49}$$

$$D_\alpha(\xi) = \int_0^\infty [f(\xi,\mu) - f(\xi,-\mu)]\, K_1(R/\mu)\, I_1(R/\mu)\, \mu^{\alpha-1}\, e^{-\mu^2}\, d\mu \quad , \tag{6.50}$$

and

$$S_\alpha = \int_0^\infty K_1(R/\mu)\, I_1(R/\mu)\, \mu^\alpha\, e^{-\mu^2}\, d\mu \quad . \tag{6.51}$$

In order to establish a complete solution that is accurate for all values of R, it is required to use the approximations as they are given explicitly by equations (6.43) and (6.44), with w(R)=1, while the simple polynomial approximations obtained by setting w(R)=0

$$\phi_p(R,\mu) = \mu^2 \sum_{\alpha=0}^{N} A_\alpha\, \mu^\alpha \tag{6.52}$$

and

$$X(R,\mu) = \mu^2 \sum_{\alpha=0}^{N} B_\alpha\, \mu^\alpha \quad , \tag{6.53}$$

can be used to establish an accurate solution only for selected values of R.

It is easy to show that $D_\alpha(\xi)$ and $E_\alpha(\xi)$ may be computed for $0<\xi<\infty$ from the explicit formulas

$$D_\alpha(\xi) = \xi^{\alpha-1} K_1(R/\xi)\, I_1(R/\xi)\, [\sqrt{\pi} - \xi \int_0^\infty \frac{e^{-\mu^2}}{\mu+\xi}\, d\mu]$$

$$- \xi^\alpha \int_0^\infty \frac{K_1(R/\xi)\, I_1(R/\xi) - K_1(R/\mu)\, I_1(R/\mu)}{\xi - \mu}\, e^{-\mu^2}\, d\mu$$

$$+ (-\xi)^\alpha \int_0^\infty K_1(R/\mu)\, I_1(R/\mu)\, \frac{e^{-\mu^2}}{\mu+\xi}\, d\mu$$

$$- \int_0^\infty K_1(R/\mu)\, I_1(R/\mu) \sum_{m=0}^{\alpha-2} \mu^m \xi^{\alpha-1-m} [1 + (-1)^{\alpha-2-m}]\, e^{-\mu^2}\, d\mu \quad (6.54)$$

and

$$E_\alpha(\xi) = \xi^\alpha K_o(R/\xi)\, I_1(R/\xi)\, [\sqrt{\pi} - \xi \int_0^\infty \frac{e^{-\mu^2}}{\xi+\mu}\, d\mu]$$

$$- \xi^{\alpha+1} \int_0^\infty \frac{K_o(R/\xi)\, I_1(R/\xi) - K_o(R/\mu)\, I_1(R/\mu)}{\xi - \mu}\, e^{-\mu^2}\, d\mu$$

$$+ (-\xi)^{\alpha+1} \int_0^\infty K_o(R/\mu)\, I_1(R/\mu)\, \frac{e^{-\mu^2}}{\mu+\xi}\, d\mu$$

$$- \int_0^\infty K_o(R/\mu)\, I_1(R/\mu) \sum_{m=0}^{\alpha-1} \mu^m\, \xi^{\alpha-m}\, [1 + (-1)^{\alpha-1-m}]\, e^{-\mu^2}\, d\mu\,, \quad (6.55)$$

or can be readily generated from the recursion formulas

$$D_\alpha(\xi) = \xi^2 D_{\alpha-2}(\xi) - 2\xi \int_0^\infty K_1(R/\mu)\, I_1(R/\mu)\, \mu^{\alpha-2}\, e^{-\mu^2}\, d\mu \quad (6.56)$$

and

$$E_\alpha(\xi) = \xi^2 E_{\alpha-2}(\xi) - 2\xi \int_0^\infty K_o(R/\mu)\, I_1(R/\mu)\, \mu^{\alpha-1}\, e^{-\mu^2}\, d\mu \quad , \quad (6.57)$$

where the starting functions $D_0(\xi)$, $D_1(\xi)$, $E_0(\xi)$ and $E_1(\xi)$ may be obtained from equations (6.54) and (6.55) by setting $\alpha=0,1$, and neglecting the summation terms.

We note that the elements of the two matrices of coefficients in (6.45), (6.46) and (6.47),(6.48) corresponding to the two problems under consideration are the same. The solution of these equations, with respect to inversion of the known matrix, can be computed only once to minimize computational cost. For each problem an Nth order approximation results in N+1 unknowns A_α, $\alpha=0,1,\ldots N$ for the Poiseuille flow problem and B_α, $\alpha=0,1,2\ldots,N$ for the pseudo thermal creep problem. Evaluating equations (6.45) and (6.47) at N distinct values of $\xi\varepsilon[0,\infty)$ leads clearly to a system of N+1 linear algebraic equations in each case:

$$\begin{bmatrix} \sum_{\alpha=0}^{N} [E_\alpha(\xi_1) + \xi_1 \frac{I_o(R/\xi_1)}{I_1(R/\xi_1)} D_\alpha(\xi_1)] \\ \vdots \\ \sum_{\alpha=0}^{N} [E_\alpha(\xi_N) + \xi_N \frac{I_o(R/\xi_N)}{I_1(R/\xi_N)} D_\alpha(\xi_N)] \\ \sum_{\alpha=0}^{N} S_\alpha \end{bmatrix} \begin{bmatrix} x_1 \\ \vdots \\ x_N \\ x_{N+1} \end{bmatrix} = \frac{\pi}{4} \begin{bmatrix} 2\xi_1 , \xi_1 \\ \vdots \quad \vdots \\ 2\xi_N , \xi_N \\ \frac{R}{2} , \frac{R}{2} \end{bmatrix}, \tag{6.58}$$

where the first and second column on the right hand side vector correspond to the Poiseuille flow and "PT" problems respectively, while the matrix of coefficients remains the same.

These equations may be solved straightforwardly to find the required constants A_α and B_α, $\alpha=0,1,\ldots N$ and consequently yield explicit results for the approximated unknown surface distributions $\phi_P(R,\mu)$ and $X(R,\mu)$ through equations (6.43) and (6.44), with $w(R)=1$. These results may, in turn, as it is shown in next section, be used to obtain flow rates and velocity profiles in terms of the expansion coefficients C_0 and $C(\xi)$ or surface quantities only.

6.4 Macroscopic Velocity Profile and Flow Rate

For a complete solution of the problem we need the functions $\phi_P(r,\mu)$ and $X(r,\mu)$ for all r and thus we proceed by establishing the expansion coefficients C_0 and $C(\xi)$ which are contained in the general solution. Evaluating the integral equations (6.32) and (6.34) at r=R leads to the following expressions:

$$C_o = \frac{3\sqrt{\pi}}{2} + \frac{4}{\sqrt{\pi}} \int_0^\infty Y(R,\mu)\, e^{-\mu^2}\, d\mu \quad , \tag{6.59}$$

and

$$C(\xi) = \frac{1}{N(\xi)\, I_o(R/\xi)} \left\{ \int_0^\infty [f(\xi,\mu) - f(\xi,-\mu)]\, Y(R,\mu)\, \frac{e^{-\mu^2}}{\mu^2}\, d\mu - \frac{\pi}{2}\, \xi \right\} . \tag{6.60}$$

If we now substitute the attempted F_N approximation (6.43)

and (6.44), (w(R)=1) into the last two expressions we find

$$C_o = \frac{3\sqrt{\pi}}{2} + \frac{4}{\sqrt{\pi}} \sum_{\alpha=0}^{N} R_\alpha A_\alpha \tag{6.61}$$

and

$$C(\xi) = \frac{1}{N(\xi)\ I_o(R/\xi)} \left\{ \sum_{\alpha=0}^{N} E_\alpha(\xi)\ A_\alpha - \frac{\pi}{2}\ \xi \right\} \tag{6.62}$$

for the Poiseuille flow problem and

$$C_o = \frac{3\sqrt{\pi}}{4} + \frac{4}{\sqrt{\pi}} \sum_{\alpha=0}^{N} R_\alpha B_\alpha \tag{6.63}$$

and

$$C(\xi) = \frac{1}{N(\xi)\ I_o(R/\xi)} \left\{ \sum_{\alpha=0}^{N} E_\alpha(\xi)\ B_\alpha - \frac{\pi}{4}\ \xi \right\} \tag{6.64}$$

for the pseudo thermal creep problem where

$$R_\alpha = \int_0^\infty K_o(R/\mu)\ I_1(R/\mu)\ \mu^{\alpha+1}\ e^{-\mu^2}\ d\mu \quad , \tag{6.65}$$

in terms of the known F_N coefficient A_α and B_α, a=0,1,...N.

Using equations (6.5), (6.6), (6.9) and (6.11) for the Poiseuille problem and (6.5), (6.7), (6.16) and (6.11) for the pseudo thermal creep problem the velocity profiles may be expressed as

$$V_P(r) = \frac{2}{\pi} \int_0^\infty \phi_P(r,\mu)\ \frac{e^{-\mu^2}}{\mu^2}\ d\mu \tag{6.66}$$

and

$$V_{PT}(r) = \frac{2}{\pi}\int_0^\infty X(r,\mu)\,\frac{e^{-\mu^2}}{\mu^2}\,d\mu + \frac{1}{4} \quad , \tag{6.67}$$

respectively. After we substitute the general solution (6.23) into the last two equations and integrate analytically over μ from 0 to ∞ we deduce that

$$V_P(r) = \frac{1}{4}\,(R^2 - r^2) + \frac{C_o}{\sqrt{\pi}} + \frac{2}{\sqrt{\pi}}\int_0^\infty C(\xi)\; I_o(r/\xi)\; d\xi - \frac{1}{2} \tag{6.68}$$

and

$$V_{PT}(r) = \frac{1}{4}\,(R^2 - r^2) + \frac{C_o}{\sqrt{\pi}} + \frac{2}{\sqrt{\pi}}\int_0^\infty C(\xi)\; I_o(r/\xi)\; d\xi - \frac{1}{4} \quad , \tag{6.69}$$

while the velocity profile for the thermal creep problem is given by equation (6.8). Since the volumetric flow rate is expressible as an integral of v(r) (we use a Q which is 2 times the Q defined by Ferziger [48] for direct comparison with Loyalka [37])

$$Q_{P,PT} = \frac{4}{R^3}\int_0^R V_{P,PT}(r)\; r\, dr \quad , \tag{6.70}$$

integrating over r we find finally the flow parameters Q_P and Q_{PT} in terms of the expansion coefficients C_0 and $C(\xi)$ to be given by

$$Q_P = \frac{R}{4} - \frac{1}{R} + \frac{2\,C_o}{\sqrt{\pi}\,R} + \frac{8}{\pi R^2}\int_0^\infty \xi C(\xi)\; I_1(R/\xi)\; d\xi \tag{6.71}$$

and

$$Q_{PT} = \frac{R}{4} - \frac{1}{2R} + \frac{2\,C_o}{\sqrt{\pi}\,R} + \frac{8}{\pi R^2}\int_0^\infty \xi C(\xi)\; I_1(R/\xi)\; d\xi \quad , \tag{6.72}$$

with

$$Q_T = Q_P - Q_{PT} \quad . \tag{6.73}$$

Estimation of the expansion coefficients C_0 and $C(\xi)$, $0<\xi<\infty$, leads through (6.70), (6.71), (6.67) and (6.68) to a complete solution for both problems, as far as flow rates and velocity profiles are considered.

However we can simplify the calculation of the flow rate Q_T and Q_{PT} using several useful relationships concerning some moments of $\phi_P(R,\mu)$ and $X(R,\mu)$ in a way shown in section 9.8 of the appendices. It has been found that we can express the flow rate and the velocity jump on the wall simply in terms of surface quantities as

$$Q_P = \frac{R}{4} - \frac{1}{R} + \frac{8}{\pi}\sum_{\alpha=0}^{N} A_\alpha \left\{\frac{1}{R}\,R_\alpha + \frac{2}{R^2}\,S_{\alpha+2}\right\} \tag{6.74}$$

and

$$V_P(R) = \frac{2}{\pi}\sum_{\alpha=0}^{N} A_\alpha\, R_{\alpha-2} \tag{6.75}$$

for the Poiseuille flow problem and similarly

$$Q_{PT} = \frac{R}{4} - \frac{2}{R} + \frac{8}{\pi}\sum_{\alpha=0}^{N} B_\alpha \left\{\frac{1}{R}\,R_\alpha + \frac{2}{R^2}\,S_{\alpha+2}\right\} \tag{6.76}$$

and

$$V_{PT}(R) = \frac{2}{\pi} \sum_{\alpha=0}^{N} B_\alpha R_{\alpha-2} \tag{6.77}$$

for the "PT" problem, while the corresponding quantities for the thermal creep problem are obtained through equations (6.73) and (6.8). The constants A_α and B_α, $\alpha=0,1,2,\ldots,N$, are the F_N coefficients, while the functions S_α and R_α are given by equations (6.51) and (6.65) respectively. Clearly these expressions for Q_P, Q_T, $v_P(R)$ and $v_T(R)$ are much simpler than the alternative expressions given by equations (6.68), (6.69), (6.71) and (6.72), since they do not require integration over the eigenvalues ξ in the range 0 to ∞. They are practical and economical to be used as far as overall quantities are desired. Of course they can also be used as numerical checks for the previous expressions.

6.5 Numerical Results

To solve the linear system of equations given by (6.58) we first choose a set of collocation points $\{\xi_\beta\}$. To have a simple and effective scheme we take the ξ_β, $\beta=1,2,3,\ldots,N$ to be the positive zeros of the Hermite polynomial $H_{2N}(\xi)$. In particular for an Nth order F_N approximation, which implies N+1 unknowns, we select the N+1 collocation points to be the positive zeros of the (2N+2)th order Hermite polynomial. We

then determine the matrix elements of equation (6.58) by computing the functions $D_\alpha(\xi)$ and $E_\alpha(\xi)$ from equations (6.54) and (6.55) or equations (6.56) and (6.57) and the function S_α from equation (6.51). To find the desired values of some of these integrals requires the use of l'Hospital's rule when $\xi=\mu$. Finally expanding equation (6.51), as it is pointed out in the section 9.9 of the appendices, we obtain an analytical evaluation of the integral S_α. This analysis was used successfully as a benchmark for testing the accuracy of the numerical results obtained by a Gaussian quadrature numerical scheme. Next the linear system (6.58) is solved for the unknown F_N coefficients A_α, $\alpha=0,1,\ldots,N$ for the Poiseuille flow problem and B_α, $\alpha=0,1\ldots,N$ for the pseudo thermal creep flow problem. The F_N coefficients are in turn used in equations (6.73), (6.74),(6.75) and (6.76) to yield the flow rate and the velocity jump at the wall, or in equation (6.60), (6.61), (6.62) and (6.63) to obtain the expansion coefficient C_0 and $C(\xi)$, which lead through (6.67) and (6.68) to a complete solution of the two problems under consideration.

In Tables 6.1 and 6.2 the convergence rate of the F_N method is illustrated and the converged results for the flow rates $Q_P(R)$ and $Q_T(R)$, as they are computed from equations (6.74) and (6.76) or (6.71) and (6.72), are compared to those of Loyalka [37], which as far we know represent the

most accurate complete solution existing in the literature. The variable R is the inverse Knudsen number given as the ratio of the actual radius of the cylindrical pipe over the mean free path. It is seen that for R<0.1 and R>1 a low order F_N approximation results in up to 5 and 4 significant figure accuracy for the Poiseuille flow and thermal creep flow problems respectively. For 0.1<R<1 a higher order approximation is required to yield the same accuracy. Although Table 6.2 illustrates results for the thermal creep flow problem, it actually demonstrates the convergence of the "PT" (pseudo thermal creep) problem and the accuracy of the solution drops from 5 to 4 significant figures because of the formulation of the problem ($Q_T=Q_P-Q_{PT}$). In general the agreement with Loyalka [37] appears best in the inverse Knudsen number range 0.02<R<4.0, although our most accurate results are achieved outside this range where convergence is faster. Considered over the complete Knudsen number spectrum the agreement ranges between 2 and 5 digits. We consider our stable results to be correct to within +1 in the last digit shown, which implies that Loyalka's results are correct to within 1%.

We have also found that the simple polynomial approximations given by equations (6.52) and (6.53) work well for all values of R>0.5 listed in Tables 6.1 and 6.2, reducing computational cost, but fail completely for R<0.5.

Table 6.3 contains values for the velocity slip at the

wall as it is computed from equations (6.75) and (6.77) for both Poiseuille flow and thermal creep flow. To our knowledge these results have not previously been reported. We believe the results to be correct to within +1 in the fourth significant figure.

In Table 6.4 we compare our results for the complete velocity profiles in both Poiseuille flow and thermal creep flow (inverse Knudsen number R=2) to those of Loyalka [37]. The degree of agreement is even better to that found for the flow rates Q_P and Q_T throughout the range of r, except very close to the boundary where the presence of the kinetic layer dominates and the agreement drops only to 1 significant figure.

In figures 6.1 and 6.2 we show the flow rates $Q_P(R)$ and $Q_T(R)$ vs the inverse Knudsen number R for the Poiseuille flow and thermal creep problems respectively, while in figures 6.3 and 6.4 we illustrate the dependence of the velocity discontinuity at the wall on the inverse Knudsen number (R) for the same two problems.

Finally in figure 6.5 the velocity profile for the Poiseuille flow problem (dashed line) is compared with the velocity profile calculated by considering the effect of the thermal creep flow problem (dotted line) at R=2.0. In addition we illustrate the continuum hydrodynamic velocity profile (solid line). It is evident that the effect of the thermal creep on the velocity profile of Poiseuille flow is

large, while the continuum solution, as it is expected, fails completely.

Table 6.1 Convergence of the Poiseuille flow rate Q_P

R	Order of the Approximation									
	4	8	12	16	20	22	24	26	28	30
0.0001	1.5038	1.5038								
0.001	1.4995	1.4995								
0.01	1.4760	1.4760								
0.02	1.4597	1.4597	1.4598	1.4598						
0.03	1.4474	1.4475	1.4475	1.4475	1.4475	1.4475	1.4475	1.4475	1.4476	1.4476
0.04	1.4375	1.4375	1.4376	1.4376	1.4377	1.4377				
0.05	1.4292	1.4293	1.4293	1.4294	1.4294	1.4295	1.4295			
0.07	1.4159	1.4161	1.4162	1.4163	1.4164	1.4164	1.4165	1.4165		
0.09	1.4057	1.4060	1.4062	1.4063	1.4064	1.4065	1.4065	1.4066	1.4066	
0.1	1.4015	1.4018	1.4020	1.4022	1.4024	1.4024	1.4025	1.4025	1.4026	1.4026
0.3	1.3715	1.3730	1.3739	1.3744	1.3748	1.3750	1.3751	1.3752	1.3753	1.3754
0.5	1.3819	1.3842	1.3852	1.3858	1.3862	1.3863	1.3864	1.3864		
0.7	1.4066	1.4090	1.4099	1.4103	1.4104	1.4105	1.4105			
0.9	1.4384	1.4405	1.4411	1.4413	1.4413					
1.0	1.4559	1.4577	1.4582	1.4583	1.4583					
1.25	1.5027	1.5039	1.5041	1.5041						
1.5	1.5524	1.5531	1.5532	1.5532						
2.0	1.6574	1.6576	1.6576							
2.5	1.7670	1.7671	1.7671	1.7672	1.7672	1.7672				
3.0	1.8798	1.8799	1.8799	1.8800	1.8800					
3.5	1.9948	1.9949	1.9949	1.9950	1.9950					
4.0	2.1114	2.1115	2.1116	2.1116						
5.0	2.3481	2.3482	2.3483	2.3483						
6.0	2.5880	2.5881	2.5882	2.5882						
7.0	2.83005	2.83017	2.83021	2.83022	2.83024	2.83024				
9.0	3.31835	3.31847	3.31850	3.31851	3.31853	3.31853				
10.0	3.56394	3.56405	3.56408	3.56409	3.56411	3.56411				
100.0	26.0215	26.0216	26.0216							

Table 6.1 (cont.) Convergence of the Poisuille flow rate $Q_p(R)$

R	Converged Results	Ref. [37]
0.0001	1.5038	--
0.001	1.4995	1.5013
0.01	1.4760	1.4763
0.02	1.4598	1.4601
0.03	1.4476	1.4481
0.04	1.4377	1.4384
0.05	1.4295	1.4303
0.07	1.4165	1.4165
0.09	1.4066	1.4077
0.1	1.4026	1.4037
0.3	1.3754	1.3759
0.5	1.3864	1.3864
0.7	1.4105	1.4101
0.9	1.4413	1.4408
1.0	1.4583	1.4578
1.25	1.5041	1.5035
1.5	1.5532	1.5526
2.0	1.6576	1.6571
2.5	1.7672	1.7667
3.0	1.8800	1.8796
3.5	1.9950	1.9948
4.0	2.1116	2.1116
5.0	2.3483	2.3493
6.0	2.5882	2.5906
7.0	2.8302	2.8346
9.0	3.3185	3.3291
10.0	3.5641	3.5791
100.0	26.021	--

Table 6.2 Convergence of the thermal creep flow rate Q_T

R	Order of the Approximation								
	4	8	12	16	20	22	24	26	28
0.0001	0.7515	0.7515							
0.001	0.7466	0.7466							
0.01	0.7177	0.7177							
0.02	0.6956	0.6956							
0.03	0.6777	0.6778	0.6778						
0.04	0.6624	0.6624	0.6624	0.6625	0.6625				
0.05	0.6488	0.6489	0.6489	0.6489	0.6489	0.6489	0.6490	0.6490	
0.07	0.6253	0.6254	0.6255	0.6255	0.6256	0.6256			
0.09	0.6054	0.6055	0.6056	0.6056	0.6057	0.6057	0.6058	0.6058	
0.1	0.5964	0.5965	0.5966	0.5967	0.5967	0.5968	0.5968		
0.3	0.4806	0.4812	0.4815	0.4817	0.4819	0.4819	0.4820	0.4820	0.4821
0.5	0.4155	0.4162	0.4166	0.4168	0.4169	0.4169	0.4170	0.4170	
0.7	0.3702	0.3709	0.3711	0.3712	0.3713	0.3713	0.3713		
0.9	0.3357	0.3362	0.3363	0.3364	0.3364				
1.0	0.3211	0.3216	0.3217	0.3217					
1.25	0.2903	0.2906	0.2906	0.2906	0.2906	0.2906	0.2907	0.2907	
1.5	0.2654	0.2655	0.2656	0.2656					
2.0	0.2270	0.2271	0.2271						
2.5	0.1986	0.1986	0.1986	0.1987	0.1987				
3.0	0.1766	0.1766							
3.5	0.1589	0.1590	0.1590						
4.0	0.1445	0.1445							
5.0	0.1222	0.1222							
6.0	0.1058	0.1058							
7.0	0.09319	0.09321	0.09322	0.09322					
9.0	0.07521	0.07522	0.07522	0.07522	0.07523	0.07523			
10.0	0.06856	0.06857	0.06858	0.06858					
100.0	0.007581	0.007582	0.007583	0.007583					

Table 6.2 (cont.) Convergence of the thermal creep flow rate $Q_T(R)$

R	Converged Results	Ref. [37]
0.0001	0.7515	--
0.001	0.7466	0.7466
0.01	0.7177	0.7177
0.02	0.6956	0.6958
0.03	0.6778	0.6780
0.04	0.6625	0.6628
0.05	0.6490	0.6493
0.07	0.6256	0.6261
0.09	0.6058	0.6063
0.1	0.5968	0.5973
0.3	0.4821	0.4823
0.5	0.4170	0.4169
0.7	0.3713	0.3712
0.9	0.3364	0.3363
1.0	0.3217	0.3215
1.25	0.2907	0.2906
1.5	0.2656	0.2655
2.0	0.2271	0.2271
2.5	0.1987	0.1987
3.0	0.1766	0.1767
3.5	0.1590	0.1591
4.0	0.1445	0.1447
5.0	0.1222	0.1224
6.0	0.1058	0.1060
7.0	0.09322	0.0934
9.0	0.07523	0.0755
10.0	0.06858	0.0688
100.0	0.007583	--

Table 6.3 Velocity Slip at the Wall

R	Poiseuille Flow $v_P(R)$	Thermal Creep Flow $v_T(R)$
0.0001	0.5639(-4)	0.2817(-4)
0.001	0.5615(-3)	0.2792(-3)
0.01	0.5484(-2)	0.2647(-2)
0.03	0.1594(-1)	0.7340(-2)
0.05	0.2597(-1)	0.1151(-1)
0.07	0.3570(-1)	0.1531(-1)
0.1	0.4987(-1)	0.2044(-1)
0.5	0.2167	0.5957(-1)
1.0	0.4049	0.8032(-1)
2.0	0.7659	0.9679(-1)
3.0	0.1120(+1)	0.1027
4.0	0.1472(+1)	0.1054
5.0	0.1824(+1)	0.1068
7.0	0.2529(+1)	0.1081
10.0	0.3587(+1)	0.1088
100.0	0.3541(+2)	0.1094

Table 6.4 Velocity Profiles

RADIUS	POISEUILLE FLOW		THERMAL CREEP FLOW	
	Present Work	Ref.[37]	Present Work	Ref.[37]
0.000	2.3533	--	0.2970	--
0.004	2.3533	2.3531	0.2970	0.2970
0.026	2.3531	2.3529	0.2970	0.2970
0.070	2.3518	2.3516	0.2969	0.2969
0.135	2.3476	2.3474	0.2966	0.2966
0.219	2.3381	2.3381	0.2959	0.2959
0.321	2.3212	2.3210	0.2946	0.2946
0.437	2.2934	2.2932	0.2925	0.2925
0.567	2.2521	2.2522	0.2893	0.2893
0.706	2.1958	2.1958	0.2848	0.2848
0.851	2.1230	2.1229	0.2788	0.2788
1.000	2.0329	2.0328	0.2710	0.2710
1.149	1.9262	1.9261	0.2613	0.2613
1.294	1.8050	1.8044	0.2495	0.2494
1.433	1.6710	1.6703	0.2354	0.2354
1.563	1.5273	1.5272	0.2190	0.2190
1.679	1.3806	1.3095	0.2006	0.2005
1.781	1.2326	1.2323	0.1802	0.1802
1.865	1.0915	1.0906	0.1585	0.1583
1.930	0.9624	0.9609	0.1364	0.1364
1.974	0.8550	0.8523	0.1160	0.1159
1.996	0.7845	0.7733	0.1011	0.0995

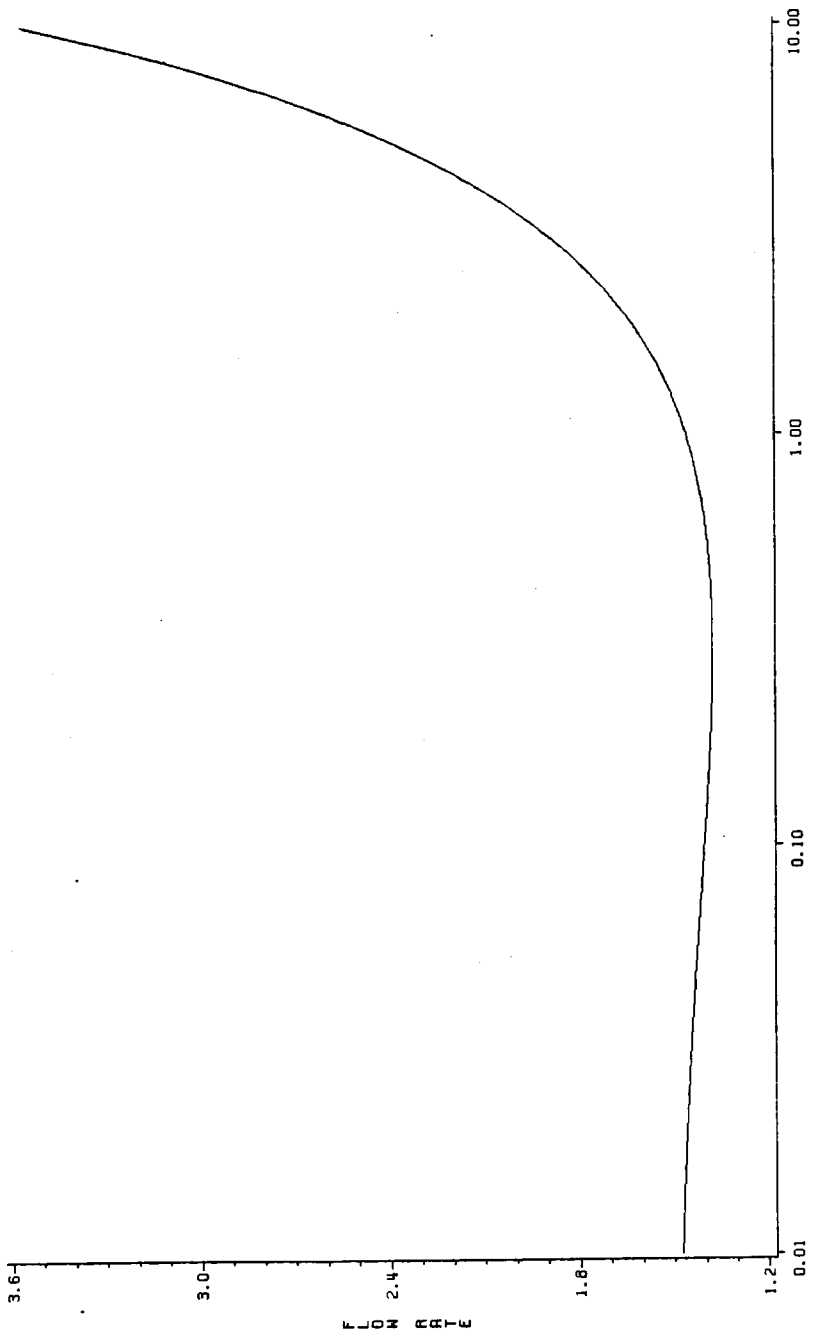

FIGURE 6.1 THE POISEUILLE FLOW RATE VERSUS INVERSE KNUDSEN NUMBER

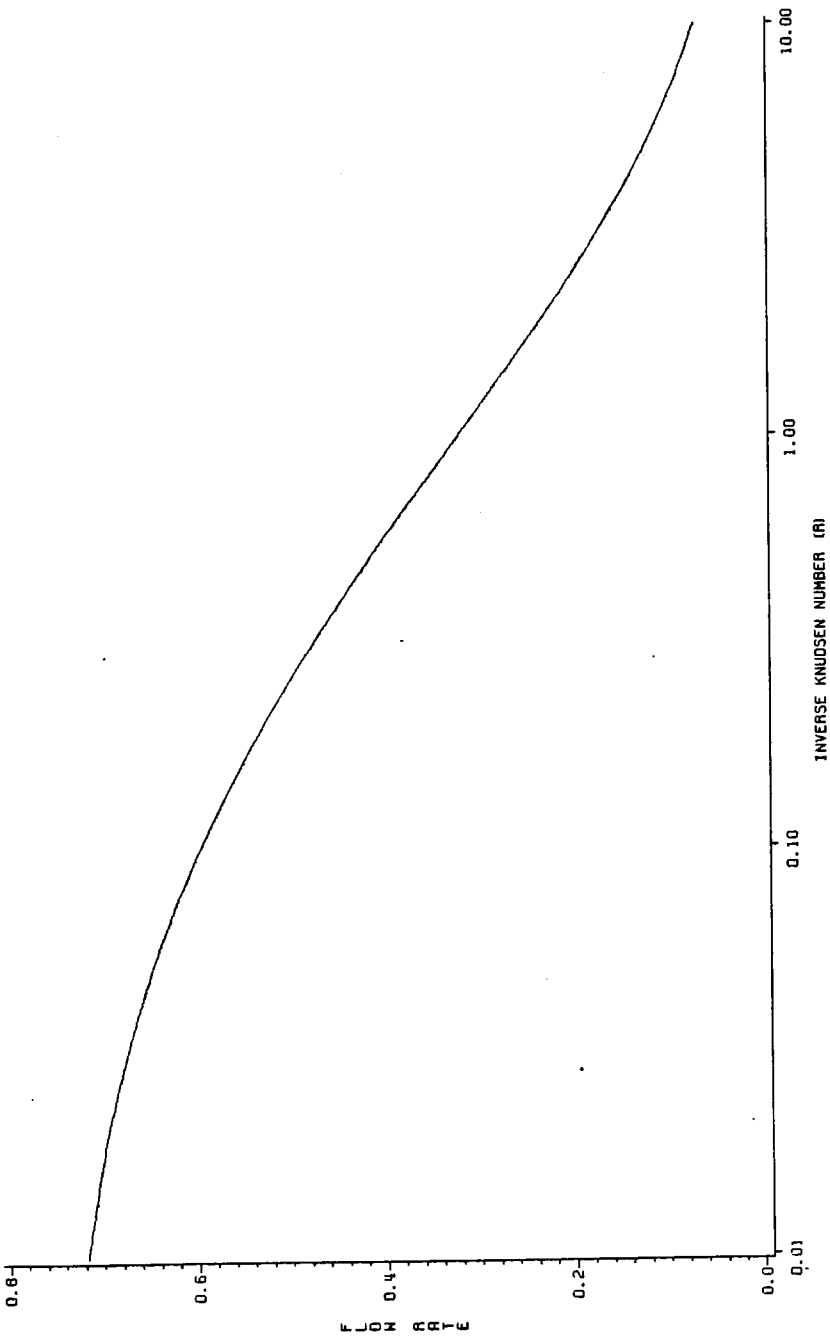

FIGURE 6.2 THE THERMAL CREEP FLOW RATE VERSUS INVERSE KNUDSEN NUMBER

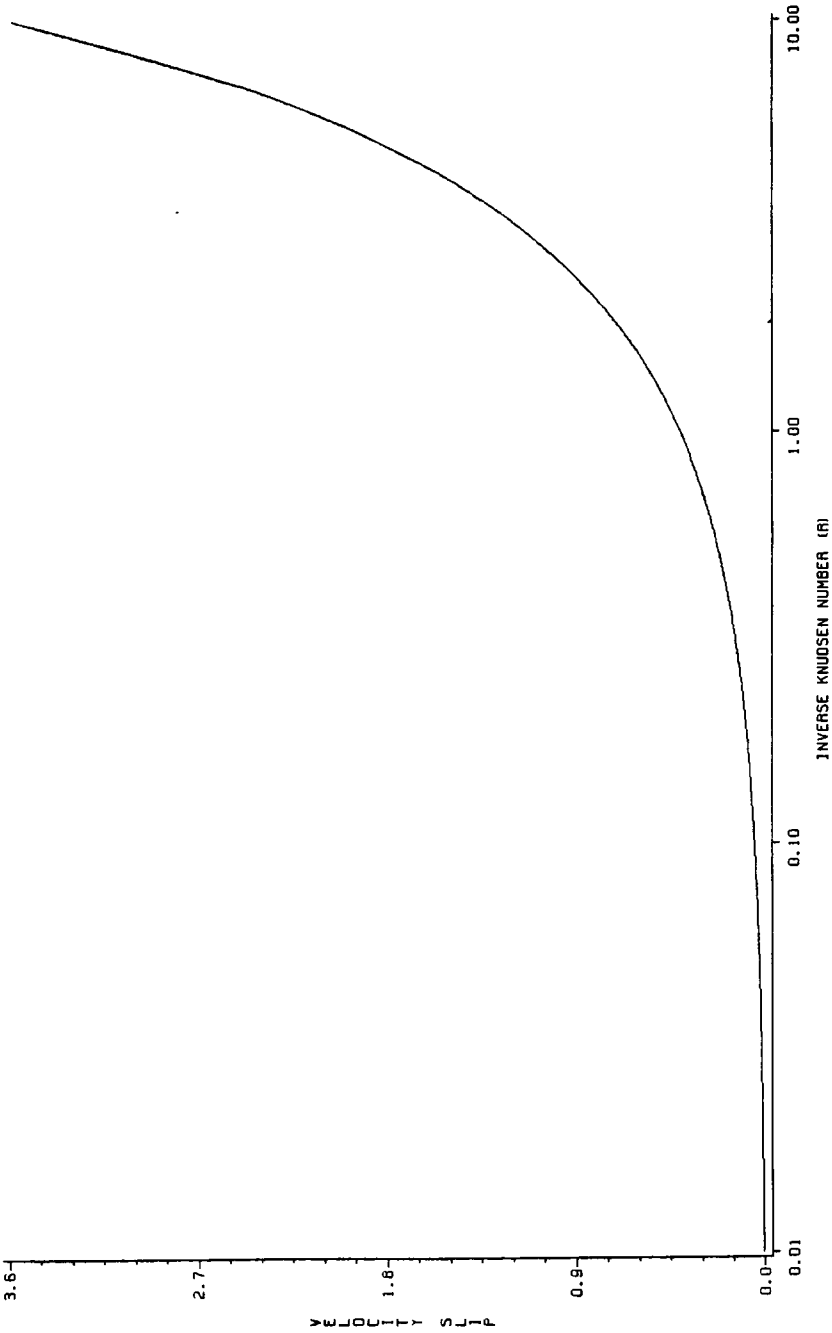

FIGURE 6.3 VELOCITY SLIP AT THE WALL FOR THE POISEUILLE FLOW PROBLEM

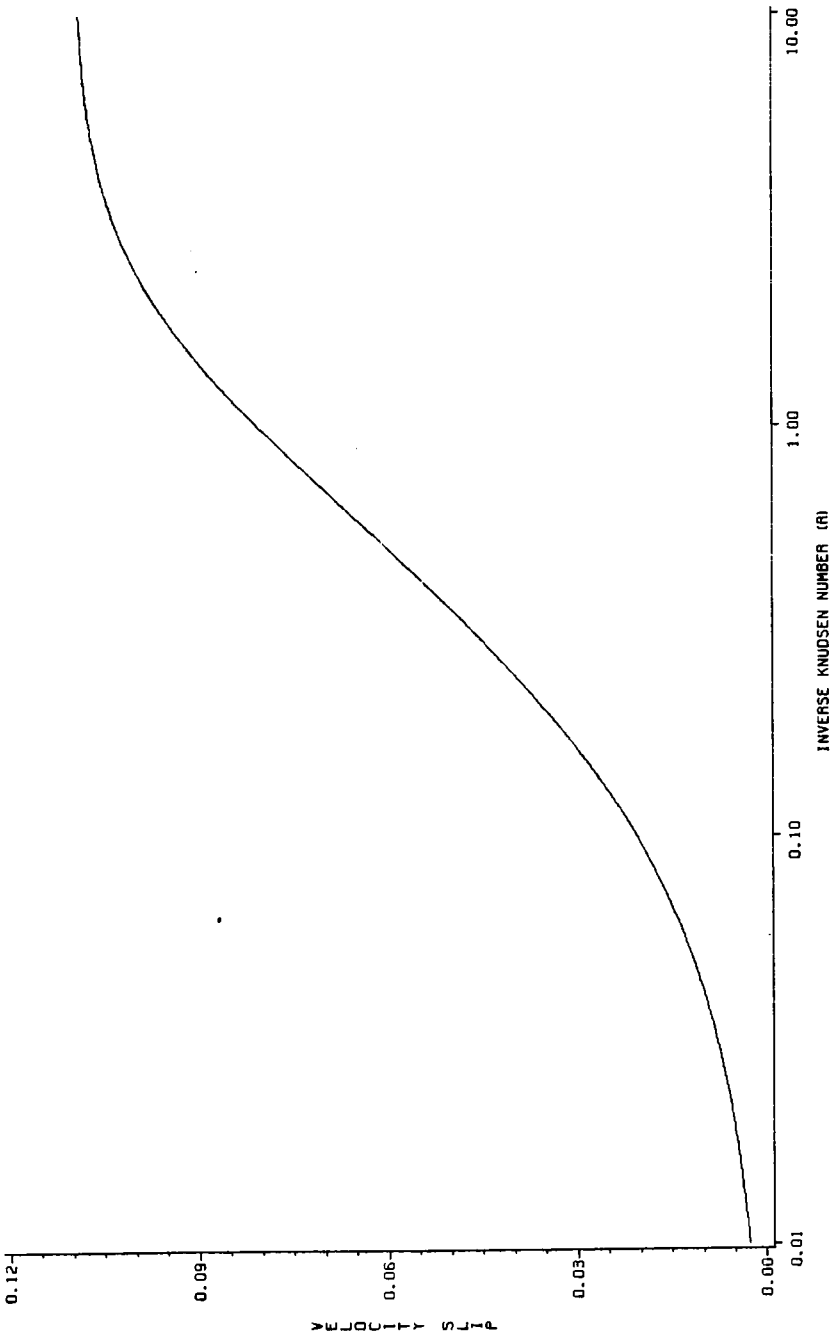

FIGURE 6.4 VELOCITY SLIP AT THE WALL FOR THE THERMAL CREEP FLOW PROBLEM

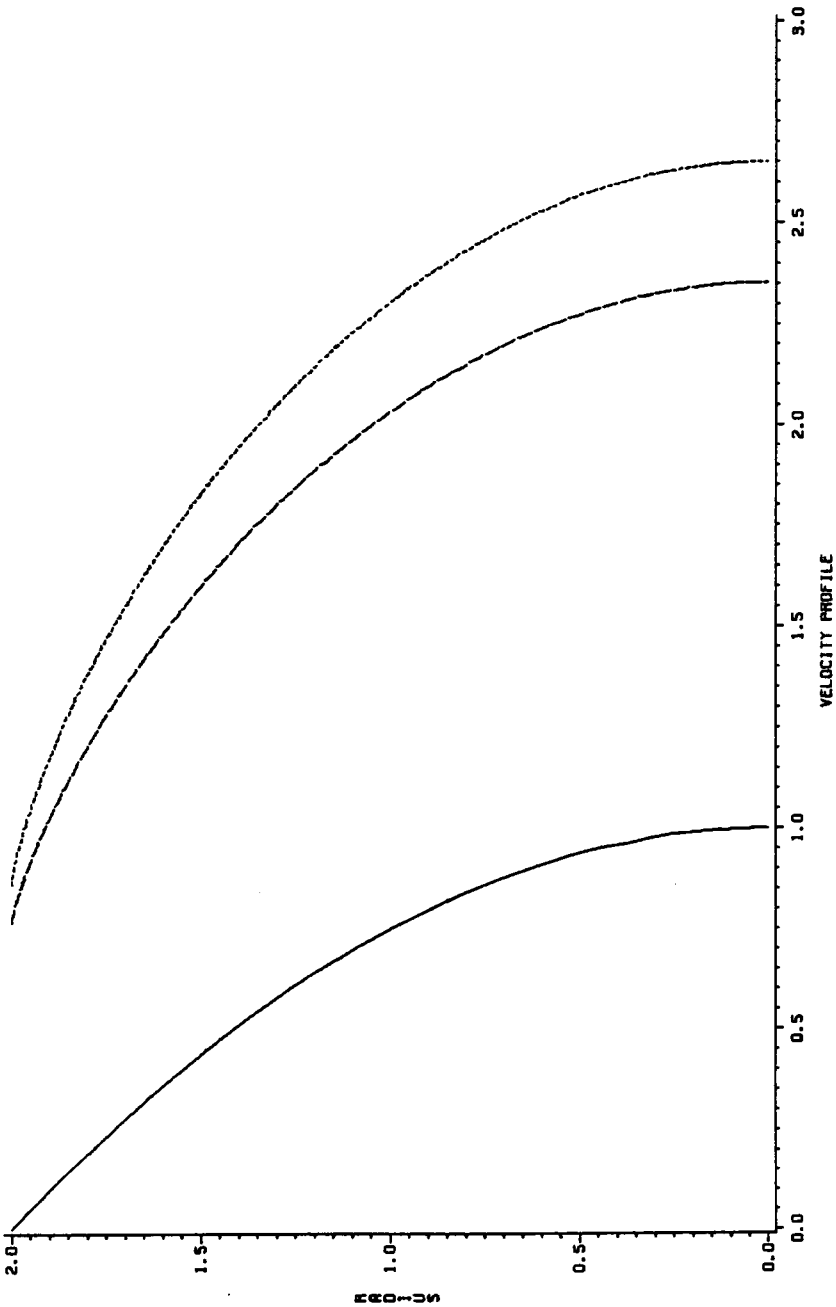

FIGURE 6.5 VELOCITY PROFILES FOR THE THERMAL TRANSPIRATION PROBLEM

7. Summary, Conclusions and Recommendations

As a result of this study, it has been shown that the powerful F_N method, originated by Siewert [7,8], can be extended to kinetic theory. A complete formulation of the method in kinetic theory problems has been presented and the accuracy of this advanced semi-analytical-numerical technique has been demonstrated by applying the method to several problems in rarefied gas dynamics. It is clear that the F_N method, which is relatively easy to use, can readily be generalized to all kinetic theory problems, when linearization is permitted, by judicial choice of basis functions.

In chapter 3 the existing analysis of Kriese, et al. [51], based on the steady-state form of the linearized BGK equation, is utilized in introducing the F_N method in kinetic theory. A general guideline of the formulation of the method based on full-range orthogonality is presented for half space and finite media applications and the basic characteristics of a position-dependent approximate solution are introduced.

In the following two chapters we have chosen problems which have previously been solved [52,54] by relatively exact methods in order to have a basis of comparison. Singular integral equations for the unknown distribution function have been derived and solved by polynomial

expansion and collocation.

In chapter 4, the half-space weak evaporation and heat transfer problems with purely diffuse reflection at the interface are solved to give accurate results for the macroscopic and microscopic temperature and density slip coefficients as well as the complete temperature and density profiles. Although the general method of formulation is quite similar from problem to problem, the choice of the F_N approximation is somewhat problem-dependent. In this chapter we concentrate on half-space problems, and develop an effective approximation, given by

$$\sum_{\alpha=0}^{n} A_\alpha/(\nu_\alpha+\mu)$$

which we think will be useful for other half-space problems in kinetic theory. A relatively low-order F_N approximation, for the fully coupled kinetic equations, produces results accurate to six significant figures for modest computational effort.

Next in chapter 5 we turn to a problem in a finite medium, that of heat transfer in a gas confined between plates with arbitrary accommodation coefficients. Testing the F_N method in finite geometry we find that a different form for the approximate solution is required. Expansion of the unknown molecular distribution function in terms of the simple polynomial F_N approximation

$$\sum_{\alpha=0}^{n} A_\alpha \mu^\alpha$$

provides best results. The total heat flux, temperature and density profiles and the molecular distribution function at various locations between the plates are all computed to high accuracy with very short computation time. Computation of the reduced distribution function itself is possible only through a position-dependent approximation and this interesting analysis is also presented in this chapter.

By studing these two different geometry problems it has been found that the applied F_N approximations yield results that are consistently accurate to three or four significant figures for N<10 and up to five or six significant figures for N<30. The choice of the basis functions is as important as the method itself and it seems advisable to seek alternative schemes of basis functions, if some difficulty with the convergence of the F_N method is encountered, than to resort to high order approximations. We have further demonstrated that the F_N method is a viable solution technique for kinetic theory problems in a half space and in finite media yielding results of benchmark accuracy for the full Knudsen number range of interest. The obtained numerical results help in judging the accuracy to expect of the method. The F_N method may be applied with confidence to problems for which more exact methods of analysis do not appear possible.

Future work in this area will be applied to solving the two-surface evaporation-condensation problem. Study of the

distribution function itself, as is discussed in the fifth chapter, can be useful in understanding the physics of the phenomena related to the severe changes in the kinetic layer, and can be helpful in explaining the reverse temperature gradient paradox [59].

Finally in chapter 6 the kinetic theory shear flow problems of Poiseuille flow and thermal creep flow in a cylindrical tube, which are not amenable to exact treatment, are solved to benchmark accuracy. Extending the work of Thomas and Siewert [71,72], the F_N method is formulated and tested successfully for the first time in cylindrical geometry in kinetic theory. The complete solution of the two aforementioned problems is based on the linearized BGK model in cylindrical coordinates. The volumetric flow rates and the velocity profiles have been computed, approximating the incoming distribution function at the wall by a finite expansion in terms of

$$K_0(R/\mu)I_1(R/\mu)\sum_{\alpha=0}^{n} A_\alpha \mu^{\alpha+1}.$$

We believe that the numerical results we quote as converged to be of reference quality accurate to four or five significant figures.

Inspite of the importance of the cylindrical Poiseuille and thermal creep flow problems, detailed solutions, that could be considered numerically "exact" have not previously been available. The present complete solutions of the two

problems demonstrate the efficiency of the method of solving basic transport problems in the fields of kinetic theory and rarefied gas dynamics. The method, though approximate, can yield very accurate numerical results.

An interesting possible continuation of the work discussed in chapter 6 is provided by the problems of cylindrical Poiseuille, thermal creep and Couette flows for a combination of diffuse and specular reflection at the wall. General speaking, in cylindrical geometry, we rely on the boundary condition to derive the governing integro-differential equation of the problem. It is this reliance on the combined diffuse-specular boundary condition which makes the formulation of the problem and the choice of a suitable F_N approximation difficult and challenging.

Finally an exploration of binary mixture or polyatomic gas problems, such as evaporation in binary mixtures, heat transfer in a polyatomic gas, or internal and external binary flows in plane and cylindrical geometry, based on the F_N method, might lead to highly accurate numerical results. In addition, although we are less certain, we are optimistic about the extension of the F_N method to higher order collision models.

8. REFERENCES

1. Bhatnagar P. L., E. P. Gross, and M. Krook, A Model for Collision Processes in Gases. I. Small Amplitude Processes in Charged and Neutral One-Component Systems, Phys. Rev., 94, 511, 1954.

2. Welander P., On the Temperature Jump in a Rarefied Gas, Arkiv. Fysik., 7, 507, 1954.

3. Case K. M., Elementary Solutions of the Transport Equation and their Applications, Ann. Phys., 9, 1, 1960.

4. Cercignani C., Mathematical Methods in Kinetic Theory, Plenum Press, New York, 1969.

5. Cercignani C., Theory and Application of the Boltzmann Equation, Scottish Academic Press, New York, 1975.

6. Case K.M., and P.F. Zweifel, Linear Transport Theory, Addison-Wesley Publishing Company, Reading, Massachusetts, 1967.

7. Siewert C.E., and P. Benoist, The F_N method in Neutron-Transport Theory. Part I : Theory and Applications, Nucl. Sci. Eng., 69, 156, 1979.

3. Granjean P., and C. E. Siewert, The F_N method in Neutron-Transport Theory. Part II : Applications and Numerical Results, Nucl. Sci. Eng., 69, 161, 1979.

9. Boltzmann L., Sitzungsberichte Akad. Wiss. Vienna, Part II, 66, 275, 1872.

10. Maxwell J. C., The Scientific Papers of J. C. Maxwell, p. 703, Dover, 1965.

11. Grad H., Asymptotic Theory of the Boltzmann Equation, Phys. Fluids, 6, 147, 1963.

12. Krook M., Continuum Equations in the Dynamics of Rarefied Gases, J. Fluid Mech., 6, 523, 1959.

13. Gross E. P., and E. A. Jackson, Kinetic Models and the Linearized Boltzmann Equation, Phys. Fluids, 2, 432, 1959.

14. Kogan M. N., Recent Developments in the Kinetic Theory of Gases, Rarefied Gas Dynamics, L. Trilling and H.

Wackman eds., Vol I, p.1, Academic Press, 1969.

15. Bird G. A., Direct Simulation Monte Carlo Method, Rarefied Gas Dynamics, L. Trilling and H. Wachman eds., Vol I, p.85, Academic Press, 1969.

16. Nanbu K, Direct Simulation Scheme Derived from the Boltzmann Equation. I, II, III, and IV, J. Phys. Soc. Japan, 49, 2042, 1980, 49, 2050, 1980, 49, 2055, 50, 2829, 1981.

17. Nanbu K., On the Simulation Method for the Bhatnager-Gross-Krook Equation, J. Phys. Soc. Japan, 50, 3154, 1981.

18. Yen S. M., Numerical Solution of the Nonlinear Boltzmann Equation for Nonequilibrium Gas Flow Problems, Ann. Rev. Fluid. Mech., 16, 67, 1984.

19. Hilbert D., Math Ann., 72, 562, 1912.

20. Hilbert D., Grundzuge einer Allgemeinen Theory der Linearen Integralgleichungen, Chelsea Publishing Co., New York, 1953.

21. Chapman S., and T. G. Cowling, The Mathematical Theory of Non-Uniform Gases, Cambridge University Press, Cambridge 1958.

22. Willis D. R., A Study of Some Nearly-Free-Molecular Flow Problems, Ph.D. Thesis, Princeton University, 1958.

23. Cercignani C., Higher Order Slip According to the Linearized Boltzmann Equation, Univ. of Calif. Rept. N.AS.-64-18, 1964.

24. Sone Y., Asymptotic Thepry of Flow of Rarefied Gas over a Smooth Boundary, I, Rarefied Gas Dynamics, L. Trilling and H. Wachman eds., Vol I, p. 243, Academic Press, 1969.

25. Darrozes J. S., Approximate Solutions of the Boltzmann Equation for Flows past Bodies of Moderate Curvature, Rarefied Gas Dynamics, L. Trilling and H. Wachman, eds, Vol. I, p.111, Academic Press, 1969.

26. Sone Y., Kinetic Theory of Evaporation and Condensation-Linear and Nonlinear Problems., J. Phys. Soc. Japan, 45, 315, 1978.

27. Onishi Y., Kinetic Theory of Evaporation and Condensation for a Cylindrical Condensed Phase, Phys. Fluids, 26, 659, 1983.

28. Onishi Y., Kinetic Theory Treatment of Nonlinear Half-Space Problem of Evaporation and Condensation, J. Phys. Soc. Japan, 46, 303, 1979.

29. Aoki K., T. Inamuro, and Y. Onishi, Slightly Rarefied Gas flow over a Body with Small Accommodation Coefficient, J. Phys. Soc. Japan, 47, 663, 1979.

30. Grad H., Singular Limits of Solutions of Boltzmann's Equation, Rarefied Gas Dynamics, K. Karamceti, Academic Press, p.337, 1972.

31. Bassanini P., C. Cercignani, and C. D. Pagani, Comparison of Kinetic Theory Analyses of Linearized Heat Transfer between Parallel Plates, Int. J. Heat Mass Transfer., 10, 447, 1966.

32. Cercignani C., and F. Sernagiotto, Cylindrical Poiseuille Flow of a Rarefied Gas, Phys. Fluids, 9, 40, 1966.

33. Cergignani C., and A. Daneri, Flow of a Rarefied Gas between two Parallel Plates, J. Appl. Phys., 34, 3509, 1963.

34. Cergignani C., and C. D. Pagani, Variational Approach to Boundary-Value Problems in Kinetic Theory, Phys. Fluids, 9, 1167, 1966.

35. P. Bassanini, C. Cercignani, and F. Sernagiotto, Flow of a Rarefied Gas in a Tube of Annular Section, Phys. Fluids, 9, 1174, 1966.

36. Loyalka S. K., Kinetic Theory of Thermal Transportation and Mechanocaloric Effect. I, J. Chem. Physics, 55, 4497, 1971.

37. Loyalka S. K., Kinetic Theory of Thermal Transpiration and Mechanocaloric Effect. II. , J. Chem. Physics, 63, 4054, 1975.

38. Cercignani C., P. Foresti, and F. Sernagiotto, Nuovo Cimento, X, 57B, 297, 1968.

39. Loyalka S. K., and J. Ferziger, Model Dependence of the Slip Coefficient Phys. Fluids, 10, 1833, 1967.

40. Loyalka S. K., Velocity Profile in the Knudsen Layer for the Kramer's problem, Phys. Fluids, 18, 1666, 1975.

41. Loyalka S. K., Strong Evaporation in Half Space : Integral Transport Solutions for one-dimensional Bhatnagar-Gross-Krook model, Phys. Fluids, 24, 2154, 1981.

42. Van Kampen N. G., On the Theory of Stationary Waves in Plasmas, Physica, 21, 949, 1955.

43. Dirac P. A. M., The Principles of Quantum Mechanics, Clarendon Press, Oxford, London, 1930.

44. Cercignani C., Elementary Solutions of the Linearized Gas-Dynamics Boltzmann Equation and their Application to the Slip-Flow Problem, Ann. Physics, 20, 219, 1962.

45. Cercignani C., The Kramers Problem for a not Completely Diffusing Wall, J. Math. Anal. Appl., 10, 568, 1965.

46. Cercignani C., Plane Couette Flow According to the Method of Elementary Solutions, J. Math. Anal. Appl., 11, 93, 1965.

47. Cercignani C., Plane Poiseuille Flow According to the Method of Elementary Solutions, J. Math. Anal. Appl., 12, 254, 1965.

48. Ferziger J. H., Flow of a Rarefied Gas Through a Cylindrical Tube, Phys. Fluids, 10, 1448, 1967.

49. Mitsis G. J., Transport Solutions of the Monoenergetic Critical Problems, Ph.D. thesis, University of Michigan, 1963.

50. Loyalka S. K., Thermal Transpiration in a Cylindrical Tube, Phys. Fluids, 12, 2301, 1969.

51. Kriese J. T., T. S. Chang, and C. E. Siewert, Elementary Solutions of Coupled Model Equations in the Kinetic Theory of Gases, Int. J. Eng. Sci., 12, 441, 1974.

52. Thomas J. R., Applications of the Method of Elementary Solutions in Radiative Transfer and Kinetic Theory, Ph.D. Thesis, North Carolina State University, 1973.

53. Thomas J. R., Temperature Slip Problem with Arbitrary Accommodation at Surface Phys. Fluids, 16, 1162, 1973.

54. Thomas J. R., T. S. Chang, and C. E. Siewert, Heat Transfer between Parallel Plates with Arbitrary Surface Accommodation, Phys. Fluids, 16, 2166, 1973.

55. Thomas J. R., Transition Regime Heat Conduction : Influence of Unequal Surface Accommodation, Rarefied Gas Dynamics, S. S. Fisher ed., 54, 363, 1981.

56. Thomas J. R., and C. E. Siewert, Half Space Problems in the Kinetic Theory of Gases, Phys. Fluids, 16, 1557, 1973.

57. Siewert C. E., and J. R. Thomas, Strong Evaporation into a Half Space, ZAMP, 32, 421, 1981.

58. Siewert C. E., and J. R. Thomas, Strong Evaporation into a Half Space. II. The Three-dimensional BGK Model, ZAMP, 33, 202, 1982.

59. Thomas J. R., T. S. Chang, and C. E. Siewert, Reverse Temperature Gradient in the Kinetic Theory of Evaporation, Physical Review Letters, 33, 680,1974.

60. Loyalka S. K., N. Petrellis, and T. S. Storvick, Some Exact Numerical Results for the BGK Model : Couette, Poiseuille and Thermal Creep Flow between Parallel Plates, ZAMP, 30, 514, 1979.

61. Benoist P., and A. Kavenoky, A New Method of Approximation of the Boltzmann Equation, Nucl. Sci. Eng., 32, 225, 1968.

62. Kavenoky A., The C_N Method of Solving the Transport Equation Application to Plane Geometry, Nucl. Sci. Eng., 65, 209, 1978.

63. Carlson, et al., Solution of the Transport Equation by the S_N Method, Proc. 2nd Int. Conf. Peaceful Uses At. Energy, United Nations, New York, 1958.

64. Williams M. M. R., Mathematical Methods in Particle Transport Theory, Wiley-Interscience Publishers, Inc, New York, 1971.

65. Case K. M., F. de Hoffmann, and G. Placzek, Introduction to the Theory of Neutron Diffusion, Vol i, U.S. Government Printing Office, Washington D.C., 1953.

66. Garcia R. D. M., and C. E. Siewert, A Multiregion

Calculation in the Theory of Neutron Diffusion, Nucl. Sci. Eng., 76, 53, 1980.

67. Garcia R. D. M., and C. E. Siewert, Multislab Multigroup Transport Theory with Lth Order Anisotropic Scattering, J. Comput. Phys., 50, 181, 1983.

68. Siewert C. E., and P. Benoist, Multigroup Transport Theory. I. Basic Analysis, Nucl. Sci. Eng., 78, 311, 1981.

69. Garcia R. D. M., and C. E. Siewert, Multigroup Transport Theory II Numerical Results, Nucl. Sci. Eng., 78, 315, 1981.

70. Garcia R. D. M., and C. E. Siewert, Multigroup Transport Theory with Anisotropic Scattering, J. Comput. Phys., 46, 237, 1982.

71. Thomas J. R., J. D. Southers, and C. E. Siewert, The Critical Problem for an Infinite Cylinder, Nucl. Sci. Eng., 84, 79, 1983.

72. Siewert C. E., and J. R. Thomas, Neutron Transport Calculations in Cylindrical Geometry, Nucl. Sci. Eng., 87, 107, 1984.

73. Siewert C. E., On using the F_N Method for Polarization Studies Finite Plane-parallel Atmospheres, J. Quant. Spectrosc. Radiat. Transfer, 21, 35, 1979.

74. Maiorino J. R., and C. E. Siewert, The F_N Method for Polarization Studies - II Numerical Results, J. Quant. Spectrosc. Radiat. Transfer, 24, 159, 1980.

75. Garcia R. D. M., and C. E. Siewert, Radiative Transfer in Finite Inhomogeneous Plane - Parallel Atmospheres, J. Quant. Spectrosc. Radiat. Transfer, 27, 141, 1982.

76. Garcia R. D. M., and C. E. Siewert, Radiative Transfer in Inhomogeneous Atmospheres - Numerical Results, J. Quant. Spectrosc. Radiat. Transfer, 25, 277, 1981.

77. Siewert C. E., and J. R. Maiorino, A Point Source in a Finite Sphere, J. Quant. Spectrosc. Radiat. Transfer, 22, 435, 1979.

78. Devaux C., C. E. Siewert, and Y. L. Yuan, The Complete Solution for Radiative Transfer Problems with Reflecting Boundaries and Internal Sources, The Astrophysical Journal, 253, 773, 1982.

79. Dunn W. L., R. D. M. Garcia, and C. E. Siewert, Concise and Accurate Solutions for Chandrasekhar's X and Y Functions, The Astrophysical Journal, 260, 849, 1982.

80. Siewert C. E., R. D. M. Garcia, and P. Grandjean, A Concise and Accurate Solution for Poiseuille Flow in a Plane Channel, J. Math. Phys., 21, 2760, 1980.

81. Loyalka S. K., C. E. Siewert, and J. R. Thomas, an Approximate Solution concerning Strong Evaporation into a Half Space, ZAMP, 32, 745, 1981.

82. Pao Y. P., Application of Kinetic Theory to the Problem of Evaporation and Condensation Phys. Fluids, 14, 306, 1971.

83. Pao Y. P., Temperature and Density Jumps in the kinetic Theory of Gases and Vapors, Phys. Fluids, 14, 1340, 1971.

84. Cassell J. S., and M. M. R. Williams, An Exact Solution of the Temperature Slip Problem in Rarefied Gases, Transport Theory and Statistical Physics, 2, 81, 1972.

85. Sone Y., and Y. Onishi, Kinetic Theory of Evaporation and Condensation, J. Phys. Soc. Japan, 35, 1773, 1973.

86. Gajewski P., A. Kulicki, A. Wisniewski, and M. Zhorzelski, Kinetic Theory Approach to the Vapor-Phase Phenomena in a Condensation Process, Phys. Fluids, 17, 321, 1974.

87. Kogan M. N., and N. K. Makashev, Role of the Knudsen Layer in the Theory of Heterogeneous Reactions and in Flows with Surface Reactions, Fluid Dynamics, 6, 913, 1974.

88. Murakami M., and K. Oshima, Kinetic Approach to the Transient Evaporation and Condensation Problems, Rarefied Gas Dynamics, F6, 1974.

89. Yen S. M., and T. J. Akai, Nonlinear Solutions for an Evaporation-Effusion Problem, J. L. Potter, ed., AIAA, New York, 1977.

90. Ytrehus T., and J. Alrestad, A Mott-Smith Solution for Nonlinear Condensation, Rarefied Gas Dynamics, S.S. Fisher ed., Part I, 74, p.330, 1977.

91. Sone Y., Kinetic Theory of Evaporation and

CondensationLinear and Nonlinear Problems, J. Phys. Soc. Japan, 45, 315, 1978.

92. Carnahan B., H. A. Luther, and J. O. Wilkes, Applied Numerical Methods, John Wiley & Sons, 1969.

93. Wilkinson J. H., Some Recent Advances in Numerical Linear Algebra, The State of the Art in Numerical Analysis, London, 1977.

94. Dongarra J. J., C. B. Moler, J. R. Bunch, and G. W. Stewart, Linpack Users' Guide, Siam, Philadelphia, 1979.

95. Gross E. P., and S. Ziering, Heat Flow between Parallel Plates, Phys. Fluids, 2, 701, 1959.

96. Willis R. D., Heat Transfer in a Rarefied Gas between Parallel Plates at Large Temperature Ratios, Rarefied Gas Dynamics, Laurmann ed., p.209, Academic Press, New York, 1963.

97. Bassanini P., C. Cercignani, and C. D. Paganini, Influence of the Accommodation Coefficient on the Heat Transfer in a Rarefied Gas, Int. J. Heat Mass Transfer, 11, 1359, 1968.

98. Hsu S. K., and T. F. Morse, Kinetic Theory of Parallel Plate Heat Transfer in a Polyatomic Gas, Phys luids, 15, 584, 1972.

99. Loyalka S. K., and J. R. Thomas, Heat Transfer in a Rarefied Gas enclosed between Parallel Plates: Role of Boundary Conditions, Phys. Fluids, 25, 7, 1162, 1982.

100. Garcia R.D.M., and C.E. Siewert, On Angular Flux Computations in Neutron-Transport Theory, Nuc. Sci. Eng., 81, 474, 1982.

101. Garcia R. D. M., G. C. Pomraning, and C. E. Siewert, on the Transport of Neutral Hydrogen Atoms in a Hydrogen Plasma, Plasma Physics, 24, 903, 1982.

102. Thomas J. R., personal communication.

103. Sone Y., and K. Yamamoto, Flow of Rarefied Gas through a Circular Pipe, Phys. Fluids, 11, 8, 1968.

104. Siewert C.E., and J.R. Thomas, The Critical Problem for an Infinite Cylinder, Nucl. Sci. Eng., 84, 285, 1983.

105. Handbook of Mathematical Functions, AMS-55, M.Abramowitz and I.A. Stegun, Eds., U.S. National Bureau of Standards ,1964.

106. Bateman Manuscript Project, Higher Transcendental Functions, A. Erdelui, Ed., Vol. II, p.333, 1954.

9. APPENDICES

9.1 The F_N Approximation in half space problems

Evaluating the general solution (4.12) at x=0 and $\mu<0$ we obtain

$$\underset{\sim}{\psi}(0,-\mu) = \sum_{\alpha=1}^{2} A_\alpha \underset{\sim}{\phi}_\alpha(-\mu) + \sum_{\alpha=3}^{4} A_\alpha \underset{\sim}{\psi}_\alpha(x,-\mu) + \sum_{\alpha=1}^{2} \int_0^\infty A_\alpha(\eta) \underset{\sim}{\phi}_\alpha(\eta,-\mu)\, d\eta \quad , \quad \mu > 0 \quad , \tag{9.1}$$

since $A_\alpha(\eta)=0$, $\eta<0$, $\alpha=1,2$. If we substitute the eigenvectors $\underset{\sim}{\phi}_\alpha(\mu)$, $\underset{\sim}{\psi}_\alpha(x,\mu)$ and $\underset{\sim}{\phi}_\alpha(\eta,\mu)$ given in equations (3.3-3.6) into equation (9.1) and take into consideration the properties of the delta function we find

$$\underset{\sim}{\psi}(0,-\mu) = \sum_{\alpha=1}^{2} A_\alpha \underset{\sim}{Q}(\mu) \begin{vmatrix} \delta_{1,\alpha} \\ \delta_{2,\alpha} \end{vmatrix} - \mu \sum_{\alpha=3}^{4} A_\alpha \underset{\sim}{Q}(\mu) \begin{vmatrix} \delta_{1,\alpha-2} \\ \delta_{2,\alpha-2} \end{vmatrix} + \sum_{\alpha=1}^{2} \int_0^\infty A_\alpha(\eta) \frac{\eta}{\sqrt{\pi}} e^{-\eta^2} \begin{vmatrix} \mu^2 - \frac{1}{2} & 1 \\ 1 & 0 \end{vmatrix} \frac{d\eta}{\eta+\mu} \quad , \tag{9.2}$$

which can be written as

$$\underset{\sim}{\psi}(0,-\mu) = \underset{\sim}{Q}(\mu) \left\{ \begin{vmatrix} A_1 \\ A_2 \end{vmatrix} - \mu \begin{vmatrix} A_3 \\ A_4 \end{vmatrix} + \int_0^\infty \begin{vmatrix} \sqrt{\frac{3}{2}} A_1(\eta) \\ A_2(\eta) \end{vmatrix} \frac{\eta}{\sqrt{\pi}} e^{-\eta^2} \frac{d\eta}{\eta+\mu} \right\} , \tag{9.3}$$

We can rewrite the above expression for the unknown distribution function by approximating the integral term as

$$\underset{\sim}{\psi}(0,-\mu) = \underset{\sim}{Q}(\mu) \left\{ \begin{vmatrix} A_1 \\ A_2 \end{vmatrix} - \mu \begin{vmatrix} A_3 \\ A_4 \end{vmatrix} + \frac{1}{\sqrt{\pi}} \sum_{\alpha=1}^{\infty} \begin{vmatrix} \sqrt{\frac{3}{2}}\, A_1(\eta_\alpha) \\ A_2(\eta_\alpha) \end{vmatrix} \frac{\eta_\alpha}{\eta_\alpha+\mu} e^{-\eta_\alpha^2} \right\} . \tag{9.4}$$

Substitution of the appropriate expansion coefficients for each particular problem into the version of equation (9.4) yields equations (4.21) and (4.42), which are the basis of the structure of the F_N approximations (4.22) for the evaporation problem and (4.43) for the heat transfer problem.

9.2 Formulation of the Functions related to the Half Space Problems.

We are concerned with deriving the coefficients of the known matrix and the right-hand-side vector, which are presented directly through the two vector functions $P_b(\nu_\alpha)$, $R_b(\eta)$, $R_b(\eta,\nu_\alpha)$, $S_b(\eta)$ and $T_b(\eta)$ given by equations (4.28) through (4.31). Since the orthonormal full-range adjoint set $\underset{\sim}{X}_\alpha(\eta,\mu)$ is given by linear combinations of the continuum eigenvectors $\underset{\sim}{\phi}_\alpha(\eta,\mu)$, first we develop the following expression:

$$\int_0^\infty \tilde{\underset{\sim}{\phi}}_1(-\eta,\mu)\, \mu^2\, e^{-\mu^2}\, d\mu = \eta e^{-\eta^2} \begin{Bmatrix} \eta f(\eta) + \frac{1}{4\sqrt{\pi}} \\ \eta h(\eta) - \frac{\eta}{2} + \frac{1}{2\sqrt{\pi}} \end{Bmatrix} , \tag{9.5}$$

$$\int_0^\infty \tilde{\Phi}_2(-\eta,\mu)\ \mu^2\ e^{-\mu^2}\ d\mu = \eta e^{-\eta^2} \begin{Bmatrix} \eta h(\eta) - \frac{\eta}{2} + \frac{1}{2\sqrt{\pi}} \\ 0 \end{Bmatrix} \tag{9.6}$$

$$\int_0^\infty \tilde{\Phi}_1(\eta,\mu)\ \underset{\sim}{Q}(\mu)\ \mu e^{-\mu^2}\ d\mu = \eta e^{-\eta^2} \begin{Bmatrix} \sqrt{\frac{2}{3}} \left[\left(\frac{1}{2} - \eta^2\right)\ f(\eta) - h(\eta) - \frac{\eta}{4\sqrt{\pi}} + \frac{3}{4}\right] \\ -f(\eta) \end{Bmatrix}, \tag{9.7}$$

$$\int_0^\infty \tilde{\Phi}_2(\eta,\mu)\ \underset{\sim}{Q}(\mu)\ \mu e^{-\mu^2}\ d\mu = \eta e^{-\eta^2} \begin{Bmatrix} -\sqrt{\frac{2}{3}}\ f(\eta) \\ -\ h(\eta) + \frac{1}{2} \end{Bmatrix}, \tag{9.8}$$

$$\int_0^\infty \tilde{\Phi}_1(\eta,\mu)\ \underset{\sim}{Q}(\mu)\ \frac{\mu}{\mu + \nu_\alpha}\ e^{-\mu^2}\ d\mu$$

$$= \frac{\eta e^{-\eta^2}}{\eta + \nu_\alpha} \begin{Bmatrix} \sqrt{\frac{2}{3}} \left[\left(\frac{1}{2} - \eta^2\right)\ f(\eta) + \left(\frac{1}{2} - \nu_\alpha^2\right)\ f(\nu_\alpha) - h(\eta) - h(\nu_\alpha) + \frac{\eta+\nu_\alpha}{4\sqrt{\pi}} + \frac{3}{2}\right] \\ -\ f(\eta) - f(\nu_\alpha) \end{Bmatrix}, \tag{9.9}$$

and

$$\int_0^\infty \tilde{\Phi}_2(\eta,\mu)\ \underset{\sim}{Q}(\mu)\ \frac{\mu}{\mu + \nu_\alpha}\ e^{-\mu^2}\ d\mu = \frac{\eta e^{-\eta^2}}{\eta + \nu_\alpha} \begin{Bmatrix} \sqrt{\frac{2}{3}}\ [-f(\eta) - f(\nu_\alpha)] \\ -\ h(\eta) - h(\nu_\alpha) + 1 \end{Bmatrix} \tag{9.10}$$

where

$$f(\xi) = h(\xi) \left[\xi^2 - \frac{1}{2}\right] + \frac{\xi}{2\sqrt{\pi}} - \frac{\xi^2}{2}\ , \tag{9.11}$$

and

$$h(\xi) = \xi\, I(\xi) \quad , \tag{9.12}$$

while $I(\xi)$ is the basic integral which we evaluate numerically using Gaussian quadrature. The two-vector functions $P_\beta(\nu_\alpha)$, $R_\beta(\eta)$, $R_\beta(\eta,\nu_\alpha)$, $S_\beta(\eta)$ and $T_\beta(\eta)$ can be easily deduced integrating equations (3.13) and (3.14) term by term with respect to μ and substituting the above expressions into the resulting equations. Finally following a similar procedure we find

$$P_1 = (3 - 2\nu_\alpha^2)\, f(\nu_\alpha) - 2h(\nu_\alpha) - \frac{\nu_\alpha}{2\sqrt{\pi}} + \frac{3}{2} \quad , \tag{9.13}$$

$$P_2 = \sqrt{6}\, (-\, 2f(\nu_\alpha) + 2h(\nu_\alpha) - 1) \quad , \tag{9.14}$$

$$P_3 = (\nu_\alpha^2 - 4)\, f(\nu_\alpha) + h(\nu_\alpha) + \frac{\nu_\alpha}{4\sqrt{\pi}} - \frac{3}{4} \quad , \tag{9.15}$$

and

$$P_4 = 4f(\nu_\alpha) - 14h(\nu_\alpha) + 7 \quad . \tag{9.16}$$

9.3 The F_N Approximation in Finite Medium Problems

In order to simplify matters we decide to take $a_1=a_2$, impose the anti-symmetry condition

$$\underset{\sim}{\psi}(x,\mu) = -\, \underset{\sim}{\psi}(-x,-\mu) \quad , \tag{9.17}$$

and take the origin of the coordinate system midway between the two plates, which then lie at $x=\delta/2$ and $x=-\delta/2$. This way the equations are not lengthy and presentation of the analysis is possible. Applying the above condition to the general solution given by equation (5.5) allows us to write the general solution as

$$\underset{\sim}{\psi}(x,\mu) = \sum_{\alpha=3}^{4} A_\alpha \, \underset{\sim}{\psi}_\alpha(x,\mu) + \sum_{\alpha=1}^{2} \int_0^\infty A_\alpha(\eta) \, [\underset{\sim}{\phi}_\alpha(\eta,\mu) \, e^{-\frac{x}{\eta}} - \underset{\sim}{\phi}_\alpha(\eta,-\mu) \, e^{\frac{x}{\eta}}] \, d\eta \quad . \tag{9.18}$$

Evaluating equation (9.18) at $x=\delta/2$ and $x=-\delta/2$, and operating on the resulting equations we find

$$\underset{\sim}{\psi}(\tfrac{\delta}{2},\mu) - \underset{\sim}{\psi}(-\tfrac{\delta}{2},\mu) \, e^{-\frac{\delta}{\mu}} = \sum_{\alpha=3}^{4} A_\alpha [\underset{\sim}{\psi}_\alpha(\tfrac{\delta}{2},\mu) - \underset{\sim}{\psi}_\alpha(-\tfrac{\delta}{2},\mu) \, e^{-\frac{\delta}{\mu}}]$$

$$+ \sum_{\alpha=1}^{2} \int_0^\infty A_\alpha(\eta) \, e^{\frac{\delta}{2\eta}} \left\{ \underset{\sim}{\phi}_\alpha(\eta,\mu) \, [e^{-\frac{\delta}{\eta}} - e^{-\frac{\delta}{\mu}}] \right.$$

$$\left. - \underset{\sim}{\phi}_\alpha(\eta,-\mu) \, [1 - e^{-\frac{\delta}{\eta} - \frac{\delta}{\mu}}] \right\} d\eta \quad , \tag{9.19}$$

which, after we substitute the boundary condition

$$\underset{\sim}{\psi}(-\tfrac{\delta}{2}, \mu) = (1-a) \, \underset{\sim}{\psi}(-\tfrac{\delta}{2}, -\mu) + a\sqrt{\pi} \begin{vmatrix} \mu^2 + B \\ 1 \end{vmatrix} \quad , \quad \mu > 0 \quad , \tag{9.20}$$

and apply the anti-symmetry condition, can be written as

$$\{1 - (1-a) \, e^{-\frac{\delta}{\mu}}\} \, \psi(\tfrac{\delta}{2},\mu) = a\sqrt{\pi} \, e^{-\frac{\delta}{\mu}} \begin{vmatrix} \mu^2 + B \\ 1 \end{vmatrix}$$

$$+ \underset{\sim}{Q}(\mu) \left\{ \left[\mu\left(1 - e^{-\frac{\delta}{\mu}}\right) - \frac{\delta}{2}\left(1 + e^{-\frac{\delta}{\mu}}\right) \right] \begin{vmatrix} A_3 \\ A_4 \end{vmatrix} \right.$$

$$\left. + \frac{1}{\sqrt{\pi}} \int_0^\infty \left[\frac{\eta\left(e^{-\frac{\delta}{\eta}} - e^{-\frac{\delta}{\mu}}\right)}{(\eta - \mu)} + \frac{\eta\left(1 - e^{-\frac{\delta}{\eta}} e^{-\frac{\delta}{\mu}}\right)}{\eta + \mu} \right] e^{\frac{\delta}{2\eta}} - \eta^2 \begin{vmatrix} \sqrt{\frac{3}{2}} A_1(\eta) \\ A_2(\eta) \end{vmatrix} d\eta \right\}. \tag{9.21}$$

Equation (9.21) yields a closed form expression for the perturbed distribution function in the form

$$\underset{\sim}{\psi}\left(-\frac{\delta}{2}, \mu\right) = a\sqrt{\pi} \left[e^{\frac{\delta}{\mu}} - (1 - a) \right]^{-1} \begin{vmatrix} \mu^2 + B \\ 1 \end{vmatrix}$$

$$+ \underset{\sim}{Q}(\mu) \left\{ \left[1 - (1-a)\, e^{-\frac{\delta}{\mu}} \right]^{-1} \left\{ \mu\left(1 - e^{-\frac{\delta}{\mu}}\right) - \frac{\delta}{2}\left(1 + e^{-\frac{\delta}{\mu}}\right) \right\} \begin{vmatrix} A_3 \\ A_4 \end{vmatrix} \right.$$

$$\left. + \frac{1}{\sqrt{\pi}} \int_0^\infty \left\{ \left[\frac{e^{-\frac{\delta}{2\eta}}}{\eta - \mu} + \frac{e^{\frac{\delta}{2\eta}}}{\eta + \mu} \right] - \left[\frac{e^{\frac{\delta}{2\eta}}}{\eta - \mu} + \frac{e^{-\frac{\delta}{2\eta}}}{\eta + \mu} \right] e^{-\frac{\delta}{\mu}} \right\} \eta e^{-\eta^2} \begin{vmatrix} \sqrt{\frac{3}{2}} A_1(\eta) \\ A_2(\eta) \end{vmatrix} d\eta \right\} \tag{9.22}$$

Although this last expression looks very promising in order to present an explicit formulation for the distribution function at the boundary, it has two major difficulties. First the constant B is given only in terms of the integral of $\underset{\sim}{\psi}(\delta/2, \mu)$, and secondly the kernel of the integral term in equation (9.22) is too complicated to suggest any simple basis functions for the F_N approximation. It was not found possible to come up with a better

formulation for the distribution function and the matter is still considered open for research. However, we decided to simplify matters and avoid these difficulties by introducing the two simple polynomial F_N approximations given by (5.20) and (5.21), which in fact turn out to give results with high accuracy, although the choice of the basis functions is not fully justified.

9.4 Explicit Formulation and Recursive Relation for the Functions related to the Finite Media Problem

If we substitute the discrete eigenvectors $\underset{\sim}{X}_\alpha(\mu)$, $\alpha=1,2$, into (5.30) and (5.31) we find

$$\underset{\sim}{C}_m = \frac{\sqrt{6}}{5\sqrt{\pi}} \begin{Bmatrix} \Gamma\left(\frac{m+3}{2}\right) - \frac{3}{2}\Gamma\left(\frac{m+1}{2}\right) \\ \Gamma\left(\frac{m+1}{2}\right) \end{Bmatrix} , \tag{9.23}$$

and

$$\underset{\sim}{D}_m = \frac{4}{5\sqrt{\pi}} \begin{Bmatrix} -\frac{1}{2}\Gamma\left(\frac{m+3}{2}\right) + 2\Gamma\left(\frac{m+1}{2}\right) \\ -\frac{1}{2}\Gamma\left(\frac{m+1}{2}\right) \end{Bmatrix} , \tag{9.24}$$

where

$$\Gamma(m) = \int_0^\infty \mu^m e^{-\mu^2} d\mu \quad ,$$

represents the gamma function.

Following the same procedure as in section 9.2 we find

$$\int_0^\infty \underset{\sim}{\phi}_1(-\eta,\mu)\ \mu^{m+1}\ e^{-\mu^2}\ d\mu = \eta e^{-\eta^2}\begin{Bmatrix} M_m(\eta) \\ K_m(\eta) \end{Bmatrix}\ , \tag{9.25}$$

$$\int_0^\infty \underset{\sim}{\phi}_2(-\eta,\mu)\ \mu^{m+1}\ e^{-\mu^2}\ d\mu = \eta e^{-\eta^2}\begin{Bmatrix} K_m(\eta) \\ 0 \end{Bmatrix}\ , \tag{9.26}$$

$$\int_0^\infty \phi_1(\eta,\mu)\ \mu^{m+1}\ e^{-\mu^2}\ d\mu$$

$$= \eta e^{-\eta^2}\begin{Bmatrix} -\sum_{i=0}^{m} \frac{\eta^{m-i}}{2\sqrt{\pi}}\left[\Gamma\left(\frac{i+3}{2}\right) - \frac{1}{2}\Gamma\left(\frac{i+1}{2}\right)\right] - \eta^m f(\eta) \\ -\sum_{i=0}^{m} \frac{\eta^{m-i}}{2\sqrt{\pi}}\Gamma\left(\frac{i+1}{2}\right) - \eta^m h(\eta) + \frac{3}{2}\eta^m \end{Bmatrix}\ , \tag{9.27}$$

$$\int_0^\infty \underset{\sim}{\phi}_2(\eta,\mu)\ \mu^{m+1}\ e^{-\mu^2}\ d\mu = \eta e^{-\eta^2}\begin{Bmatrix} -\sum_{i=0}^{m} \frac{\eta^{m-i}}{2\sqrt{\pi}}\Gamma\left(\frac{i+1}{2}\right) - \eta^m h(\eta) + \eta^m \\ \frac{\eta^m}{2} \end{Bmatrix}\ , \tag{9.28}$$

$$\int_0^\infty \tilde{\underset{\sim}{\phi}}_1(\pm\eta,\mu) \begin{vmatrix} \mu^2 + B \\ 1 \end{vmatrix} \mu e^{-\mu^2}\ d\mu$$

$$= \eta e^{-\eta^2}\left[-f(\eta)\ (\eta^2 + B) - h(\eta) - \frac{\eta}{4\sqrt{\pi}} + \frac{3}{4}\right] \tag{9.29}$$

and

$$\int_0^\infty \tilde{\underset{\sim}{\phi}}_2(\pm\eta,\mu) \begin{vmatrix} \mu^2 + B \\ 1 \end{vmatrix} \mu e^{-\mu^2}\ d\mu$$

$$= \eta e^{-\eta^2}\left[-f(\eta) + \frac{1}{4} - B\left(h(\eta) - \frac{1}{2}\right)\right]\ , \tag{9.30}$$

where $f(\eta)$ and $h(\eta)$ are given by equation (9.11) and (9.12) and the functions $M_m(\eta)$ and $K_m(\eta)$ satisfy the recursive relations

$$M_m(\eta) = -\eta\, M_{m-1}(\eta) + \frac{1}{\sqrt{\pi}} \int_0^\infty (\mu^2 - \tfrac{1}{2})\, \mu^m\, e^{-\mu^2}\, d\mu \quad , \tag{9.31}$$

and

$$K_m(\eta) = -\eta\, K_{\eta-1}(\eta) + \frac{1}{\sqrt{\pi}} \int_0^\infty \mu^m\, e^{-\mu^2}\, d\mu \quad , \tag{9.32}$$

with

$$M_o(\eta) = f(\eta)/\eta \quad ,$$

and

$$K_o(\eta) = I(\eta) \quad ,$$

or can be deduced directly from

$$M_{m+1}(\eta) = (-1)^{m+1}\, \eta^m\, f(\eta) + \frac{1}{2\sqrt{\pi}} \sum_{\alpha=0}^{m} \eta^{m-\alpha}\, (-1)^{m-\alpha} \left\{ \Gamma\left(\frac{\alpha+3}{2}\right) - \frac{1}{2}\, \Gamma\left(\frac{\alpha+1}{2}\right) \right\} , \tag{9.33}$$

and

$$K_{m+1}(\eta) = (-1)^{m+1}\, \eta^m\, h(\eta) + \frac{1}{2\sqrt{\pi}} \sum_{\alpha=0}^{m} \eta^{m-\alpha}\, (-1)^{m-\alpha}\, \Gamma\left(\frac{\alpha+1}{2}\right) . \tag{9.34}$$

The two-vector functions $S_m(\eta)$, $T_m(\eta)$, $R_m(\eta)$, $P_m(\eta)$, $W_1(\eta)$, and $W_2(\eta)$ are derived by direct substitution of the above

expressions into the integrated version of equations (3.13) and (3.14).

9.5 The Reduced Distribution Function

We define the perturbed distribution function $h(x,\underset{\sim}{\xi})$ by the relation

$$f(x,\underset{\sim}{\xi}) = f_1(\underset{\sim}{\xi}) \left[1 + \frac{\Delta T}{T_1} h(x,\underset{\sim}{\xi})\right] \quad , \tag{9.35}$$

where $f(x,\underset{\sim}{\xi})$ is the distribution function and $f_1(\underset{\sim}{\xi})$ is the Maxwellian distribution at x=0 given by

$$f_1(\underset{\sim}{\xi}) = \frac{n_1}{(2\pi RT_1)^{3/2}} \exp\left[-\frac{\xi^2}{2RT_1}\right] \quad . \tag{9.36}$$

If we integrate equation (9.35) over all ξ_2 and ξ_3 we find

$$\phi(x,\mu) = \frac{n_1}{(2\pi RT_1)^{1/2}} e^{-\mu^2} \int_{-\infty}^{\infty}\int \left[1 + \frac{\Delta T}{T_1} h(x,\underset{\sim}{c})\right] e^{-c_2^2 - c_3^2} \, dc_2 \, dc_3 \quad , \tag{9.37}$$

where $\underset{\sim}{c}=\underset{\sim}{\xi}/(2RT_1)^{0.5}$ and $\mu=c_1$.

Next, following Cercignani [2,12] we project $h(x,\underset{\sim}{c})$ as follows

$$h(x,\underset{\sim}{c}) = \sum_{\ell=1}^{4} \psi_\ell(x,\mu) \, g(c_2,c_3) + \psi_5(x,\underset{\sim}{c}) \quad , \tag{9.38}$$

where

$$g_1(c_2,c_3) = \pi^{-\frac{1}{2}} \quad ,$$

$$g_2(c_2,c_3) = \pi^{-\frac{1}{2}} (c_2^2 + c_3^2 - 1) \quad ,$$

$$g_3(c_2,c_3) = \left(\frac{\pi}{2}\right)^{-\frac{1}{2}} c_2 \quad ,$$

and

$$g_4(c_2,c_3) = \left(\frac{\pi}{2}\right)^{-\frac{1}{2}} c_3 \quad .$$

It has been shown [4] that the $\{g_i\}$ form an orthogonal set with respect to the inner product

$$(g_\ell, g_m) = \int_{-\infty}^{\infty} dc_2 \int_{-\infty}^{\infty} dc_3 \; g_\ell(c_2,c_3) \; g_m(c_2,c_3) \; \exp(-c_2^2 - c_3^2) \; .$$

We can now deduce equation (5.65) by projecting equation (9.37) according to equation (9.38).

In order to obtain equation (5.66) we linearize the Maxwellian at some x, using a Taylor series expansion about the same absolute Maxwellian $f_1(c)$ and write

$$f_x(\underset{\sim}{\xi}) = f_1(\underset{\sim}{\xi}) + \left.\frac{\partial f_x}{\partial \eta_x}\right|_{\eta_1,T_1} (\eta_x - \eta_1) + \left.\frac{\partial f_x}{\partial T_x}\right|_{\eta_1,T_1} (T_x - T_1) + \ldots \; , \qquad (9.39)$$

After we take the partial derivatives with respect to density and temperature the above expression can be written as

$$f_x(\underset{\sim}{\xi}) = f_1(\xi) \left[1 + \frac{\Delta\eta_x}{\eta_1} + \frac{\Delta T_x}{T_1}\left(\frac{\underset{\sim}{\xi}^2}{2RT_1} - \frac{3}{2}\right)\right] \; . \qquad (9.40)$$

Integrating equation (9.40) in a similar manner as equation

(9.35) and invoking the fact that $\Delta n_x/n_1=-\Delta T_x/T_1$ we obtain the reduced Maxwellian distribution given by equation (5.66).

9.6 General Solution of the Cylindrical Shear Flow Equation based on the Method of Elementary Solutions

In this section we outline the method of elementary solutions as it is used in obtaining equation (6.23). The procedure and the formulation of the method, for the particular problems under consideration, was pointed out to the author by J. R. Thomas. We reproduce here his work for reasons of completeness and better understanding of the material.

The complete solution of the derived integro-differential equation

$$\frac{\partial^2 Y}{\partial r^2}+\frac{1}{r}\frac{\partial Y}{\partial r}-\frac{Y}{\mu^2}=-\frac{2}{\sqrt{\pi}}\int_0^\infty Y(r,\mu)\, e^{-\mu^2}\frac{d\mu}{\mu^2}-\frac{\sqrt{\pi}}{2} \quad , \tag{9.41}$$

can be written in the form

$$Y(r,\mu)=\psi(r,\mu)+g(r,\mu) \quad , \tag{9.42}$$

where $g(r,\mu)$ is the particular solution of equation (9.41) given by equation (6.31) and the function $\Psi(r,\mu)$ is the solution of the homogeneous part of equation (9.41); that is $\psi(r,\mu)$ satisfies the following equation :

$$\left(\frac{\partial}{\partial r^2} + \frac{1}{r}\frac{\partial}{\partial r} - \frac{1}{\mu^2}\right) \psi(r,\mu) = -\frac{2}{\sqrt{\pi}} \int_0^\infty \psi(r,\mu)\, e^{-\mu^2} \frac{d\mu}{\mu^2} \quad . \tag{9.43}$$

Following Case [2] the function $\psi(r,\mu)$ is separated in the form

$$\psi(r,\mu) = R(r) \cdot M(\mu) \quad . \tag{9.44}$$

Substitution of equation (9.44) into the integral equation (9.43) yields

$$\left(\frac{\partial}{\partial r^2} + \frac{1}{r}\frac{\partial}{\partial r} - \xi^2\right) R(r,\xi) = 0 \tag{9.45}$$

and

$$(\xi^2 - \mu^2)\, M(\mu,\xi) = \frac{2}{\sqrt{\pi}}\, \xi^2\, \mu^2 \quad , \tag{9.46}$$

where ξ is the eigenvalue of the homogeneous equation and the normal mode $M(\mu,\xi)$ has been normalized such that

$$\int_0^\infty M(\mu',\xi)\, e^{-\mu^2} \frac{d\mu'}{\mu'^2} = 1 \quad . \tag{9.47}$$

The general solution, which is bounded at r=0, of equation (9.45) can be written as

$$R(r,\xi) = a_o\, I_o(r/\xi) \quad . \tag{9.48}$$

When ξ takes values between $-\infty$ and ∞ equation (9.46) is singular for $\mu=\xi$. In this case the most general solution of

equation (9.46) is given as

$$M(\mu,\xi) = \frac{2}{\sqrt{\pi}} [f(\xi,\mu) + f(-\xi,\mu)] \quad , \tag{9.49}$$

where $f(\mu,\xi)$ and $f(\mu,-\xi)$ are given explicitly by equation (6.24) and possess completeness and orthogonality properties on the full range $-\infty<\mu<\infty$ as proved by Cercignani [44].

For $\xi=\zeta\varepsilon(-\infty,\infty)$ equation (9.46) can be solved to yield

$$M(\mu,\xi) = \frac{2}{\sqrt{\pi}} \frac{\zeta^2\mu^2}{\zeta^2 - \mu^2} \quad , \tag{9.50}$$

where ζ must be a zero of

$$\Lambda(\zeta) = 1 - \frac{2\zeta^2}{\sqrt{\pi}} \int_0^\infty e^{-\mu^2} \frac{d\mu}{\zeta^2 - \mu^2} \quad . \tag{9.51}$$

In the limit $\zeta\to\infty$ the corresponding discrete normal modes which are solutions to equation (9.43) are

$$\phi_o = C_o \mu^2$$

and

$$\phi_1 = C_1 \mu^2 \ell n(r) \ .$$

Having established the elementary solutions the general solution to equation (9.43) can be written as

$$\psi(r,\mu) = \mu^2 \{C_o + C_1 \ell n r + \frac{1}{\sqrt{\pi}} \int_0^\infty C(\xi) [f(\xi,\mu) + f(-\xi,\mu)] I_o(r/\xi) d\xi\} \ , \tag{9.52}$$

where the expansion C_0 and $C(\xi)$ are to be determined once the boundary conditions of a particular problem are specified.

9.7 The F_N Approximation in Cylindrical Geometry in Rarefied Gas Dynamics.

The simple polynomial approximations (6.52) and (6.53), used to solve the finite media problem and also used extensively in previous work with the F_N method [71,72,106], are not complete enough to establish an accurate solution throughout the Knudsen number range. We start our search for an advanced F_N approximation by considering the general solution of the two problems under consideration

$$Y(R,\mu) = \mu^2 \{C_o + \int_0^\infty C(\xi) \, [f(\xi,\mu) + f(-\xi,\mu)] \, I_o(R/\xi) \, d\xi - \sqrt{\pi} \, \mu^2 \} \quad (9.53)$$

and the first derivative with respect to r

$$\left.\frac{\partial Y}{\partial r}\right|_{r=R} = \mu^2 \left\{ \int_0^\infty C(\xi) \, [f(\xi,\mu) + f(-\xi,\mu)] \, I_1(R/\xi) \, \frac{d\xi}{\xi} - \sqrt{\pi} \, R \right\} , \quad (9.54)$$

where $Y(R,\mu) \equiv \Phi(R,\mu)$ for the Poiseuille flow problem and $Y(R,\mu) \equiv X(R,\mu)$ for the pseudo thermal creep problem. If we multiply (9.54) by $\mu I_o(R/\mu)/I_1(R/\mu)$ and subtract the resulting expression from (9.53) we find

$$Y(R,\mu) - \mu \frac{I_o(R/\mu)}{I_1(R/\mu)} \cdot \frac{\partial Y}{\partial r}\bigg|_{r=R} = \mu^2 C_o - \sqrt{\pi}\,\mu^4 + \sqrt{\pi}\,R\,\mu^3 \frac{I_o(R/\mu)}{I_1(R/\mu)}$$

$$+ \mu^2 \int_0^\infty \xi C(\xi) \left[\frac{1}{\xi-\mu} + \frac{1}{\xi+\mu}\right]\left[I_o(R/\xi) - \frac{\mu}{\xi}\frac{I_1(R/\xi)}{I_1(R/\mu)} I_o(R/\mu)\right] d\xi\Bigg\} , \quad (9.55)$$

invoking the fact that always

$$\int_0^\infty \delta(\xi-\mu)\,[g(\xi) - g(\mu)] = 0 \quad .$$

We now substitute the boundary conditions (6.19) and (6.23) into equation (9.55) and use the identity (6.15) to obtain

$$\phi_P(R,\mu) = R\,\mu\,K_o(R/\mu)\,I_1(R/\mu)\,\{C_o + \sqrt{\pi}\,R\,\mu\,\frac{I_o(R/\mu)}{I_1(R/\mu)} - \sqrt{\pi}\,\mu^2$$

$$+ \int_0^\infty C(\xi)\,\frac{2\xi^2}{\xi^2 - \mu^2}\,[I_o(R/\xi) - \frac{\mu}{\xi}\frac{I_1(R/\xi)}{I_1(R/\mu)} I_o(R/\mu)]\,d\xi \qquad (9.56)$$

and

$$X(R,\mu) = -\frac{\sqrt{\pi}}{2}\mu^4 + R\,\mu\,K_o(R/\mu)\,I_1(R/\mu)\,\{C_o + \sqrt{\pi}\,R\,\mu\,\frac{I_o(R/\mu)}{I_1(R/\mu)}$$

$$-\frac{\sqrt{\pi}}{2}\mu^2 + \int_0^\infty C(\xi)\,\frac{2\xi^2}{\xi^2 - \mu^2}\,[I_o(R/\xi) - \frac{\mu}{\xi}\frac{I_1(R/\xi)}{I_1(R/\mu)} I_o(R/\mu)]\,d\xi \quad , \qquad (9.57)$$

for the Poiseuille and pseudo thermal creep problems respectively. These two integral equations represent closed form expressions for the surface functions and lead directly to the attempted F_N approximations given by equation (6.43) and (6.44).

9.8 Flow Rate and Velocity Jump in terms of Surface Quantities

It is seen that $Y(r,\mu)$ is the solution of equation (9.41). If we let

$$Y_\alpha(r) = \int_0^\infty Y(r,\mu)\, \mu^\alpha\, e^{-\mu^2}\, \frac{d\mu}{\mu^2} \quad , \tag{9.58}$$

then we can multiply equation (9.41) by $\exp(-\mu^2)$ and integrate over all μ from 0 to ∞ to deduce

$$\frac{d}{dr}\left[r\,\frac{dY_2}{dr}\right] = -\frac{\pi}{4}\, r \quad , \tag{9.59}$$

which, after we multiply by r and integrate over all r from 0 to R, yields

$$\int_0^R Y_2(r)\, r dr = \frac{R^2}{2}\, Y_2(R) + \frac{\pi}{64}\, R^4 \quad , \tag{9.60}$$

invoking the requirement

$$\left.\frac{dY_2}{dr}\right|_{r=R} = -\frac{\pi}{8}\, R \quad . \tag{9.61}$$

If we multiply equation (9.41) by $\mu^2\exp(-\mu^2)$ and integrate over all μ we find

$$\frac{d^2Y_4(r)}{dr^2} + \frac{1}{r}\,\frac{dY_4(r)}{dr} - Y_2(r) = -\frac{Y_o(r)}{2} - \frac{\pi}{8} \quad , \tag{9.62}$$

which we can integrate over r and equation (9.60) to obtain

$$R\frac{dY_4(R)}{dr} - \frac{R^2}{2}Y_2(R) - \frac{\pi}{64}R^4 + \frac{\pi}{16}R^2 = -\frac{1}{2}\int_0^R r\,Y_o(r)\,dr \quad . \tag{9.63}$$

Now since the macroscopic velocity is

$$V_P(r) = \frac{2}{\pi}\phi_{P_o}(r) \quad , \tag{9.64}$$

and

$$V_{PT}(r) = \frac{2}{\pi}X_o(r) + \frac{1}{4} \quad , \tag{9.65}$$

and the flow rate is given by equation (6.69) we conclude that

$$Q_P = \frac{R}{4} - \frac{1}{R} + \frac{8}{\pi}\left\{\frac{1}{R}\phi_{P_2}(R) - \frac{2}{R^2}\frac{d\phi_{P_4}(R)}{dr}\right\} \quad , \tag{9.66}$$

for the Poiseuille flow problem and

$$Q_{PT} = \frac{R}{4} - \frac{1}{2R} + \frac{8}{\pi}\left\{\frac{1}{R}X_2(R) - \frac{2}{R^2}\frac{dX_4(R)}{dr}\right\} \tag{9.67}$$

for the pseudo thermal creep flow problem. If we use the appropriate moments of $\phi_P(r,\mu)$ and $X(r,\mu)$ and the boundary conditions (6.19) and (6.22) to eliminate the derivative terms we can write

$$Q_P = \frac{R}{4} - \frac{1}{R} + \frac{8}{\pi}\left\{\frac{1}{R}\int_0^\infty \phi_P(R,\mu)\,e^{-\mu^2}\,d\mu + \frac{2}{R^2}\int_0^\infty \frac{K_1(R/\mu)}{K_o(R/\mu)}\phi_P(R,\mu)\,\mu e^{-\mu^2}\,d\mu\right\} \quad , \tag{9.68}$$

and

$$Q_{PT} = \frac{R}{4} - \frac{1}{2R} + \frac{8}{\pi}\left\{\frac{1}{R}\int_0^\infty X(R,\mu)\ e^{-\mu^2}\,d\mu + \frac{2}{R^2}\int_0^\infty \frac{K_1(R/\mu)}{K_o(R/\mu)}\ X(R,\mu)\ \mu e^{-\mu^2}\,d\mu\right.$$

$$\left. + \frac{\sqrt{\pi}}{R^2}\int_0^\infty \frac{K_1(R/\mu)}{K_o(R/\mu)}\ \mu^5\ e^{-\mu^2}\,d\mu\right\}\ , \qquad (9.69)$$

so that Q_P and Q_{PT} finally are expressed in terms only of $\phi_P(R,\mu)$ and $X(R,\mu)$ respectively.

By a similar procedure we find

$$V_P(R) = \frac{2}{\pi}\int_0^\infty \phi_P(R,\mu)\ \frac{e^{-\mu^2}}{\mu^2}\,d\mu \qquad (9.70)$$

and

$$V_{PT}(R) = \frac{2}{\pi}\int_0^\infty X(R,\mu)\ \frac{e^{-\mu^2}}{\mu^2}\,d\mu + \frac{1}{4} \qquad (9.71)$$

After we substitute the F_N approximation (6.43) into equations (9.68) and (9.70) for the Poiseuille flow problem and (6.44) into equation (9.69) and (9.71) for the pseudo thermal creep flow problem we find equation (5.73), (5.74) and (5.75), (5.76) respectively.

9.9 Analytical Evaluation of Integral (6.51) via a Mellin Transform

We have mentioned in section 6.5 that the integral (6.51), which can be written as

$$S_\alpha(R) = \int_0^\infty K_1(R/\mu)\ I_1(R/\mu)\ \mu^\alpha\ e^{-b\mu^2}\,d\mu \quad , \quad b = 1\ , \qquad (9.72)$$

can be compputed analytically, and thus we now proceed to derive this alternative expression. If we set $\alpha=1,2$ in equation (9.72) we obtain

$$S_o(R) = \int_0^\infty K_1(R/\mu)\ I_1(R/\mu)\ e^{-b\mu^2}\ d\mu \quad , \quad b = 1 \ , \tag{9.73}$$

and

$$S_1(R) = \int_0^\infty K_1(R/\mu)\ I_1(R/\mu)\ e^{-b\mu^2}\ \mu\, d\mu \quad , \quad b = 1 \ . \tag{9.74}$$

respectively. It has been found that the intergrals $S_\alpha(R)$, $\alpha=1,2,3...$ can be generated, by taking the partial derivatives of $S_0(R)$ and $S_1(R)$ with respect to b, through the recursive formulas

$$S_{2n}(R) = (-1)^n \left.\frac{\partial^n S_o(R)}{\partial b^n}\right|_{b=1} \quad , \qquad n = 1,2,\ldots, \tag{9.75}$$

and

$$S_{2n+1}(R) = (-1)^n \left.\frac{\partial^n S_1(R)}{\partial b^n}\right|_{b=1} \quad , \qquad n = 1,2,\ldots. \tag{9.76}$$

To initate our calculations we use

$$S_o(R) = R \int_0^\infty K_1(1/t)\ I_1(1/t)\ e^{-bt^2R^2}\ dt \quad , \tag{9.77}$$

and

$$S_1(R) = R^2 \int_0^\infty K_1(1/t)\ I_1(1/t)\ e^{-bt^2R^2}\ t\, dt \quad , \tag{9.78}$$

where $t=\mu/R$. Here we concentrate on $S_0(R)$ and for convenience we introduce $f(z)=R^{-1}S_0(R)$ where $z=bR^2$ and

$$f(z) = \int_0^\infty K_1(1/t)\ I_1(1/t)\ e^{-t^2 z}\ dt \quad . \tag{9.79}$$

Taking the Mellin transform of f(z) with respect to z we have [37]

$$M[f(z)] \triangleq \int_0^\infty z^{x-1}\ f(z)\ dz = \Gamma(s) \int_0^\infty t^{-2s}\ K_1(1/t)\ I_1(1/t)\ dt \quad . \tag{9.80}$$

After evaluating this integral we find [106,37]

$$M[f(z)] = \frac{1}{4\sqrt{\pi}} \frac{\Gamma(s)\ \Gamma(s-\frac{1}{2})\ \Gamma(s+\frac{1}{2})\ \Gamma(1-s)}{\Gamma(\frac{5}{2}-s)} z^{-s}\ ds \quad , \tag{9.81}$$

while f(z) is deduced from the inversion formula

$$f(z) = \frac{1}{2\pi i} \int_{c-i\infty}^{c+i\infty} M[f(z)]\ z^{-s}\ ds \quad , \tag{9.82}$$

where $0.5<c<1$. It is clear that the last integral can be expressed in terms of the residues of the integrand at the poles of $M\{f(z)\}$. After we find the poles and evaluate the residues, using Cauchy's residue theorem and invoke the fact that $S_0(R)=Rf(z)$, we obtain

$$S_o(b,R) = \frac{\sqrt{\pi}}{4\sqrt{b}} - \frac{2}{3}R - \frac{\sqrt{\pi}\ R^2}{8}\left(\ell n\ b + 2\ \ell n\ R + 3\gamma - \frac{5}{2}\right)\sqrt{b}$$

$$- \frac{1}{4} \sum_{n=1}^{\infty} \frac{(-1)\ R^{2n+1}\ b^n}{(n+\frac{3}{2})(n+\frac{1}{2})^2\ \{(n-\frac{1}{2})!\}^3}$$

$$- \frac{\sqrt{\pi}}{4} \sum_{n=1}^{\infty} \frac{(-1)^n R^{2n+2} b^{n+\frac{1}{2}}}{(n+2)(n+1)^2(n!)^3} \left(\ell\eta\, b + 2\, \ell\eta\, R + 3\gamma - \frac{2}{n+1} - \frac{1}{n+2} \right.$$

$$\left. - 3 \sum_{k=1}^{n} \frac{1}{k} \right) \quad . \tag{9.83}$$

By setting b=1, we have $S_0(R)$ and of course if we now use equations (9.73) and (9.74) we can deduce from equation (9.82) analytical expressions for the higher order functions $S_\alpha(R)$, $\alpha=2,4,6,\ldots$, similar to (9.82). The computed exact results of $S_\alpha(R)$, $\alpha=2,4,\ldots30$, are compared with numerical results obtained directly through a 400 points Gaussion quadrature scheme and agreement is achieved from 9 up to 14 significant figures.

The vita has been removed from the scanned document